The Dissertation Committee for Nai-Jung Hung certifies that this is the approved version of the following dissertation:

The ribosome biogenesis factor Arx1p: characterization of its

recycling mechanism and its role in ribosome export.

Committee:

_____

Arlen Johnson, Supervisor

_____

David Hoffman

_____

Makkuni Jayaram

_____

Paul Macdonald

_____

Scott Stevens

The ribosome biogenesis factor Arx1p: characterization of its recycling mechanism and its role in ribosome export.

by

Nai-Jung Hung, B.S.

Dissertation

Presented to the Faculty of the Graduate School of

The University of Texas at Austin

in Partial Fulfillment

of the Requirements

for the Degree of

Doctor of Philosophy

The University of Texas at Austin

August 2007

Dedication

This dissertation is dedicated to my parents, younger sister for their love and support throughout my graduate study, and to my lovely kitty for her accompany.

Acknowledgements

I would like to express my sincere appreciation to my thesis supervisor Dr. Arlen Johnson for affording me the opportunity to serve in his laboratory and for his constant support, guidance, patient and encouragement throughout my graduate career. This dissertation could not have possible without him. Considerable discoveries throughout this manuscript were driven by his brilliant insight into the molecular mechanism of the late-60S subunit biogenesis. I am grateful to Dr. Scott Stevens for his insightful suggestion into this work. I offer my sincerest thanks to my thesis committee members, David Hoffman, Dr. Makkuni Jayaram and Dr. Paul Macdonald, for their support and expertise during the course of my dissertation work. I would like to acknowledge Dr. Elizabeth Craig and Alison Meyer for the establishment of rewarding collaborations, especially Alison for her thorough analysis and discussions. I also would like to acknowledge former my former laboratory colleagues, John Hedges, Matt West and Ligna Wang, for providing me with experimental guidance and encouraging research environment early in my graduate career. My thanks are also extended to current lab members, Kai-Yin Lo, Cyril Bussiere, Peggy Huang, Joshua White and Richa Sardana, for their sound advice and accompany lately. I wish to thank Kai-Yin Lo, especially, for her assistance in identifying *ARX1* synthetic lethal and suppressor mutants and her helpful discussions. I am indebted to Zhihua Li and Dr. Edward Marcotte for providing me with useful strains and reagents. Finally, I would also like to thank lab members of the Stevens's lab for their suggestions throughout this work.

The ribosome biogenesis factor Arx1p: characterization of its recycling mechanism and its role in ribosome export.

Publication no. _____

Nai-Jung Hung, Ph.D.
The University of Texas at Austin, 2007

Supervisor: Arlen Johnson

Translation is an essential and fundamental process that coverts genetic codes into functional polypeptides by an apparatus called ribosome. In eukaryotic cells, ribosomes are composed of two subunits: the large (60S) subunit and small (40S) subunits. In *Saccharomyces cerevisiae*, ribosome biogenesis is complex and requires the involvement of over ~170 trans-acting factors. As a growing number of factors were identified related to this essential metabolic pathway, our lab has contributed to functional characterization of the late 60S subunit biogenesis pathway that centers on Nmd3p. This work particularly focuses on characterizing of the nuclear shuttling trans-acting factor Arx1p found in the Nmd3p-60S subunit particle. A working model that describes how Rei1p, another cytosolic trans-acting factor, recycles Arx1p is presented. This work also shows a similar mode of Arx1p recycling by the Hsp40 J-protein, Jjj1p. Furthermore, I have investigated functional interplay between Arx1p and Rpl25p, a 60S ribosomal protein at the polypeptide exit

tunnel. These findings further reveal the involvement of Arx1p at the polypeptide exit tunnel in mediating association of other factors with 60S subunits.

Beyond its function at the polypeptide exit tunnel, this work also focuses on a function for Arx1p in the export of 60S subunits. In yeast and higher eukaryotes, 60S subunit export depends on the export adaptor Nmd3p via Crm1-dependent pathway. I show that *ARX1* interacts with the NES of Nmd3p and nucleoporins. From these results, I propose that Arx1p acts as another export receptor to facilitate 60S subunit export.

Table of Contents

Chapter 1: Introduction

Chapter 2: Description of materials and methods

Chapter 4: Interplay of the Hsp-40 J-protein, Jjj1p, with Arx1p and Rei1p in the 60S subunit biogenesis

Chapter 5: Arx1p interacts with 60S subunit export constituents: Nmd3p, Crm1p and nucleoporins

List of Tables

List of Figures

List of Illustrations

Chapter 1: Introduction

1.1 Overview

Translation is initiated by the binding of the large subunit to the pre-initiation complex, containing the small ribosomal subunit and messenger RNA. However, assembling the complex structure of a ribosome poses a first challenge for a cell far before translation can take place. The eukaryotic ribosome is composed of two subunits: the large (60S) and small (40S) subunits which together form an 80S ribosome. In *Saccharomyces cerevisiae*, the 40S subunit consists of one rRNA (18S) and 30 r-proteins while the 60S subunit is comprised of three rRNA (5S, 5.8S and 25S) and 45 r-proteins. The synthesis and assembly of both ribosomal subunits are initiated in the nucleolus, and as they are exported from the nucleus to the cytoplasm, they are finally matured and ready to engage in translation. As ribosomal subunits move along on their itinerary from the nucleolus to the cytoplasm, different factors are involved in distinct steps of the assembly and transport pathway. A growing number of these trans-acting factors (now over ~170) have been identified. While a large pool of nucleolar factors contribute to early rRNA processing coordinated with ribosome precursor assembly, late nuclear/cytoplasmic factors largely function in supporting subunit export across the nuclear pore complex (NPC), as well as final cytoplasmic maturation prior to translation.

Unlike pre-40S particles, which are exported to the cytoplasm immediately after their release from the nucleolus, nascent 60S subunits are subjected to nucleoplasmic maturation events that further simplify the complexity of the pre-60S particle prior to nuclear export. In an attempt to expand our understanding towards these late maturation events, my dissertation work began with the functional

characterization of two novel 60S subunit biogenesis factors, Arx1p and Rei1p, that co-purified with 60S subunit in complex with the export adaptor protein Nmd3p. My work has established a functional connection between these two factors and also revealed a novel linkage between a cytoplasmic chaperone Jjj1p and late 60S subunit biogenesis. Lastly, my work has also suggested a separate function for Arx1p in modulating Nmd3-dependent 60S subunit export.

1.2 Ribosome biogenesis in the nucleolus

Ribosome biogenesis is one of the major metabolic activities in cells. In eukaryotic cells, ribosome biogenesis initiates in a specialized cellular compartment- the nucleolus. The nucleolus is a membraneless organelle within the nucleus, and in *Saccharomyces cerevisiae*, it appears as a single crescent occupying approximately one-third to one-half of the nucleus (Thiry, 2005)(Shaw, 2005)(Raska, 2006). Within the nucleolus, transcription of rDNA is highly active and accounts for more than half of total transcription. The rRNAs are encoded by a 9.1 Kb rDNA unit with 100 to 200 repeats on the long arm of chromosome XII (Kempers-Veenstra, 1986). Three of the four rRNAs (18S, 5.8S, and 25S) are transcribed as a single large pre-rRNA (35S) by RNA polymerase I, whereas the fourth rRNA (5S) is independently transcribed as a short pre-rRNA by RNA pol III (Fromont-Racine, 2003).

Actively transcribed rDNA was first observed in *Xenopus* oocytes as the 5' end of nascent pre-rRNA transcripts are decorated with highly condensed terminal knobs (Miller, 1969). Later, Kumar *et al* showed, by metabolic labeling and density gradient sedimentation analysis, that the primary pre-rRNA transcripts from HeLa and yeast cells are packaged into large 90S complexes, reminiscent of the size of the terminal knobs (Kumar, 1972). While similar structures have been observed in

various eukaryotic organisms, the exact components and biochemical functions of these complexes have remained mysteries for decades. In the early 1990s, U3 snoRNA complexes corresponding to pre-rRNA processing activity within terminal knobs were resolved from mouse cell extracts (Kass, 1990). The 90S complex contains 35S rRNA and U3 snoRNA, and trans-acting factors that are involved in 40S subunit formation, and the components of the SSU processome complex (Granneman, 2004). While the 90S complex can be considered as a common precursor which gives rise to both the pre-40S (43S) and the pre-60S (66S) complex, a major feature of this complex is the lack of trans-acting factors involved in the 60S subunit synthesis (Grandi, 2002). Along the same line, recent evidence from yeast suggests that the small subunit is assembled first and largely independently of the large subunit. This is consistent with the 18S rRNA of the small subunit being encoded in the 5' portion of the primary 35S transcript and thus being transcribed first.
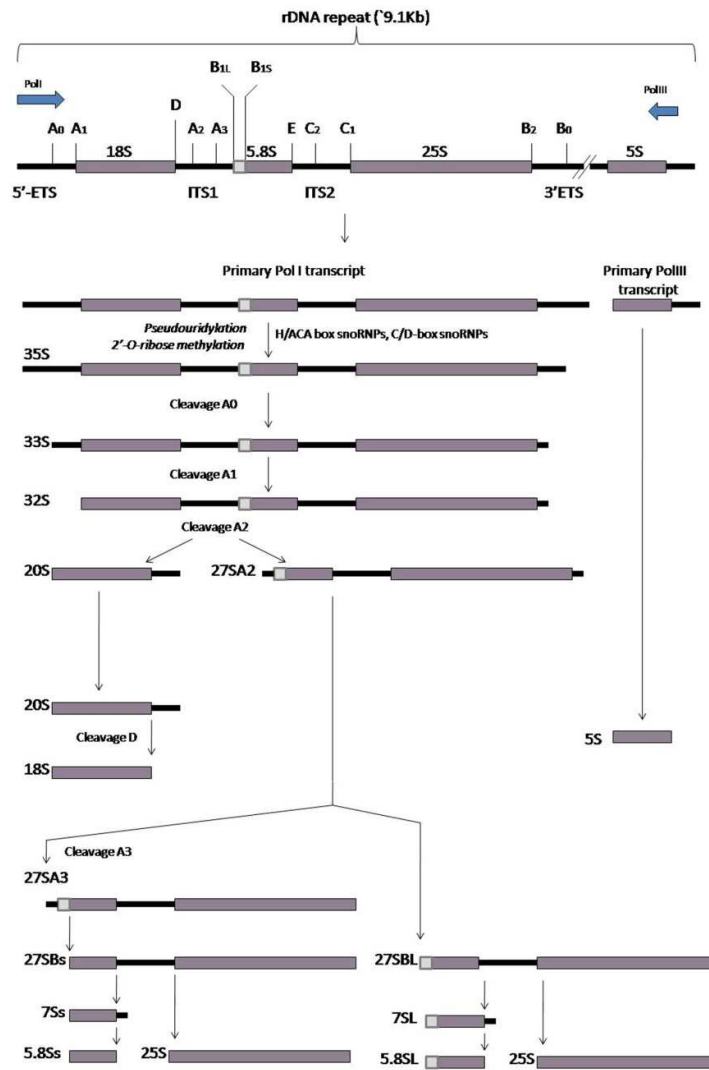
Illustration 1.1 Overview of pre-rRNA processing in *S. cerevisiae*

Each rDNA repeated unit in yeast contains a large operon encoding 18S, 5.8S and 25S rRNAs, which is transcribed by RNA PolI as a long 35S rRNA transcript, and a RNA PolIII transcribed 5S rRNA gene (Illustration 1.1). Maturation of the 35S pre-rRNA transcript involves extensive cleavage and modification on intermediates, which finally gives rise to mature rRNA sequences that were separated by two internal transcribed spacer (ITS) sequences, ITS1 and ITS2, and flanked by two external transcribed spacer (ETS) sequences, a 5' ETS and a 3' ETS. On the other hand, pre-5S rRNA processing is independent of the 35S pre-rRNA maturation and is kinetically faster than formation of 18S, 5.8S and 25S rRNAs. The earliest cleavage at the 35S pre-rRNA is at sites A0, A1 (5'ETS) and A2 (ITS1). Cleavage at A2 separates the 18S precursor (20S) from the 25S and 5.8S precursor (27S). The 20S pre-RNA is subsequently transported to the cytoplasm where the cleavage at site D finally yields the mature rRNA of the 40S subunit – the 18S rRNA. In contrast, the 27SA2 pre-rRNA precursor still undergoes multiple steps of cleavage and processing within ITS1 and ITS2 regions to produce the fully matured 60S rRNA- 25S and 5.8S rRNAs, before they can be exported to the cytoplasm.

To date, more than 170 factors have been identified in the ribosome biogenesis pathway (Hurt, 1999)(Stage-Zimmermann, 2000)(Gavin, 2002) (Illustration 1.2). These factors can be classified into subgroups according to functions or their action period of time along with the 60S particle maturation pathway. Factors involved in early nucleolar pre-rRNA processing include U3 snoRNA, H/ACA-box snoRNPs , C/D-box snoRNPs, endonucleases, exonucleases and RNA helicases (Fromont-Racine, 2003). The U3 snoRNA complex (U3 snoRNP) targets the 5'ETS and the 5' terminus of 18S rRNA by base pairing and thus facilitates cleavages at sites Ao, A1 and A2 and subsequent 18S pre-rRNA processing. Other

snoRNPs are complexes formed by snoRNAs and r-RNA-modifying enzymes, functioning in extensive steps of chemical modifications of pre-rRNA processing. These snoRNPs target pre-rRNA, guided by base-pairing of sno-RNAs and to pre-rRNA by 2'-O-methylation of the sugar moiety and pseudouridylation of uridine residues. Endonucleases and exonucleases (i.e. Rnt1, Rat1, Xrn1, RNase MRP) carry out various endonucleolytic and exonucleolytic cleavages as pre-35S rRNA is processed into shorter intermediates and finally the mature rRNA. Other than these well characterized rRNA modifications described above, recent studies have implicated post-translational modifications of proteins as well. For instance, phosphorylation, ubiquitination and sumoylation are associated with maturation of ribosomal subunits at various steps (Panse, 2006)(Schafer, 2006)(Neumann, 2003).

During the course of ribosome biogenesis, subsets of factors govern the nucleolar-nuclear transit of pre-60S particles. The first example is the Noc protein family, and at least three Noc proteins have been well documented as their role in nuclear passage of nascent 60S subunits. Exchange of the nucleolar Noc1p/Noc2p complex with their nucleoplasmic counterpart, the Noc2p/Noc3p complex, coincides with nucleolar-nucleoplasmic passage of the pre-60S particles (Milkereit, 2001). Rix7p, a member of the AAA-ATPase family, has also been shown to play an important role in nucleolar release of pre-60S subunits. Inter-migration between the nucleolus and nucleoplasm of Rix7p corresponds to the status of ribosome synthesis, and its intrinsic ATPase activity may couple its role as a "chaperone" in remodeling pre-60S particles prior to export (Gadal, 2001).
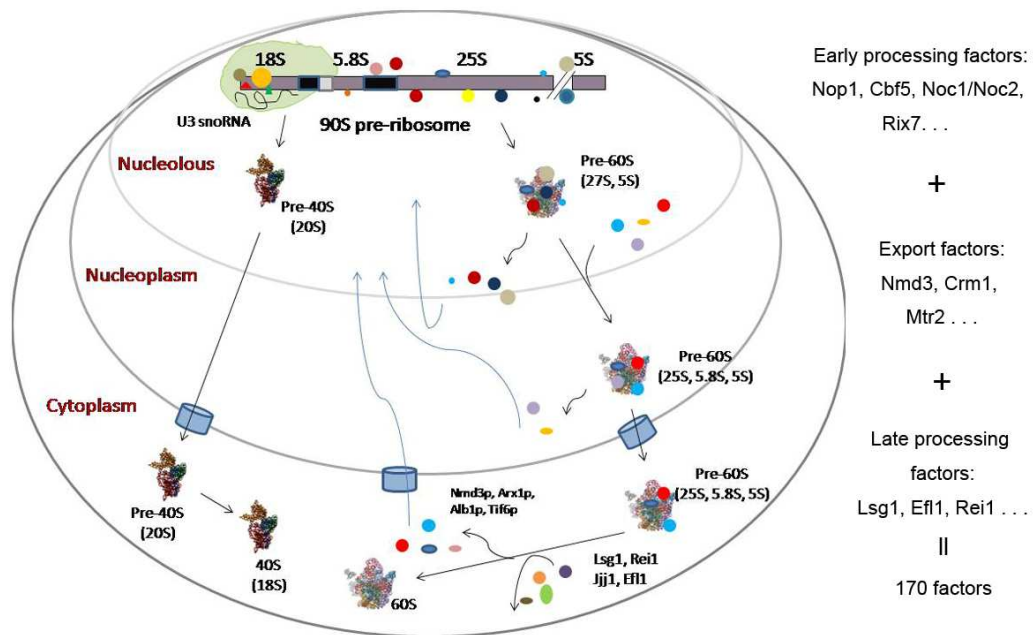
Illustration 1.2 Ribosome biogenesis in *Saccharomyces cerevisiae*

Over 170 trans-acting factors participate in the ribosome biogenesis in *Saccharomyces cerevisiae*. Maturations of both 40S and 60S ribosomes from the nucleolous to the cytoplasm are shown above. While pre-40S subunits are exported into the cytoplasm immediately after their release from the nucleolous, nascent 60S subunits undergo extensive maturation events in the nucleoplasm to further simplify the complexity of the pre-60S particle prior to nuclear export.Example factors involved in distinct steps of 60S subunits biogenesis are listed on the right margin.

1.3 Nuclear export of the 60S subunit

The nuclear envelope compartmentalizes the nucleus and the cytoplasm. The specialized structure, nuclear pore complex (NPC), is embedded within the nuclear envelope and serves as a passage channel accommodating the flux of molecules travelling between these two major cellular compartments. Molecules with size smaller than 40kDa are thought to freely traverse the NPC by simple diffusion; however, such a permeability barrier impedes larger molecules from entering the nucleus by the same manner. In most cases, nuclear transport of larger molecules or complexes is mediated by karyopherins, with a gradient of RanGTP across the nuclear envelope (Gorlich, 1996)(Yoneda, 1999). In general, karyopherins can be simply divided into two classes: importins and exportins, based upon their function in nuclear import or export, respectively (Ullman, 1997)(Ohno, 1998). Importins bind to their cargos in the cytoplasm independent of Ran, and upon translocation to the nucleus, RanGTP binding stimulates dissociation of cargos from importins. Conversely, the exportin-mediated nuclear export pathway operates in a reciprocal fashion. In the nucleus, exportin-cargo interaction is enhanced by the presence of RanGTP, which cooperatively promotes the formation of a cargo-exportin-RanGTP ternary complex. Upon translocation of the export complex in the cytoplasm, the intrinsic low GTPase activity of Ran is strongly induced by the recruitment of RanGAP (RanGTP activating protein, Rna1), and RanBP1 (RanGTP-binding proteins, Yrb1) to the export complex. Upon GTP hydrolysis, Ran switches to GDP-bound form that has low affinity for exportins, which in turn triggers rapid dissociation of export complexes in the cytoplasm (Bischoff, 2002)(Bischoff, 1994)(Bischoff, 1995)(Becker, 1995).

Among various nuclear export pathways, one of the best characterized examples is the Crm1p-mediated pathway. Crm1p, belonging to the importin β-like

family, recognizes cargos harboring well characterized Leucine-rich nuclear export signals (NESs) (Fornerod, 1997). These Leucine-rich NESs share a common feature in primary sequence ($\Phi X_{2-3}\Phi X_{2-3}\Phi X\Phi$) with hydrophobic amino acids (Φ) interspaced by any amino acids (X) (Fornerod, 2002)(Kutay, 2005). As seen from the secondary structure of the well defined Leucine-rich NES of cAMP-dependent protein kinase inhibitor (PKI), the NES forms an amphipathic helix. The hydrophobic amino acids sitting on one side of the helix presumably form the interaction face for Crm1p (Hauer, 1999).

In most cases, Crm1p has only very low affinity for these NESs and must bind cargos cooperatively with RanGTP to achieve a stable complex for export (Fornerod, 1997). The efficient release of cargo in the cytoplasm also relies on GTP hydrolysis by Ran, which triggers dissociation of export complexes. Excitingly, the molecular mechanism of assembly and disassembly of the Crm1p export complex was highlighted by a recent structural analysis of the human Crm1p (Petosa, 2004). The architecture of Crm1p comprises 19 HEAT repeats and a large loop dedicated to Ran binding. The flexible loop is usually positioned in a conformation that blocks its interaction surface for cargos and impedes its stable interaction with Ran. A conformational change of the Ran-binding loop was evidenced when Crm1p was bound by its cargo or RanGTP that allows the formation of the stable export complex in the nucleus. The mechanism of a flexible loop is also seen in an importin system but has an opposite effect on the transport complex. In this case, a conformational change of the loop dislodges the import complex upon RanGTP binding in the nucleus (Chook, 2002). The counter behavior of these transporters may serve as a general theme in mediating nuclear transport events in response to the steep RanGTP gradient across the nuclear envelop.

Early experiments in *Xenopus* oocytes suggested that ribosome export is energy-dependent, saturable and may be mediated by export receptors that are conserved among various living species (Bataille, 1990). Later, nuclear export of both nascent 40S and 60S ribosomal subunits was shown to utilize Crm1p as the export receptor to traverse nuclear pore complex (Ho, 2000)(Gadal, 2001)(Moy, 2002). While Nmd3p is now accepted as the *bona fide* Crm1p-dependent 60S subunit export adaptor (Ho, 2000)(Gadal, 2001), bridging 60S subunit interaction with Crm1p, no such comparable 40S subunit export factor has been identified thus far.

While Nmd3p was first identified as a putative mRNA decay factor, accumulating data have suggested that it functions instead in the biogenesis of 60S subunits. First, *nmd3* mutants have reduced 60S subunit levels but do not display obvious defects in mRNA turnover (Ho, 1999). In addition, Nmd3p was found to co-purify with 60S subunits and could bind both nascent and mature 60S subunits (Ho, 1999). The function of Nmd3 in nuclear export of 60S subunits was further investigated by employing an *nmd3* dominant-negative mutant (nmd3Δ50) lacking its last 50 C-terminal amino acids. This mutant *nmd3* protein was trapped in the nucleus and inhibited the export of 60S subunits (Ho, 2000), suggesting that a functional NES exists in the C-terminal end of Nmd3p. Indeed, sequence analysis of the C-terminus of Nmd3p revealed a putative NES sequence INIDELLDEL (from aa 491 to 500) (Ho, 2000) and mutations of hydrophobic residues within this region resulted in a 60S subunit export defect (Hedges, 2005). Finally, Nmd3p-mediated 60S subunit export is Crm1p-dependent, as both Nmd3p and 60S subunits were trapped in the nucleus upon treating sensitized yeast cells with Leptomycin B (LMB), an antibiotic inhibitor that blocks Crm1p specific export (Ho, 2000). Taken together, these results strongly suggested that Nmd3p functions in the 60S subunit export by providing a

Leucine-rich NES recognized by Crm1p.

The Nmd3p-dependent 60S subunit export mechanism is conserved in yeast, frog and human (Johnson, 2002)(Trotta, 2003)(Thomas, 2003). The Leucine-rich NES is located at the C-terminus of the protein, a region that is only present in Nmd3p orthologs from nucleated cells (Illustration1.3). As seen in the NES of PKI, the NES of Nmd3p is also predicted to form a helical structure with hydrophobic amino acids clustered at the Crm1p interacting face (Illustration 1.3). In addition to the NES, the C-terminal portion of Nmd3p protein also contains a nuclear localization signal (NLS) (Ho, 2000). The presence of a NES and a NLS in Nmd3p in nucleated cells is consistent with its function as a shuttling protein in supporting export of nascent 60S subunits from the nucleus.
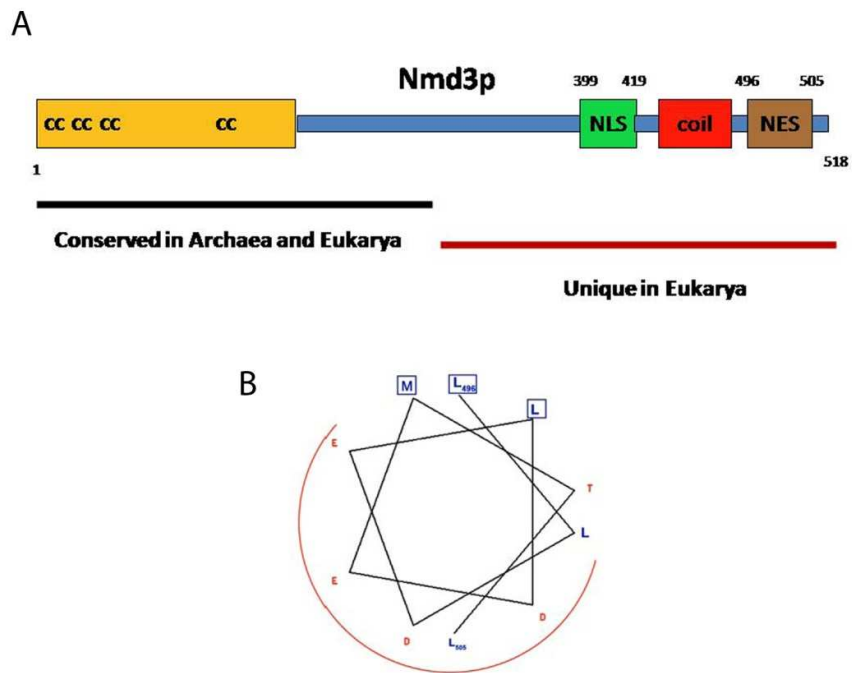
Illustration 1.3 Configuration of Nmd3p and its predicted NES structure

(A) The N-terminal domain, with four Cys-X$_2$-Cys putative zinc binding motifs responsible for ribosome binding, is conserved in Archaea and Eykarya. Nuclear shuttling sequences, including the NES and NLS, are shown at the C-terminal region of the protein. (B) Helical projection of the NES region (amino acids 496~505) of Nmd3p is shown. This region is predicted to fold into an amphipathic helical structure with three conserved residues (boxed) delineating a hydrophobic Crm1p-interacting surface. The red semicircle represents an acidic face. (Adopted from Matt West (West, 2007)).

Identification of Nmd3p as the nascent 60S subunit export adaptor was a major step forward in the field; however, more recent data have suggested the existence of other factors involved in this complex process. Recently, the discovery of a function of the general yeast mRNA export receptor Mex67p-Mtr2p in nuclear export of 60S subunits is another breakthrough (Yao, 2007). Several observations alluded to the involvement of Mex67p and Mtr2p in 60S subunit biogenesis pathway. First, *MEX67* was identified as a high copy suppressor of an *nmd3* mutant, and *MEX67* and *NMD3* show synthetic lethality (Ho, 2000). In addition, high copy *MEX67* partially rescued growth defects of *nmd3* export mutants (Lo and Johnson, unpublished data). Meanwhile, Mtr2p was found to associate with late 60S subunits, and a specific *mtr2-33* mutant exhibited defects in 60S subunit export (Nissan, 2002)(Bassler, 2001) and synthetic lethality with a *nmd3* export mutant (Lo and Johnson, unpublished data). Furthermore, Mtr2p, Mex67p, Nmd3p and Arx1p can be found in the same 60S subunit particles, raising the possibility that Mex67p-Mtr2p may participate in nuclear export of 60S subunits (Yao, 2007).

Unlike general protein export receptors, the Mtr2p-Mex67p system belongs to the family of nuclear export factor (NXF), a distinct system that is specialized for mRNA export (Stewart, 2007)(Katahira, 1999). Mtr2p-Mex67p and its metazoan counterpart p15-TAP have been shown to interact both with polyA RNAs and NPCs (Segref, 1997)(Braun, 2002). Unlike β-karyopherins, the Mtr2p-Mex67p system exports mRNAs independent of Ran. After NPC passage, the disassembly of the Mtr2p-Mex67p mRNA export complex requires the DEAD-box helicase Dbp5p, the ATPase activity of which is activated by Gle1p and inositol hexaphosphate (IP_6) (Lund, 2005)(Alcazar-Roman, 2006)(Weirich, 2006).

The interplay of Mtr2p-Mex67p with Nmd3p suggested their functional

involvement in the 60S subunit export. Strikingly, a fusion of Mex67p to an *nmd3-NES* mutant could bypass the 60S subunit export defect but not an mRNA export defect (Lo and Johnson, unpublished data), suggesting that the Mex67p-mediated 60S subunit export is not indirect or derived from a crosstalk with the mRNA export pathway. Moreover, Mex67p-mediated 60S subunit export is independent of Crm1p (Lo and Johnson, unpublished data). However, the Mtr2p-Mex67p system did not seem to fully rescue *nmd3p-NES* mutants ((Yao, 2007) and Lo and Johnson, unpublished data). These results suggested that Mtr2p-Mex67p act as assisting export factors utilizing a distinct export mechanism that is required but not sufficient for efficient 60S subunit export.

In addition to Nmd3p, several non-ribosomal transacting factors were found on the pre-60S particles as they are exported from the nucleus. These include Tif6p, Rlp24p, Arx1p and Alb1p (Nissan, 2002)(Saveanu, 2003)(Lebreton, 2006)(Hung, 2006). These factors are released in the cytoplasm before translation and recycled back to the nucleus to support subsequent runs of 60S subunit export. These factors each have corresponding cytoplasmic factors that are responsible for their release from nascent 60S subunits and contribute to cytoplasmic maturation events.

Recently, work in our lab has shown that the cytoplasmic GTPase, Lsg1p, is needed for Nmd3p release (Hedges, 2005)(West, 2005). A working model was proposed, in which the release of Nmd3p requires the GTP hydrolysis by Lsg1p in concert with the proper loading of Rpl10p into cytoplasmic 60S particles. A similiar cytoplasmic maturation event is carried out by another GTPase Efl1p. Mutations in *efl1* retained Tif6p, a nucleolar 60S biogenesis factor, in the cytoplasm. This was suppressed by either higher level of Tif6p expression or a *tif6* mutant that is defective in 60S subunit association (Basu, 2001)(Senger, 2001). Tif6p, the yeast homolog of

mammalian eIF6 (eukaryotic translation initiation factor 6) has been shown to inhibit subunits joining *in vitro* (Russell, 1979)(Raychaudhuri, 1984). Thus, failure of release Tif6p from the 60S subunit results in a block of translation initiation, and therefore its persistence on the cytoplasmic 60S subunit would provide the latest maturation check point before translation initiation.

Whereas the mechanisms for recycling Nmd3p and Tif6p are at least partially understood, how Arx1p is recycled to the nucleus was not known. In Chapter 3, I show that the cytoplasmic zinc finger protein Rei1p is required for releasing Arx1p from 60S subunits for recycling to the nucleus. As my work was in progress, similar results were reported by (Lebreton, 2006). In collaboration with Dr. Craig and her graduate student A. Meyer in University of Wisconsin-Madison, in Chapter4, I go on to show that Rei1p acts with Jjj1p, a cytoplasmic J-protein belonging to the Hsp40 chaperone family (Meyer, 2007). Beyond its function as a ribosome-associated chaperone, Jjj1p also acts as a 60S subunit biogenesis factor and its function in recycling Arx1p to the nucleus is shown in Chapter. 4.

1.4 Factors at the polypeptide exit tunnel

Active ribosomes execute two main functions: decoding the mRNA and polypeptide synthesis. These tasks are accomplished by joining of the 60S subunits to the 48S initiation complex followed by peptidyl-transfer activity carried out by the PTC (peptidyl transferase center). The PTC is located in the middle of the face of 60S subunit that interacts with the 40S subunit. Although the PTC first catalyzes polypeptide bond formation and can thus be considered as the "birthplace" of polypeptides, emerging nascent chains from the large subunits were first detected on the side of the large subunits opposite its subunits joining face (Bernabeu, 1982). This

observation suggested that the large subunit contains an internal channel connecting from the PTC center to the site where nascent chains emerge. The existence of such channel (the exit tunnel), first observed in the mid-1980s (Milligan, 1986), has been elucidated in atomic detail using 50S ribosomes from *Haloarcula marismortui* (Nissen, 2000) and *Deinococcus radiodurans* (Harms, 2001) and was further proven by cryo-electron microscopy (Frank, 1995). The lateral dimension of the tunnel is between 10 and 20 Å, which is just enough to accommodate a nascent polypeptide chain. Studies from several groups have suggested that a nascent polypeptide chain could only adopt a "α-helix" like structure, possibly resulting from the geometry of the exit tunnel. The nature of this narrow tunnel also prohibits complete folding of protein domains. The distance from the PTC to the surface of the large subunit is about 100Å. This generally agrees with the fact that a nascent chain less than 35-40 amino acids is protected from proteolytic cleavage by the ribosome and that the minimum chain length for antibody recognition at the tunnel is about 40-50 amino acids (Picking, 1992).

As the nascent polypeptide chain emerges from the exit tunnel, it must fold into the proper protein structure in the crowded environment of the cytosol. To prevent inappropriate misfolding in these unfavorable conditions, cells have evolved a class of chaperones that are anchored to the ribosome in the proximity of the exit tunnel to promote polypeptide folding. These "ribosome-associated" chaperones have been thought to keep nascent chains from aggregation by transiently masking the hydrophobic surfaces of nascent polypeptides as these residues are buried inside of mature proteins.

Ribosome-associated chaperones have been identified both from prokaryotes

and eukaryotes (Rassow, 1996)(Craig, 2003)(Hesterkamp, 1996)(Pfund, 1998). While their functions in mediating nascent chain folding were both demonstrated by their ability of being cross-linked to short nascent polypeptides, these chaperones do not share sequence similarity. In bacteria, the specialized ribosome-associated chaperone is trigger factor (TF), a peptidyl-prolyl isomerase (PPIase). Based on the structure of TF, a model of TF-ribosome complex was proposed to explain TF-mediated *de novo* nascent polypeptide folding (Maier, 2005)(Ferbitz, 2004)(Ito, 2005). In this model, TF sits over the polypeptide exit tunnel as a monomer with an N-terminal ribosome binding domain and a hanging hydrophobic domain formed largely by the rest of the protein that is thought to mediate nascent polypeptide folding once it emerges out of the ribosome.

In eukaryotes, the co-translational nascent polypeptide folding apparatus is more complex and can be achieved by more than one class of ribosome-associated chaperones (Craig, 2003). A member of the Hsp70 chaperone family, Ssb, has been implicated as the major ribosome-associated chaperone, which binds directly with the ribosome as well as nascent polypeptides. The Hsp70 proteins all share a highly conserved N-terminal domain with intrinsic ATPase activity that is obligatory for modulating peptide binding and thus promoting subsequent protein folding. Each of the Hsp70 proteins was thought to adopt two discrete conformations according to their binding states to ATP and ADP. In the ADP bound form, Hsp70 proteins have higher peptide binding affinity, while in the presence of ATP, the Hsp70-peptide interaction is weakened, resulting in peptide release. In summary, the conformational exchange between peptide bound and unbound states, regulated by ATP hydrolysis, is the basis of Hsp70 chaperone-mediated protein folding.

Like many other Hsp70 chaperones, Ssb requires a J-protein, namely Zuo

17

(zuotin), as co-chaperone to fulfill its biological function. Furthermore, Zuo was found to form a stable complex RAC (ribosome-associated complex) with another chaperone Ssz. The critical role for RAC in modulating Ssb function was persuasive as Ssb can only be crosslinked to nascent polypeptide when both RAC and a functional Zuo's J-domain are present (Gautschi, 2002).

In eukaryotes, another complex that acts as a molecular chaperone and binds to ribosome in close proximity of the nascent polypeptide is NAC (nascent-polypeptide-associated complex). NAC generally exists as a heterodimer that is composed either of Egd2p and Egd1p or to a lesser level by Egd2p and Btt1p (Rospert, 2002). Functions of NAC have been proven to be divergent. It was not only proposed to function as a nascent-chain binding complex, it has also been shown to prevent inappropriate interaction of ribosomes to ER membrane and SRP binding to ribosomes displaying non-secretory peptides (Rassow, 1996).

Other types of co-translational modification are largely primary sequence dependent. For example, the signal recognition particles (SRPs) recognizes proteins that co-translationally bear a secretion signal, usually containing a stretch of about 9-12 hydrophobic amino acids, and thereby direct the ribosome-nascent chain complex to ER membrane for secretion. While SRP binds to a nascent polypeptide, it arrests translation elongation on ribosomes in free cytosol and only resumes translation as the ribosome is properly targeted to Sec61 complex, the translocon of the ER membrane.

Other examples of sequence dependent co-translational modifications include two classes of enzyme that specifically modify N-terminal residues of nascent polypeptides. Methionine aminopeptidase (MetAP), a unique class of proteases, binds to emerging nascent polypeptides co-translationally and removes the N-terminal

methionine if the second residue is small and uncharged (e.g. Ala, Cys, Gly, Pro, Ser, Thr or Val) (Sherman, 1985). This type of N-terminal methionine excision (NME) is conserved from eubacteria to high eukaryotes, and is of significance in regulating various cellular processes, including protein maturation, folding and cellular localization (Giglione, 2004)(Lowther, 2000). Another enzyme-catalyzed reaction at the N-terminal residues of nascent polypeptides is carried out by N-acetyltransferase (Polevoda, 2003). This enzyme transfers an acetyl-group from Acetyl-CoA and neutralizes the charged residues of the N-termini of a polypeptide chain that may impair its cellular function. N-terminal acetylation is very common in eukaryotes, and it typically occurs co-translationally when an emerging nascent chain is only about 25 to 50 amino acids in length (Driessen, 1985).

While functions of most of these co-translationally acting factors were widely studied by various means, efforts have also been made towards understanding their function in the context of ribosomes. To this end, the modes of how these factors interact with ribosomes have been illustrated extensively at the molecular level. Consistent with their proposed functions with nascent polypeptides, these factors have been shown to bind in the vicinity of the polypeptide exit tunnel. More surprisingly, many factors, including SRP, NAC and translocon (the Sec61 complex), have even been shown to adopt the same ribosomal protein (Rpl25 in yeast or Rpl23 in *E. Coli*) as their docking site on ribosome (Grallath, 2006)(Halic, 2006)(Pool, 2002)(Beckmann, 2001)(Beckmann, 2001).

1.5 Dissertation objectives

In my dissertation work, I have functionally characterized two novel 60S subunit biogenesis factors in depth. While many 60S subunit biogenesis factors have

been identified, the focus of my work was to expand our understanding of late 60S subunit biogenesis events that are linked to nucleocytoplasmic export. To this end, two novel factors, Arx1p and Rei1p, were chosen as they were found in the Nmd3p-60S subunit complex, raising the possibility of their involvement in Nmd3p-mediated 60S subunit export process.

This dissertation includes five individual chapters. Chapter one has illustrated current knowledge of ribosome biogenesis with extensive examples of the involvement of various factors from various aspects. Chapter two will provide general information of methods and materials that were used in the body of this work. Chapter three will then describe initial characterization of Arx1p and Rei1p in the context of 60S subunit biogenesis and the implication of the function of Arx1p at the polypeptide exit tunnel. Subsequently, chapter four will reveal the interplay between ribosome biogenesis and chaperone-mediated protein folding pathway by introducing a ribosome-associated Hsp40 protein, Jjj1p. Finally, chapter five will describe a separate function of Arx1p in modulating Nmd3-mediated 60S subunit export and the requirement of other factors in this process. In all, this work extensively expands our current understanding of 60S subunit export and cytoplasmic biogenesis.

Chapter 2: Description of Materials and Methods

The experimental materials and methods used in this thesis are described in detailed in this chapter. The first time that a particular plasmid, strain or method is introduced it will be described in full. Subsequent usages of the same method will refer to the first description with necessary modifications.

2.1 Materials and Methods for Chapter3

2.1.1 Strains, plasmids, and culture media

Strains used in Chapter 3 are listed in Table 2.1. The standard yeast genetics methods and media that are incorporated throughout this chapter have been described previously in (Kaiser, 1994). All yeast strains were cultured in drop-out (synthetic complete) or rich (yeast extract-peptone) media containing 2% glucose or 1% galactose as the carbon source unless stated otherwise in figure legends or text. Yeast transformations, sporulations and tetrad dissections were carried out according to (Gietz, 1992). The following strains were made for use in this section. Strains AJY1901 (*arx1Δ*) and AJY1902 (*rei1Δ*) were haploid spore clones obtained by sporulating heterozygous deletion mutants (Research Genetics). AJY1903 (*arx1Δ rei1Δ*) was obtained by sporulating the diploid made by crossing AJY1901 and AJY1902. Strains with genomic *ARX1* tagged with three tandem copies of the hemagglutinin epitope (HA) or with green fluorescent protein (GFP) (AJY1905 and AJY1909, respectively) were made by homologous recombination (Longtine, 1998) in the wild-type strain W303. Strain AJY1904 (*rei1Δrpl25Δ*pAJ908 (Rpl25-eGFP)) was obtained from a cross of AJY1395 (*rpl25Δ* pAJ908 (Rpl25-eGFP)) and AJY1902 (*rei1Δ*). AJY1904 was then crossed to Arx1-HAexpressing strain AJY1905 to make

AJY1906 (*ARX1-HA rpl25*ΔpAJ908 (Rpl25-eGFP)), AJY1907 (*ARX1-HA rei1*Δ), and AJY1908 (*ARX1-HA rei1*Δ *rpl25*ΔpAJ908 (Rpl25-eGFP)). The 13myc genomically tagged *REI1* strain (AJY1910) was made similarly in W303. Strain AJY2125 (*RPL35A-GFP RPL35B-GFP*) was obtained from a cross of genomic GFP-tagged strains *RPL35A-GFP* and *RPL35B-GFP* (Research Genetics) (Huh, 2003). Strain AJY2128 (*RPL19A-GFP RPL19B-GFP*) was made similarly from a cross of genomic tagged strains *RPL19A-GFP*and *RPL19B-GFP*.

Table 2.1 Yeast strains used in Chapter 3.

Strains		Genotype	Reference
W303	MATa	*his3-11 leu2-3,112 trp1-1 ura3-1*	
AJY1395	MATα	*ade2 his3 leu2 tp1 ura3 rpl25Δ::HIS3 + pASZ11-Rpl25-eGFP*	Bassler *et al.*
AJY1539	MATa	*his3 leu2 ura3 CRM1T539C*	Hedges *et al.*
AJY1901	MATα	*his3Δ1 leu2Δ0 ura3Δ0 arx1Δ::KanMX4*	This section
AJY1902	MATα	*his3Δ1 leu2Δ0 ura3Δ0 rei1Δ::KanMX4*	This section
AJY1903	MATα	*his3Δ1 leu2Δ0 ura3Δ0 arx1Δ::KanMX4 rei1Δ::KanMX4*	This section
AJY1904	MATα	*his3 leu2 trp1 ura3 rei1Δ::KanMX4 rpl25Δ::HIS3 + pAJ908*	This section
AJY1905	MATα	*his3-11 leu2-3,112 trp1-1 ura3-1 ARX1-3HA:His3MX6*	This section
AJY1906	MATα	*his3 leu2 ura3 rpl25Δ::HIS3 ARX1-3HA:His3MX6 + pAJ908*	This section
AJY1907	MATα	*his3 leu2 ura3 rei1Δ::KanMX4 ARX1-3HA:His3Mx6*	This section
AJY1908	MATα	*his3 leu2 ura3 rei1Δ::KanMX4 rpl25Δ::HIS3 ARX1-3HA:His3MX6 + pAJ908*	This section
AJY1909	MATa	*his3-11 leu2-3,112 trp1-1 ura3-1 ARX1-GFP:His3MX6*	This section
AJY1910	MATa	*his3-11 leu2-3,112 trp1-1 ura3-1 REI1-13myc:TRP1*	This section
AJY1911	MATα	*his3Δ1 leu2Δ0 ura3Δ0*	This section
AJY2125	MATa	*his3Δ1 leu2Δ0 ura3Δ0 Rpl35A-GFP::HIS3 RPL35B-GFP::HIS3*	This section
AJY2128	MATa	*his3Δ1 leu2Δ0 ura3Δ0 Rpl19A-GFP::HIS3 RPL19B-GFP::HIS3*	This section

Plasmids used are listed in Table 2.2. For making pAJ1001 (*NMD3-13myc*), pAJ538 (*NMD3-13myc*) was digested with BglII and HindIII and cloned into the same sites of pAJ408 (NMD3-13myc). pAJ1010 (*TIF6-13myc*) was made by cloning the EagI and PacI digested fragment from pAJ1003 (*TIF6-GFP*) into the same site of pAJ1001 (*NMD3-13myc*). pAJ1014 (*NOG2-13myc*) was made by cloning the EagI and PacI digested fragment from pAJ1007 (*NOG2-GFP*) into the same site of pAJ1001 (*NMD3-13myc*). pAJ1015 (*ARX1-13GFP*) and pAJ1016 (*ARX1-13myc*) were made by PCR amplification of ARX1 from wild-type yeast genomic DNA with the primers AJO563 (5'-CTGGGTACCCGGCCGTCATGCCTCTGTGAAGCT) and AJO564 (5'-GCGCCCGGGCTTAATTAACATTTTCATGGTTTCTTCAACTC). The PCR product was then digested with EagI and PacI and ligated into the same sites of pAJ755 (*NMD3-GFP*) and pAJ901 (*LSG1-13myc*), respectively. pAJ1017 (*REI1-GFP*) and pAJ1018 (*REI1-13myc*) were made by PCR amplification of *REI1* from wild-type yeast genomic DNA with the primers AJO567 (5'-CTGAAGCTTCGCCCGCATTATTACCACGGCGATAT) and AJO568 (5'-GCGCCCGGGCTTAATTAACTGCAGAAGTTGGTCTCT). The PCR product was digested with EagI and PacI and ligated into the same sites of pAJ755 (*NMD3-GFP*) and pAJ901 (*LSG1-13myc*). pAJ1016 was made by PCR amplification of *ARX1* from wild-type yeast genomic DNA with the primers AJO563 (5'-CTGGGTACCCGGCCGTCATGCCTCTGTGAAGCT) and AJO564 (5'-GCGCCCGGGCTTAATTAACATTTTCATGGTTTCTTCAACTC). pAJ1026 (*ARX1-13myc LEU2*) was made by EagI and PacI digestion of pAJ1016 (*ARX1-13myc URA3*). pAJ1463 (*ARX1(B6)-GFP*) was derived from an ARX1 mutagenesis screen (refer to 2.1.8 for detailed information). pAJ1464 (*ARX1(B6)-13myc*) was made from pAJ1463 (*ARX1(B6)-GFP*) digestion of KpnI and

PacI into the same sites of pAJ1016 (*ARX1-13myc*). pAJ1489 (*ES27Δ97-U1A-rDNA*) was made by recombinant PCR. Two PCR reaction products amplified by (1) AJO420 and AJO928 (5'-GCTCATATGCCTTCTAAAAACTCC); (2) AJO970 (5'-CGAGCCTCACTACCCGACCCT) and AJO666 (5'-AGTTTCCCTCAGGATAGC) were used as templates for the third PCR reaction amplified by AJO420 and AJO666. The final PCR product was digested with SpeI and MscI and cloned into the same sites of pAJ1181.

Table 2.2. Plasmids used in Chapter 3.

Plasmid	Relevant markers	Reference
pAJ538	*LEU2 CEN NMD3-13myc*	(Hedges, 2005)
pAJ543	*LEU2 CEN GAL10::NMD3*	Hedges and Johnson, unpublished
pAJ545	*LEU2 CEN GAL10:-nmd3Δ100*	Hedges and Johnson, unpublished
pAJ903	*LEU2 CEN LSG1-13myc*	(Kallstrom, 2003)
pAJ908	*URA3 CEN RPL25-eGFP*	(Kallstrom, 2003)
pAJ909	*URA3 CEN RPL25-13myc*	(Kallstrom, 2003)
pAJ1001	*LEU2 CEN NMD3-13myc*	This section
pAJ1010	*LEU2 CEN TIF6-13myc*	This section
pAJ1014	*LEU2 CEN NOG2-13myc*	This section
pAJ1015	*URA3 CEN ARX1-GFP*	This section
pAJ1016	*URA3 CEN ARX1-13myc*	This section
pAJ1017	*URA3 CEN REI1-GFP*	This section
pAJ1018	*URA3 CEN REI1-13myc*	This section
pAJ1026	*LEU2 CEN ARX1-13myc*	This section
pAJ1463	*URA3 CEN ARX1(B6)-GFP*	This section
pAJ1464	*URA3 CEN ARX1(B6)-13myc*	This section
pAJ1489	*LEU2 2µ ES27Δ97-U1A-rDNA*	This section

2.1.2 Sucrose gradient sedimentation

For sucrose density gradients in Figures 3.2, 3.3, 3.4, 3.7, 3.9 and 3.10, 2 ml overnight cultures of yeast strains (as indicated in figure legends) were diluted to OD_{600} ~0.1 into 150 ml of fresh yeast extract-peptone medium and incubated at desired temperatures (as indicated in figure legends). When cultures reached OD_{600} ~0.4, Cycloheximide (150μg/ml final concentration) was then added to each culture followed by one minute incubation. Cells were then collected on icy centrifuge containers, harvested, and pellets were frozen at –80°C until use. Subsequent steps were carried out on ice or at 4°C. Cell pellets were washed once with one ml of "polysome lysis buffer" (10mM Tris-HCl pH 7.5, 100mM KCl, 30mM $MgCl_2$, 1mM DTT, 50μg/ml cycloheximide, and protease inhibitors: 1μg/ml each of leupeptin and pepstatin A and 1mM phenylmethylsulfonylfluoride (PMSF)). Buffer conditions for Figure 3.5 are 20mM HEPES, 10mM KCl, 2.5mM $MgCl_2$, 1mM DTT, 50μg/ml cycloheximide, and protease inhibitors (1μg/ml each of leupeptin and pepstatin A and 1mM phenylmethylsulfonylfluoride (PMSF)). To prepare cell extracts, cells were pelleted and resuspended in ~ one volume of the same buffer and lysed via glass bead abrasion (4x30 second intervals on vortexer separated by one minute periods of cooling on ice). Extracts were clarified by pelleting-out insoluble material via centrifugation at 15,000Xg for 10 minutes. About 20 OD_{260} units of supernatant were loaded onto linear 7-47% sucrose gradients prepared in polysome lysis buffer. After a 2.5-hour spin at 40,000 rpm at 4°C in a Beckman SW40 rotor, gradients were fractionated while continuously monitoring absorbance at 254 nm on an ISCO density gradient fractionator. Collection of ~900μl fractions was conducted by an automated fraction collector. Protein samples were then precipitated from collected gradient fractions by the addition of 10% trichloroacetic acid followed by one hour incubation

on ice prior to centrifugation at 15,000Xg for 10 minutes at 4°C. Pellets were dried by a speed-vacuum and resuspended in about 30μl of 1X Laemmli buffer. Samples were heated at 99°C before proteins were resolved on 12% SDS-PAGE gels. Western analysis was performed as described in section 2.1.3, using specific antibodies against desired epitopes (as indicated in figure legends).

2.1.3 Western blotting

Protein samples resolved on SDS-PAGE gels were subsequently transferred to nitrocellulose membranes in a semi-dry transfer cell (BIORAD) by eletrophoresis with transfer buffer (192mM Glycine, 25mM Tris-Base, 20% methanol, and 0.01% SDS). After transfer, membranes were blocked in TBS (10mM Tris-HCl pH 8.0, 150mM NaCl) plus 5% dry milk solution for at least 30 minutes at room temperature (or 4℃ for overnight). Following blocking, membranes were then washed with TBST (TBS + 0.1% Tween 20) and incubated for at least 3 hours at room temperature with primary antibody diluted in TBST. Primary antibodies used are denoted in respective figure legends and/or method sections. After washing membranes extensively with TBST, they were incubated with appropriate secondary antibodies (horseradish peroxidase conjugates) in TBST for 30 min at room temperature, followed by extensive washing in TBST. Western blots were developed for chemiluminscent (horseradish peroxidase) analysis.

2.1.4 *In vivo* microscopy

Specific strains used for this experiment were denoted in figure legends. Overnight cultures were diluted into fresh medium to an optical density at 600 nm of

0.1 to ~ 0.2 and cultured at room temperature or 30°C to mid-log phase. Cultures were fixed with formaldehyde (3.7% final concentration) for 40 min at room temperature or 30°C, washed three times in cold 0.1 M potassium phosphate buffer, pH 6.6, and resuspended in 0.1 M potassium phosphate, pH 6.6, 1.2 M sorbitol. For 4',6'-diamidino-2-phenylindole (DAPI) staining, Triton X-100 was added to fixed cells to a final concentration of 0.1% for 5 min, and DAPI was added subsequently to a final concentration of 1 μg/ml for 1 min. Cells were then washed three times with cold phosphate-buffered saline (PBS) and resuspended in PBS with 0.02% NaN3. Fluorescence was visualized on a Nikon Eclipse E800 microscope fitted with a 100X objective and a SPOT cooled color digital camera controlled with the SPOT software package (version 1.0.02). Captured images were prepared using Adobe Photoshop 5.0.

2.1.5 Indirect immunofluorescence microscopy

Indirect immunofluorescence was performed as described previously (Ho, 1999). Specific strains used in this experiment are denoted in respective figure legends. Cell fixation was conducted as described in section 2.1.4. Fixed cells were then washed two times in KSorb buffer (0.1M potassium phosphate pH 6.6, 1.2M sorbitol) and resuspended in 100μl of KSorb containing 10mM dithiothreitol (DTT). Samples were then treated with "Yeast lytic enzyme" (Zymolyase T100) at a concentration of 0.1mg/ml and incubated at 30°C for 10 minutes. Spheroplasted cells were washed two times with KSorb plus 1mM PMSF and 10μl aliquots from cell samples were applied to an individual poly-lysine-coated well on a multi-well slide. Excess liquid was aspirated off after 1 minute incubation at room temperature. Attached cells were then permeabilized in ice cold methanol for six minutes at –20°C

followed by treatment with ice cold acetone for 30 seconds. Slides were air-dried completely and cells were then blocked in PBS plus 1% BSA solution for 30 minutes at room temperature. Cells were incubated with primary antibody (α-myc at 1:1000 dilution, Covance 9e10; α-HA at 1:500 dilution, Covance) in PBS plus 1% BSA and incubated for four hours in a damp chamber at room temperature. Cells were washed three times in PBS plus 1% BSA followed by incubation with Cy3-conjugated goat anti-mouse secondary antibody (JacksonImmunoResearch Labortories, Inc.) at a 1:500 dilution in PBS plus 0.1% BSA solution for one hour in a damp chamber at room temperature. After washing cells extensively in PBS plus 0.1% BSA, a 1μg/ml solution of DAPI (in PBS plus 0.1% BSA) was added for staining nuclei (DNA) for 1 minute. After staining, cells were washed three times and were mounted in AquaPolymount (Poly Biosciences) and sealed with a coverslip. Fluorescence was visualized as described in section 2.1.4.

2.1.6 Comparative growth assays

For Figure 3.4 and 3.9, tenfold serial dilutions of saturated cultures were spotted onto yeast extract-peptone-glucose plates and incubated for 3 days at the indicated temperatures. The strains used were the following: AJY1905 (wild-type (WT) *ARX1-HA*), AJY1901 (*arx1Δ*), AJY1907 (*rei1Δ ARX1-HA*), AJY1903 (*arx1Δ rei1Δ*), AJY1907 (*rei1Δ ARX1-HA*) carrying plasmid pAJ908 (*RPL25-eGFP*), AJY1906 (*rpl25Δ ARX1-HA* pAJ908), and AJY1908 (*rei1Δ rpl25Δ ARX1-HA* pAJ908).

2.1.7 Immunoprecipitations

For the immunoprecipitations shown in Figure 3.6, 2ml overnight cultures of strain AJY1907 (*rei1Δ ARX1-HA*) harboring pAJ1018 (*REI1-13myc*) were diluted to 200mL of fresh drop-out medium and cultured at 30°C to OD_{600}~0.4. Cells were harvested by centrifugation and stored at –80°C until use. All subsequent steps were carried out on ice or at 4°C. Cells were washed once in lysis buffer (20mM HEPES pH7.5, 50mM KCl, 5mM $MgCl_2$, 0.1% NP40, 1mM $MgCl_2$ and protease inhibitors :1μg/ml each of leupeptin and pepstatin A and 1mM phenylmethylsulfonylfluoride (PMSF)). Cells were pelleted and resuspended in one volume of lysis buffer, and extracts were prepared by glass bead abrasion (3x30 second cycles on vortexer with one-minute intervals on ice). Extracts were clarified at 15,000xg for 10 minutes at 4°C. Soluble materials were collected and normalized. Equal OD_{260} units of sample supernatants were blocked with BSA-coated protein A agarose beads (Upstate) for 30 minutes at 4°C. Unbound supernatants were collected and incubated with 1 μl of α- myc (9e10 monoclonal, Covance) or 1.5 μl of α-HA (Covance) antibodies and rocked for 2 hour at 4°C. 30μl of BSA-blocked protein A agarose beads were then added, and rocking was continued for an additional 1hour. Beads were washed 3 times with lysis buffer (ten minutes each of rocking at 4°C) and eluted with 50μl of 1x Laemmli sample buffer at 99°C for 3 minutes. Proteins were resolved on a 8% SDS-PAGE gel and transferred to nitrocellulose. Western blots were performed as described in section 2.1.3 with α-myc or α-HA.

For the immunoprecipitations shown in Figure 3.8, 2ml overnight cultures of strain AJY1901 (*arx1Δ*) harboring pAJ1016 (*ARX1-13myc*) or pAJ1464 (*ARX1(B6)-13myc*) were diluted to 200mL of fresh drop-out medium and cultured at 25°C to OD_{600}~0.4. Cells were harvested by centrifugation and stored at –80°C until use. Immunoprecipitation were carried out as described above except extracts were

prepared in buffer conditions with two concentration of KCl: 100 or 200 mM. and samples were run on a 8% gel and Western blotting carried out as described in 2.1.3 with α-c-myc or α-Rpl8 antibodies.

For the immunoprecipitions shown in Figure 3.10, 2ml overnight cultures of strains AJY2128 (Rpl19A-GFP Rpl19B-GFP), AJY2125 (Rpl35A-GFP Rpl35B-GFP), and an isogenic wild type carrying Arx1-13myc (pAJ1016) plasmids were diluted to 200mL of fresh drop-out medium and cultured at 25°C to $OD_{600}\sim0.4$. Immunoprecipitation were carried out as described above except extracts were prepared in buffer conditions with two concentration of KCl: 100 or 200 mM. Samples were run on a 8% gel and Western blotting carried out as described in 2.1.3 with α-c-myc or α-Rpl8 antibodies. For the immunoprecipitions shown in Figure 3.8C, cell extyracts were prepared from the Rpl35A-GFP Rpl35B-GFP strain (AJY2125) expressing Lsg1-13myc (pAJ901), Nmd3-13myc (pAJ1001), Tif6-13myc (pAJ1010), Nog2-13myc (pAJ1014), and Arx1-13myc (pAJ1026). Immunoprecipitation were carried out as described above with two concentration of KCl: 100 or 200 mM and samples were run on a 8% gel and Western blotting carried out as described in 2.1.3 with α-myc or α-Rpl8 antibodies.

For the immunoprecipitions shown in Figure 3.11, 2ml overnight cultures of strains AJY1911 (WT), AJY1901 (*arx1Δ*) and AJY1902 (*rei1Δ*) carrying Lsg1-13myc (pAJ901) or Tif6-13myc (pAJ1010) were diluted to 300mL of fresh drop-out medium and cultured at 25°C to $OD_{600}\sim0.4$. Immunoprecipitation were carried out as described above and samples were run on a 8% gel and Western blotting carried out as described in 2.1.3 with antibodies specific to various RPBs.

For the immunoprecipitions shown in Figure 3.12, cell extracts were prepared from strain AJY1185 where the endogenous wild type rDNA plasmids was

32

replaced by pAJ1181 (U1A tagged wild type rDNA plasmid) or pAJ1489 (U1A tagged ES27Δ97 rDNA plasmid) harboring the Arx1-13myc (pAJ1016) or Rei1-13myc (pAJ1018) plasmid. Immunoprecipitation were carried out as described above except extracts were prepared in buffer conditions with two concentration of KCl: 50 or 200 mM. Samples were run on a 8% gel and Western blotting carried out as described in 2.1.3 with antibodies specific to c-myc or Rpl8p.

2.1.8 Isolation of *ARX1* mutants that suppresses *rei1*Δ

A small scale of random mutagenesis of *ARX1* was performed by PCR using Taq polymerase (Epicentre), pAJ1015 (*ARX1-GFP*) as template (~300 ng) and primers AJO319 (5'-GCGCCATGGATTTGTATAGTTCATCCAT) and AJO563 (5'-CTGGGTACCCGGCCGTCATGCCTCTGTGAAGCT). 10 independent PCR reactions were performed in parallel, using 12 rounds of amplification in order to increase the number of independent mutagenic events. PCR products were purified, pooled, and co-transformed with BclI- and PacI-digested pAJ1015 into strain AJY1903 (*arx1*Δ *rei1*Δ) for *in vivo* homologous recombination. Cells were plated onto Ura- dropout plates, and the screen was performed at room temperature; *arx1* mutants were identified by their suppression of the cold sensitivity of *rei1*Δ. Plasmids DNA were extracted from these suppressor colonies and retransformed into *E. Coli* for amplification. Recovered plasmids were transformed back to strain AJY1903 (*arx1*Δ*rei1*Δ) to confirm suppression. Out of approximately 4000 colonies screened, 26 potential suppressors were identified. Illustration 2.1 depicts *ARX1* suppressors derived from this screen with mutated residues indicated in the context of full length Arx1p. Sequencing of mutant *ARX1* alleles was conducted by the DNA Sequencing

Facility at the ICMB Core (UTAustin). This screen was performed with the assistance of K. Lo.
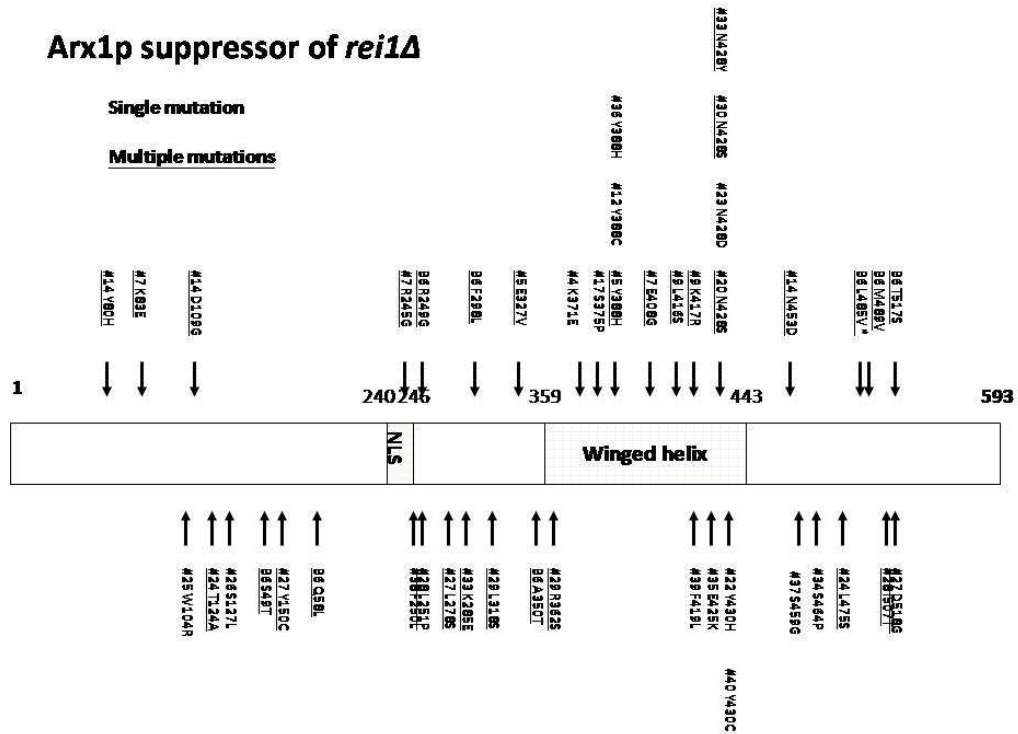
Illustration 2.1 Arx1 suppressors of *rei1*Δ

Full length Arx1p is shown above. Each suppressor mutant is indicated by number. Suppressor mutations were aligned at the corresponding residues in the context of full length Arx1p. Suppressors with more than one mutation were underlined.

2.1.9 LMB treatment

The LMB-sensitive strain AJY1539 (*CRM1T539C*) containing plasmid pAJ538 (*Nmd3-13myc*) or pAJ1018 (*REI1-13myc*) was cultured in selective media at room temperature. Cells were concentrated 20-fold in fresh media, LMB (M. Yoshida) was added to a final concentration of 0.1 μg/ml, and cultures were incubated for 30 minutes. Cells were then fixed with 3.7% formaldehyde (final concentration) and subjected to indirect immunofluorescence microscopy (IF) using antibodies specific to c-myc as described in 2.1.5.

2.2 Materials and Methods for Chapter 4
2.2.1 Strains, plasmids and culture media

Strains used in Chapter 4 are listed in Table 2.3. The following strains were made for use in this section. Strains with genomic *ARX1* tagged with three tandem copies of the hemagglutinin epitope (HA) or with green fluorescent protein (GFP) (AJY1946, AJY1947, AJY1948 and AJY1949) were made by homologous recombination (Longtine, 1998). Briefly, the *ARX1-HA* cassette were amplified from AJY1905 (ARX1-HA) by primers AJO607 (5'- GCTACCAATCCAAACGG) AND AJO600 (5'-GCGGAGCTCCCGGGTATGATATACTTATATTATTTATAT ACTAGCTTTAGAAATGATGAAG). The ARX1-GFP cassette were amplified from AJY1909 (ARX1-HA) by primers AJO607 (5'-GCTACCAATCCAAACGG) and AJO589 (TACTTATATTATTTATATACTAGCTTTAGAAATGATGAAGTTTC GAATTCGAGCTCGTTTAAA). PCR products were gel-purified and transformed into strain AJY1942 (WT) and AJY1944 (*jjj1Δ*).

Table 2.3 Yeast strains used in Chapter 4.

Strains		Genotype	Reference
AJY1539	MATa	*his3 leu2 ura3 CRM1T593C*	Hedges *et al.*
AJY1902	MATα	*his3Δ1 leu2Δ0 ura3Δ0 rei1Δ::KanMX4*	Section 2.1.1
AJY1942	MATa	*his3 leu2 met15 ura3*	A. Meyer
AJY1944	MATa	*GAL2 his3-11, 15 leu2-3, 112 lys1 lys2 Δtrp1 ura3-52 jjj1Δ::TRP1*	A. Meyer
AJY1946	MATa	*his3 leu2 met15 ura3 ARX1-3HA:His3Mx6*	This section
AJY1947	MATa	*his3 leu2 met15 ura3 ARX1-3HA:His3Mx6 jjj1Δ::URA3*	A. Meyer
AJY1948	MATa	*his3 leu2 met15 ura3 ARX1-GFP: His3Mx6*	This section
AJY1949	MATa	*GAL2 his3-11, 15 leu2-3, 112 lys1 lys2 Δtrp1 ura3-52 jjj1Δ::TRP1* *ARX1-GFP: His3Mx6*	This section
AJY2703	MATa	*GAL2 his3-11, 15 leu2-3, 112 lys1 lys2 Δtrp1 ura3-52*	A. Meyer
AJY2705	MATa	*GAL2 his3-11, 15 leu2-3, 112 lys1 lys2 Δtrp1 ura3-52 zuo11Δ::HIS3*	A. Meyer

2.2.2 Immunoprecipitations

For the immunoprecipitations shown in Figure 4.1, 2ml overnight cultures of strain AJY1946 (WT *ARX1-HA*) and a *jjj1Δ* mutant harboring Jjj1-HA plasmid (from Craig lab) were diluted to 200mL of fresh drop-out medium and cultured at 25°C to OD_{600}~0.4. Cells were harvested by centrifugation and stored at –80°C until use. Immunoprecipitation were carried out as described in 2.1.7. And samples were run on a 8% gel and Western blotting carried out as described in 2.1.3 with α-HA or α-Rpl8 antibodies.

For the immunoprecipitations shown in Figure 4.6, 2ml overnight cultures of strain AJY1946 (WT *ARX1-HA*) and AJY1947 (*jjj1Δ ARX1-HA*) were diluted to 200mL of fresh drop-out medium and cultured at 25°C to OD_{600}~0.4. Cells were harvested by centrifugation and stored at –80°C until use. Immunoprecipitation were carried out as described in 2.1.7. And samples were run on a 8% gel and Western blotting carried out as described in 2.1.3 with α-HA or α-Rpl8 antibodies.

2.2.3 Sucrose gradient sedimentation

For polysome analysis and sucrose density gradients in Figures 4.3 and 4.6, 2 ml overnight cultures of yeast strains (as indicated in figure legends) were diluted to OD_{600} ~0.1 into 150 ml of fresh yeast extract-peptone medium and incubated at room temperatures. When cultures reached OD_{600} ~0.4, Cycloheximide (150µg/ml final concentration) was then added to each culture followed by one minute incubation. Cells were then collected on icy centrifuge containers, harvested, and pellets were frozen at –80°C until use. Polysome lysis buffer conditions are: 20mM HEPES, 10mM KCl, 2.5mM $MgCl_2$, 1mM DTT, 50µg/ml cycloheximide, and protease inhibitors (1µg/ml each of leupeptin and pepstatin A and 1mM

phenylmethylsulfonylfluoride (PMSF)). All other steps were carried out as described in 2.1.2. For Figure4.6, SDS-PAGE analysis and Western blotting was carried out as described in 2.1.3 using antibodies specific to HA and Rpl8.

2.2.4 LMB treatment

The LMB-sensitive strain AJY1539 (*CRM1T539C*) was cultured in selective media at room temperature. Cells were concentrated 20-fold in fresh media, LMB (M. Yoshida) was added to a final concentration of 0.1 μg/ml, and cultures were incubated for 30 minutes. Cells were then fixed with 3.7% formaldehyde (final concentration) and subjected to indirect immunofluorescence microscopy (IF) as described in 2.1.5. Affinity purified antibodies against Jjj1 (from Craig lab) or Nmd3 (J. Hedges) were used for detecting Jjj1 or Nmd3.

2.2.5 *In vivo* microscopy

For GFP fluorescence microscopy shown in Figure 4.6, overnight cultures of strain AJY1948 (*WT ARX1-GFP*), AJY1949 (*jjj1Δ ARX1-GFP*) and *rei1Δ ARX1-GFP* were diluted into fresh medium to an optical density at 600 nm of 0.1 to ~ 0.2 and cultured at room temperature to mid-log phase. Cultures were fixed with formaldehyde (3.7% final concentration) and prepared as described in 2.1.4 for *in vivo* microscopy. Fluorescence was visualized on a Nikon Eclipse E800 microscope fitted with a 100X objective and a Photometrics CoolSNAP ES digital camera controlled with the NIS-Element AR 2.10 software. Captured images were prepared using Adobe Photoshop 7.0.

2.3 Materials and Methods for Chapter 5

2.3.1 Strains, plasmids and culture media

Strains used in Chapter 5 are listed in Table 2.4. The following strains were made for use in this section. Strain AJY1912 was made by homologous recombination (Longtine, 1998) in the wild-type strain 1974. Briefly, *arx1Δ::KanMX4* locus was PCR amplification from strain AJY1901 using primers AJO563 (CTGGGTACCCGGCCGTCATGCCTCTGTGAAGCT) and AJO569 (5'-GCGGAGCTCCCGGGTCGACTGCAAGATTCTGAGCAAATG). PCR products were then gel-purified and transformed into wild-type strain 1974 to allow in vivo recombination. Transformants were plated on YPD for one overnight and replicated to YPD plate containing G418 to select for resistance clones. Potential clones were restreaked onto same media to confirm their G418 resistance and verified by PCR.

Plasmids used are listed in Table 2.5. pAJ1029 (*ADE3 URA ARX1*) was made from PCR amplification of *ARX1* from wild-type yeast genomic DNA using primers AJO599 (5'-CTGAGCTCCCGGGTCATGCCTCTGTGAAGC) and AJO600 (5'-GCGGAGCTCCCGGGTATGATATACTTATATTATTTATATACTAGCTTTA GAAATGATGAA). PCR products were gel-purified and digested with SstI and cloned into the same site of pAJ60. pAJ1480 (GAL-UBI(M)-ARX1-GFP) were made by three parts ligation of (1) PCR amplification of ARX1 from wild-type yeast genomic DNA with primers AJO876 (CTGTCGACGCTCTAGCTATCTCCCACGA) and AJO564 (5'-GCGCCCGGGCTTAATTAACATTTTCATGGTTTCTTCAACTC), (2) SstI and SalI digested fragment of pAJ1479 (GAL-UBI; Dong, 2004 12), and (3) SstI and PacI digested vector of pAJ1025 (ARX1-GFP). pAJ1481 (GAL-UBI(M)-ARX1-13MYC) was made by SstI and PacI digestion of pAJ1480 and

cloned into same sites of pAJ1026 (ARX1-13myc). pAJ1483 (GAL-UBI(R)-ARX1-GFP) was made by three parts ligation of (1) PacI and SstI digested fragment of pAJ1025 (vector), (2) SstI and SalI digested fragment of pAJ1482 (GAL-UBI) and (3) SalI and PacI digested fragment of pAJ1481 (ARX1). pAJ1484 was made from three parts ligation similarly as pAJ1483 except using pAJ1026 (ARX1-13myc) as vector. pAJ1454 (pGAD C-1 ARX1) was made from PCR amplification of ARX1 from wild-type yeast genomic DNA with primers AJO784 (5'-CTGTCTAGAGGATCCATGGCTCTAGCTATCTCCCA) and AJO785 (GCGAAGCTTGGATCCCTACATTTTCATGGTTTCTTCAACTCCG). PCR products were then purified and digested with BamHI and cloned into same site of pAJ553 (pGAD C-1).

Table 2.4 Yeast strains used in Chapter 5.

Strains		Genotype	Reference
AJY951	MATa	*ade2 ade3 his3 leu2 trp1 ura3gal4Δ gal80ΔLYS2::GAL1-HIS3 GAL2-ADE2 met::GAL7-lacZ*	(James, 1996)
AJY1608	MATα	*hsi3 leu2 ura3 nup120Δ::KanMX4*	J. Hedges
AJY1901	MATa	*his3Δ1 leu2Δ0 ura3Δ0 arx1Δ::KanMX4*	Section 2.1.1
AJY1911	MATa	*his3Δ1 leu2Δ0 ura3Δ0*	Section 2.1.1
AJY1912	MATa	*ade2 ade3 leu2 lys52-801 ura3-52 arx1Δ::KanMX4*	This section
AJY1930	MATa	*his3Δ1 leu2Δ0 ura3Δ0 nup84Δ::KanMX4*	Z. Li
AJY1931	MATa	*his3Δ1 leu2Δ0 ura3Δ0 nup133Δ::KanMX4*	Z. Li
AJY1990	MATα	*his3 leu2 lys2 trp1 ura3 nup82Δ::HIS3+pNup82-Δ108 URA3*	M. Horwitz
AJY1994	MATa	*ade2 ade3 leu2 lys1 his3 nsp1-10A::URA3*	E. Hurt
AJY1995	MATa	*ade2 ura3 leu2 trp1 nic96Δ::HIS3+pUN100-nic96-1 LEU2*	E. Hurt
AJY2110	MATa	*his3 Δ1 leu2Δ0 ura3Δ0 lys2Δ0 nmd3Δ::KanMX4*	A. Johnson
AJY2470	MATa	*his3Δ1 leu2Δ0 ura3Δ0 nup42Δ::KanMX4*	Z. Li
AJY2471	MATa	*his3Δ1 leu2Δ0 ura3Δ0 nup100Δ::KanMX4*	Z. Li
AJY2601	MATα	*his3Δ1 leu2Δ0 ura3Δ0 arx1Δ::NatMX4*	X. Lou

Table 2.5 Plasmids used in Chapter 5.

Plasmid	Relevant markers	Reference
pAJ538	*LEU2 CEN Nmd3-13myc*	(Hedges, 2005)
pAJ582	*LEU2 CEN Nmd3-GFP*	(Hedges, 2005)
pAJ739	*URA3 CEN Crm1(T539C)-HA*	K. Weis
pAJ751	*LEU2 CEN NMD3AA-13MYC*	J. Hedges
pAJ752	*LEU2 CEN NMD3AAA-13MYC*	J. Hedges
pAJ866	*URA3 2μ pGBDU-C1*	C. Chan
pAJ908	*URA3 CEN RPL25-eGFP*	(Kallstrom, 2003)
pAJ1029	*ADE3 URA3 ARX1*	This section
pAJ1480	*LEU2 CEN GAL-UBI(M)-ARX1-GFP*	This section
pAJ1481	*LEU2 CEN GAL-UBI(M)-ARX1-13MYC*	This section
pAJ1483	*LEU2 CEN GAL-UBI(R)-ARX1-GFP*	This section
pAJ1484	*LEU2 CEN GAL-UBI(R)-1RX1-13MYC*	This section
pAJ1454	*URA3 2μ pGADC-1 ARX1*	This section
pAJ1593	*LEU2 CEN NMD3-L505A-13MYC*	(Hedges, 2006)
pAJ1594	*LEU2 CEN NMD3-SupraNES-13MYC*	(West, 2007)
pAJ2251	*TRP1 2μ pGBKT7*	(Patel, 2007)
pAJ2252	*TRP1 2μ pGBKT7 NUP116 (165-716)*	(Patel, 2007)
pAJ2253	*LEU2 2μ pGADT7*	(Patel, 2007)
pAJ2254	*LEU2 2μ pGADT7 NUP116 (165-456)*	(Patel, 2007)
pAJ2255	*LEU2 2μ pGADT7 NUP100 (1-588)*	(Patel, 2007)
pAJ2256	*LEU2 2μ pGADT7 NUP57 (1-255)*	(Patel, 2007)
pAJ2257	*LEU2 2μ pGADT7 Nsp1 (1-591)*	(Patel, 2007)
pAJ2258	*LEU2 2μ pGADT7 NUP159 (441-876)*	(Patel, 2007)
pAJ2259	*LEU2 2μ pGADT7 NUP42 (1-364)*	(Patel, 2007)

2.3.2 Synthetic lethal screen for *arx1Δ*

The synthetic lethal screen was adopted from a protocol used previously by (Johnson, 1995). UV mutagenesis experiment was carried out with strain AJY1912 carrying pAJ1029. Cells were grown in Ura- dropout medium to early stationary phase, pelleted, washed with ddH$_2$O and resuspended in ddH$_2$O at approximately 3x107 cells per ml. Cells were then sonicated briefly to avoid aggregation and placed in a plastic weigh boat and exposed for various times to UV radiation in a UV stratalinker oven (Stratagene). A 12seconds exposure resulted in 85% killing. Cells were diluted in H$_2$O and plated onto YPD plates to give approximate 300 colonies per plate. Plates were wrapped with foil and incubated at 30℃ for 5-7 days. Overall, about 34,300 colonies were screened and 490 potential solid red synthetic lethal mutants were identified. All candidate mutants were restreaked onto YPD plates to confirm their solid phenotype (24 mutants) and tested for 5-FOA sensitivity (11 mutants). These 11 mutants were then transformed with an *ARX1-LEU* plasmid to confirm their dependence on *ARX1* (4 mutants). All four mutants were mated to an *ade2 ade3 arx1Δ* mutant of the opposite mating type and were determined as recessive mutants. Diploid were sporulated and the resulting tetrads were dissected onto YPD to score for sectoring. All four mutants showed 2:2 segregation for white:solid red (indicative of single locus mutation) were picked for cloning of wild-type genes. A *LEU2* centromeric yeast genomic library was transformed into each mutant strain and plated onto Leu dropout low-adenine plates and scored for sectoring. Potential complementing clones were identified by sectored phenotype and were restreaked on the same medium plates and on 5-FOA plates to confirm their resistance of loss of the *ARX1* plasmid. Plasmids from complementing clones were

extracted and re-transformed into *E. Coli* for amplification and back to yeast to confirm their sectored phenotype. Clones containing *ARX1* were eliminated by restriction digestion. Clones that contain other library DNA fragments were submitted for sequencing using primers AJO194 (5'-GCTACTTGGAGCCACTATCGACTAC) and AJO195 (5'-CAGCAACCGCACCTGTGG), specific to the plasmid vector-genomic DNA insert junction. Among these four mutants: SYL89, SYL118, SYL348 and SYL373, two of them (SYL118 and SYL348) were identified successfully.

2.3.3 Genetic interactions between *ARX1* and nucleoporins

Selective nucleoporin mutants were selected to test for genetic interaction with an *arx1Δ* mutant. These mutants, including AJY1608 (*nup120Δ::KanMX4*), AJY1930 (*nup84Δ::KanMX4*), AJY1931 (*nup133Δ::KanMX4*), AJY1990 (*nup82Δ::HIS3+pNup82-Δ108*), AJY1994 (*nsp1-10A::URA3*), AJY1995 (*nic96Δ::HIS3+pUN100-nic96-1 LEU2*), AJY2470 (*nup42Δ::KanMX4*) and AJY2471 (*nup100Δ::KanMX4*) were crossed to *arx1Δ* strains AJY1901 (*arx1Δ::KanMX4*) or AJY2601 (*arx1Δ::NatMX4*). Diploids were selected in drop out media with corresponding marker in the presence of G418 or Clonat. The resultant diploid were sporulated, dissected to isolate spore clones and genotyped by appropriate markers.

2.3.4 Yeast two-hybrid analysis

To test for Arx1p interaction with nucleoporins, plasmids expressing Arx1p (pAJ1454 *URA3 2μ pGADC-1 ARX1*) and Nup116 (pAJ2252 *TRP1 2μ pGBKT7 NUP116*) fused to the GAL4 DNA binding domain (BD) and several nucleoporin fragments fused to

the GAL4 activating domain (AD) (pAJ2253-pAJ2259 *LEU2*, refer to table 2.5 for detailed information) were co-transformed into the reporter strain AJY951 with different combinations. Leu$^+$ Trp$^+$ or Leu$^+$ Ura$^+$ transformants were first selected on double dropout plates and then spotted onto ura$^-$ trp$^-$ his$^-$ or leu$^-$ trp$^-$ his$^-$ triple-dropout medium supplemented with various concentration of 3-AT (0, 2.5, 7.5 and 10mM). Plates were incubated at 30 ℃ for 4 days. Positive interactions were recognized by colony growth on plates.

2.3.5 *In vivo* microscopy

For GFP fluorescence microscopy shown in Figure 5.3, overnight cultures of strain AJY1911 (*WT*) carrying pAJ1480 (*LEU2 CEN GAL-UBI(M)-ARX1-GFP*) or pAJ1483(*LEU2 CEN GAL-UBI(R)-ARX1-GFP*) from 1% galactose containing dropout media were diluted into fresh medium and cultured to an optical density at 600 nm of 0.1 to ~ 0.2. Cultures were then transferred to 2% glucose containing fresh media to suppress Arx1p expression. Cells were collected at various time points after shifting to glucose media and fixed with formaldehyde (3.7% final concentration) and prepared as described in 2.2.5 for *in vivo* microscopy.

For GFP fluorescence microscopy shown in Figure 5.4, overnight cultures of strain SYL118 carrying pAJ908 (Rpl25-eGFP) or pAJ755 (Nmd3-GFP) from 1% galactose containing dropout media were diluted into fresh medium and cultured to an optical density at 600 nm of 0.1 to ~ 0.2. Cultures were then transferred to 2% glucose containing fresh media to suppress Arx1p expression. Cells were collected at various time points after shifting to glucose media and fixed with formaldehyde (3.7% final concentration) and prepared as described in 2.2.5 for *in vivo* microscopy.

For GFP fluorescence microscopy shown in Figure 5.6, overnight cultures of strain AJY1911 (*WT*), SYL348 and AJY2110 (*nmd3Δ*) carrying pAJ908 (Rpl25-eGFP) were diluted into fresh medium to an optical density at 600 nm of 0.1 to ~ 0.2 and cultured at room temperature to mid-log phase. Cultures were fixed with formaldehyde (3.7% final concentration) and prepared as described in 2.2.5 for *in vivo* microscopy.

For GFP fluorescence microscopy shown in Figure 5.7, overnight cultures of strain AJY1911 (*WT*) and AJY1901 (*arx1Δ*) carrying pAJ582 (Nmd3-eGFP) were diluted into fresh medium to an optical density at 600 nm of 0.1 to ~ 0.2 and cultured at room temperature to mid-log phase. Cultures were fixed with formaldehyde (3.7% final concentration) and prepared as described in 2.2.5 for *in vivo* microscopy.

2.3.6 Western blotting for the expression of *UBI-ARX1* constructs

For the Western blot shown in Figure 5.3, 5ml overnight cultures of strain AJY1911 (*WT*) carrying pAJ1481 (*LEU2 CEN GAL-UBI(M)-ARX1-13MYC*) or pAJ1484 (*LEU2 CEN GAL-UBI(R)-ARX1-13MYC*) from 1% galactose containing dropout media were diluted into fresh medium and cultured to an optical density at 600 nm of 0.1 to ~ 0.2. Cultures were then transferred to 2% glucose containing fresh media to suppress Arx1p expression. Cells were collected at various time points after shifting to glucose media. Subsequent procedures were performed as described in 2.1.3.

2.3.7 Indirect immunofluorescence microscopy

For IF shown in Figure 5.6, overnight cultures strain AJY1911 (WT) and SYL348 were diluted into fresh medium to an optical density at 600 nm of 0.1 to ~

0.2 and cultured at room temperature to mid-log phase. Subsequent procedures were carried out as described in 2.1.5.

2.3.8 Sucrose gradient sedimentation

For polysome analysis and sucrose density gradients in Figures 5.7 and 5.8, 2 ml overnight cultures of yeast strains AJY1911 (WT) and AJY1901 (*arx1Δ*) (carrying pAJ739 (Crm1T539C-HA) for Figure 5.8) were diluted to OD_{600} ~0.1 into 150 ml of fresh yeast extract-peptone medium and incubated at room temperatures. When cultures reached OD_{600} ~0.4, Cycloheximide (150μg/ml final concentration) was then added to each culture followed by one minute incubation. All other steps were carried out as described in 2.1.2. For Figure 5.7, SDS-PAGE analysis and Western blotting was carried out as described in 2.1.3 using antibodies specific to Nmd3p and Rpl8. For Figure 5.8, SDS-PAGE analysis and Western blotting was carried out as described in 2.1.3 using antibodies specific to HA and Rpl8.

2.3.9 Immunoprecipitations

For the immunoprecipitations shown in Figure 5.8, 2ml overnight cultures of strain AJY1911 (WT) and AJY1901 (*arx1Δ*) harboring pAJ538 (Nmd3-13myc) or pAJ1594 (Nmd3-supra-NES-13myc) were diluted to 200mL of fresh drop-out medium and cultured at 25°C to OD_{600}~0.4. Cells were harvested by centrifugation and stored at –80°C until use. Immunoprecipitation were carried out as described in 2.1.7. And samples were run on a 8% gel and Western blotting carried out as described in 2.1.3 with α-HA or α-Rpl8 antibodies.

Chapter 3: Functional characterization of Arx1p and its recycling factor, Rei1p, at the polypeptide exit tunnel

3.1 Introduction

The work presented in this chapter originated from our characterization of the late pre-60S particles. To identify additional factors that act on the subunit at this stage of its maturation, our lab purified the Nmd3p-60S complex (Kallstrom, 2003). Nmd3p is a shuttling protein that acts as an export adaptor recruiting Crm1p to the pre-60S subunit. Nmd3p-ssociated 60S subunits represent not only the pool of nuclear "export competent" pre-60S particles, but also a substantial amount of cytoplasmic 60S subunits that require further maturation before translation. Several such factors identified from this complex were subjected to further analysis for their potential functions in conjunction with Nmd3p. To understand 60S subunit biogenesis in greater depth, I decided to characterize another shuttling factor encoded by *YDR101c* (now known as *ARX1*). Here, I demonstrate that the recycling of Arx1p to the nucleus requires the zinc finger protein Rei1p. I also provide evidence that Arx1p binds to the ribosome near the polypeptide exit tunnel where it may affect the binding of other factors that act on the nascent polypeptide chain. Most of the work shown in this chapter was published in Molecular and Cellular Biology vol.26 p.3718-3727 2006 (Hung, 2006).

3.2 Background

A combination of techniques has been applied to comprehensively identify the factors required for biogenesis of the ribosomal subunits. More than ~170 transacting factors have been identified that in participate in the complex events for

both the 40S and 60S subunit biogenesis, including nuclear rRNA transcription, endo-, exoribonuclease cleavages, rRNA modification and remodeling, nuclear export and cytoplasmic maturation (Fromont-Racine, 2003)(Kressler, 1999)(Venema, 1995). While the majority of these factors are devoted to nuclear processing events, a small number of late 60S subunit biogenesis factors center around the 60S subunit export and downstream cytoplasmic maturation.

For the large subunit, the trans-acting that remain associated with nascent 60S subunits upon translocation into the cytoplasm include the export adapter Nmd3p (Ho, 2000), Tif6p (Nissan, 2002), Arx1p (encoded by *YDR101c*) (Nissan, 2002), Alb1p (Lebreton, 2006) and Rlp24p (Saveanu, 2003). As none of these proteins remains associated with subunits during translation, they are removed prior to subunit joining and must be recycled to the nucleus for subsequent rounds of export. For example, recycling of the export adapter Nmd3p requires the essential cytoplasmic GTPase Lsg1p, which may sense the correct assembly of Rpl10p into the subunit (Hedges, 2005). In addition, Tif6p has been shown to act as an anti-association factor for the ribosome and must be removed by Ria1p/Efl1p to activate the subunit for translation competence (Basu, 2001)(Senger, 2001). Rlp24p belongs to the archaeal eukaryotic Rpl24e family of ribosomal proteins and is highly related to the yeast cytoplasmic ribosomal protein Rpl24p. Loading of Rlp24p onto the 60S subunit occurs in the nucleolus and has been thought to tie into early rRNA processing (Saveanu, 2003). While Rlp24p is essential, deletion of its cytoplasmic counterpart Rpl24p has little effect on cell growth rate. Meanwhile, Rpl24p is likely to associate with the 60S subunits only after they enter the cytoplasm (Kruiswijk, 1978). Although how Rlp24p recycles is not known yet, it has been highly speculated that Rlp24p and

Rpl24p bind to the same site on the ribosome. Consequently, Rlp24p must be replaced to allow Rpl24p to bind.

More recently and just at about the same time as data present in this chapter was published, the work by Lebreton *et al.* further established a late 60S subunit biogenesis network, including recycling of Arx1p and Alb1p from the cytoplasm and the involvement of its cytoplasmic release factor, Rei1p (Lebreton, 2006). However, they reported that Arx1p can form a small complex with Alb1p in the cytoplasm in the 60S subunit unbound state. This result is inconsistent with my observation and the discrepancy will be discussed in Chapter 3.4.

3.3 Results

3.3.1 Characterization of Arx1p as a novel 60S subunit biogenesis factor

Our laboratory previously identified Arx1p as a factor associated with the Nmd3-60S particle. BLAST search and sequence alignment revealed that Arx1p is related to methionine aminopeptidases (MetAP2) (Figure 3.1). This class of enzyme is responsible for removal of the N-terminal methionine co-translationally; an activity that is important for subsequent protein function (Giglione, 2004)(Bradshaw, 1998). However, several of the residues required for the enzymatic activity of this class of peptidase are not conserved in Arx1p, suggesting that it is not catalytically active.
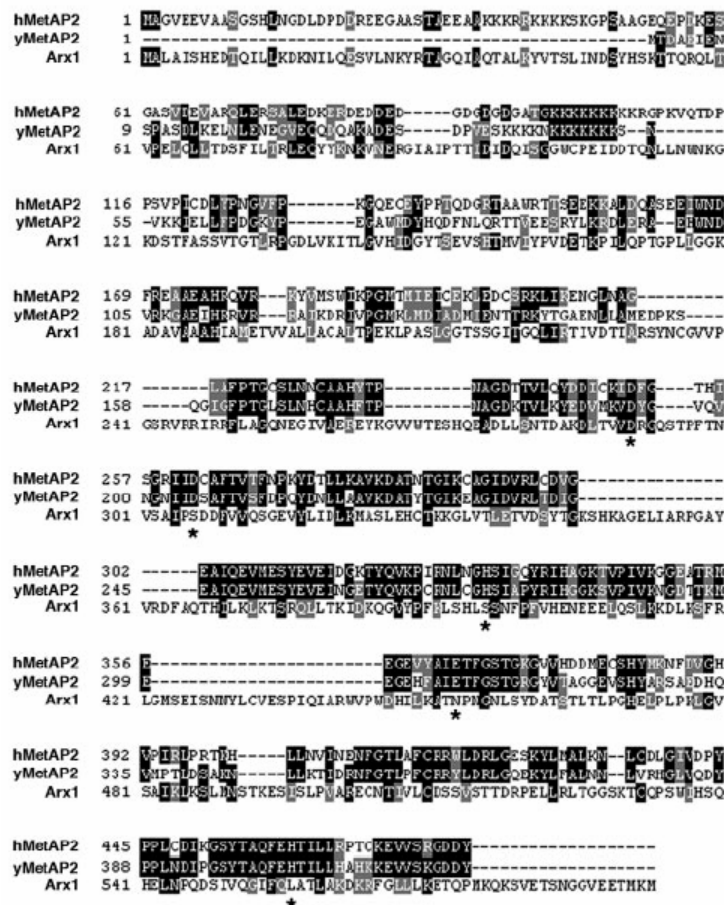
Figure 3.1 Sequence alignments of Arx1p and MetAP2.

Sequences of MetAP2 (yeast yMetAP2 and human hMetAP2) and Arx1p were aligned using ClustalW1.8 (http://searchlauncher.bcm.tmc.edu/). Black and grey blocks indicate identical residues in at least two sequences and similar residues, respectively. Asterisks point out residues responsible for MetAP2 enzymatic activity. The insertions within the Arx1 sequence are characteristic of the Arx1p protein family and are predicted to lie predominately on one face of the protein based on threading the Arx1p sequence onto the structure of MetAP.

To confirm Arx1p's association with 60S subunits, I first examined if it co-sedimentated with 60S subunit by sucrose gradient sedimentation. To determine Arx1p's behavior within the cells, I introduced epitope tags (3HA or GFP) in frame to the C-terminus of *ARX1* in the genomic locus. As seen in Figure 3.2A, Arx1p predominately cosedimented with free 60S subunits, consistent with previously published results (Nissan, 2002). In addition, its association with 60S subunits was also demonstrated by co-immunoprecipitation (data not shown), substantiating its specific binding to 60S subunits.

Because Nmd3p is a shuttling protein, 60S subunits that are co-purified with Nmd3p represent a mixture of nuclear and cytoplasmic particles. To relate Arx1p's residence on specific species of 60S subunits, it is important to determine its cellular localization. For this reason, Arx1-GFP cells were subjected to fluorescence microscopy. As seen in Figure 3.2B, genomically expressed Arx1-GFP is predominately nuclear or nucleolar with faint cytoplasmic signal. This finding is consistent with the genome-wide yeast protein localization analysis (Huh, 2003) and work by Nissan *et al* (Nissan, 2002).
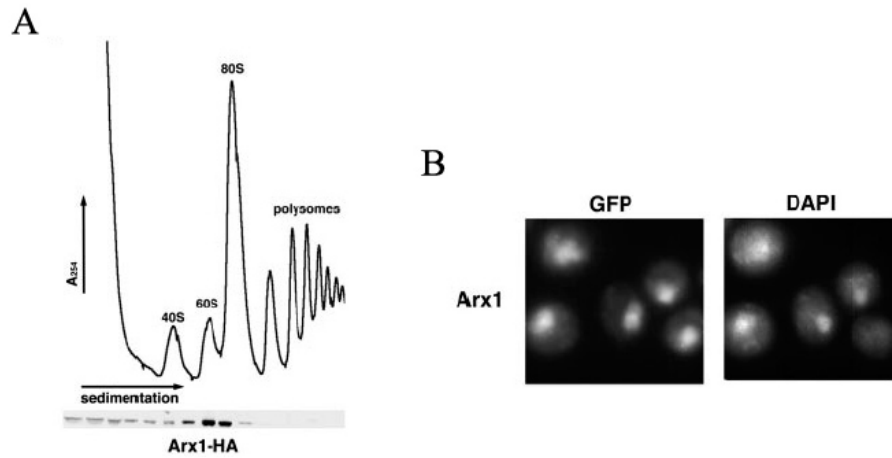
Figure 3.2 Sucrose gradient sedimentation and cellular localization of Arx1p

(A) Lysates were prepared from AJY1905 (*ARX1-3HA*) in the presence of cycloheximide (50 μg/ml) and fractioned on 7% to 47% sucrose gradients by ultracentrifugation (refer to Chapter 2.1.2 for buffer condition). Fractions were collected, and the absorbance at 254 nm was monitored continuously. Proteins were precipitated with trichloroacetic acid, separated by SDS-polyacrylamide gel electrophoresis, transferred to nitrocellulose membrane, and immunoblotted for HA (Covance) visualization of Arx1p. (B) Culture of AJY1909 (*ARX1-GFP*) was grown to mid-log phase and the in vivo localizations of Arx1-GFP were monitored by fluorescence microscopy. DAPI staining was used to identify the position of nuclei.

To relate Arx1p's function to 60S subunit biogenesis, I next asked if deletion of *ARX1* impaired 60S subunit levels in the cells. Cell extracts from wild type and *arx1Δ* strains were prepared and subjected to sucrose gradient velocity sedimentation in the presence of cycloheximide (an inhibitor of translation elongation in eukaryotic organisms). By using cycloheximide, translating ribosomes can be trapped on mRNAs, and populations of various ribosome species, including 40S, 60S, 80S and polysomes containing multiple translating 80S ribosomes bound by mRNAs, can be monitored by absorbance at A_{254} as sucrose gradients are fractionated (refer to Chapter 2.1.2 for detailed information). Wild type cells usually give a profile in which a smaller 40S peak is followed by a higher 60S peak. However, several 60S subunit associated defects can be observed in the *arx1Δ* strain (Figure 3.3A). Particularly, *arx1Δ* showed a moderate reduction in the free 60S peak and the appearance of half-mers. Half-mer peaks are indicative of the presence of pre-initiation 48S complexes on mRNAs awaiting 60S subunit joining. The lower free 60S peak and the formation of half-mers are classic index of 60S subunit biogenesis defects seen in many previously characterized mutants.

To examine the *arx1Δ* mutant associated-60S subunit export defect, a reporter plasmid carrying Rpl25-eGFP was introduced into wild type and an *arx1Δ* strains. Rpl25p is a ribosomal protein that assembles into pre-60S particles in the nucleolus by direct binding to rRNA on the pre-60S particle. This reporter plasmid has been widely used to monitor 60S subunit export (Hurt, 1999)(Gadal, 2001)(Ho, 2000). In wild type cells, Rpl25-eGFP signal was ubiquitously distributed throughout the cytoplasm, indicating that high levels of ribosomes are engaged into translation pool. Conversely, a nuclear retention of Rpl25-eGFP was observed in an *arx1Δ* strain, suggesting a block of 60S subunit export from the nucleus (Figure 3.3B). Considering

that Arx1p accompanies 60S subunit export out of the nucleus, the nuclear export defect of an *arx1Δ* strain likely reflects a direct function of Arx1p in facilitating 60S subunit export. (Arx1p's function in supporting 60S subunit export will be discussed in Chapter 5). Together, these data suggested that Arx1p is a 60S subunit biogenesis factor.
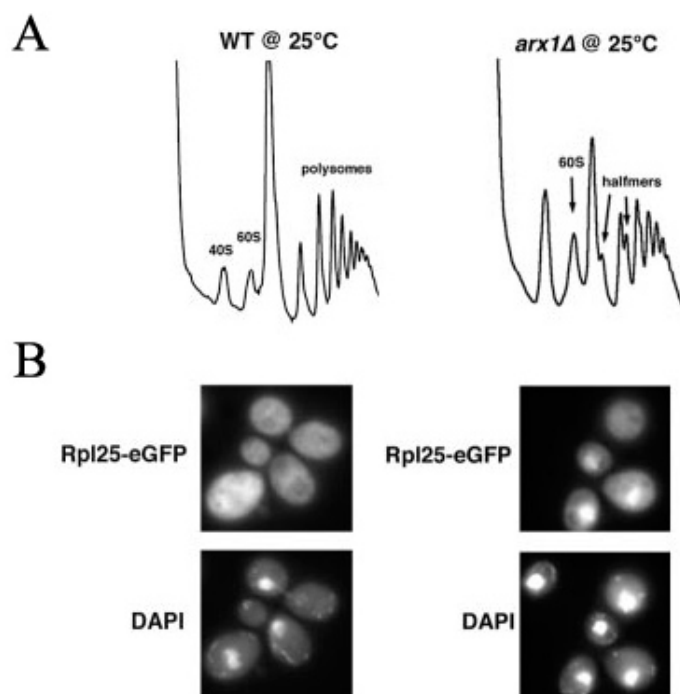
Figure 3.3 Deletion of ARX1 affect 60S subunit levels and export.

(A) Cell extracts, prepared from mid-log-phase cultures of strain AJY1911 wild type (WT)) and AJY1901 (*arx1Δ*) grown at 25°C, were fractionated by sucrose gradient sedimentation as described in the legend to Figure 3.2. (B) Cultures of AJY1911 (WT) and AJY1901 (*arx1Δ*) carrying plasmid pAJ908 (*RPL25-eGFP*) were incubated at 25°C, and the in vivo localization of Rpl25-eGFP was monitored by fluorescence microscopy.

3.3.2 Interplay of *ARX1* and *REI1*

Identification of Arx1p as a novel 60S subunit biogenesis factor inspired us to further characterize its interplay with additional players in the same metabolic pathway. Considering that Arx1p was identified from the Nmd3p-associated 60S subunit complex, it is likely that Arx1p interacts with other factors residing in the same complex. As a first attempt to characterize its functional involvement with other players, an *arx1Δ* mutant was crossed to a collection of mutants to test for genetic interaction. From this, we found that deletion of *ARX1* suppressed the cold sensitivity of *rei1Δ* cells (Hung and Johnson).

Rei1p, encoded by *YBR267w*, also co-purified with the Nmd3p-60S subunit complex (Kallstrom, 2003). Sequence alignment revealed that Rei1p is a C_2H_2 zinc finger protein that has been implicated in the mitotic signaling network (Iwase, 2004). Similar to *ARX1*, *REI1* is also dispensable; however, deletion of *REI1* displayed severe cold sensitivity (Figure 3.4A). Interestingly, the growth defect can be suppressed by raising temperature and is fully rescued to a wild type level at 37 ℃

(Figure 3.4A, compare growth at 25℃ and at 37℃). Strikingly, the cold sensitivity of a *rei1Δ* mutant can also be suppressed by an additional deletion of *ARX1* (Figure 3.4A, compare *rei1Δ* with *arx1Δ rei1Δ*). I next asked if the suppression of cold sensitivity of a *rei1Δ* mutant by deletion of *ARX1* would result in rescued 60S subunit levels. Extracts from wild type, *rei1Δ* and *arx1Δrei1Δ* strains were subjected to sucrose gradient sedimentation. Indeed, the free 60S and polysome peaks were largely rescued in the *arx1Δrei1Δ* strain (Figure 3.4B). Thus the improved polysome profile may reflect the suppression of growth seen in the *arx1Δrei1Δ* strain.
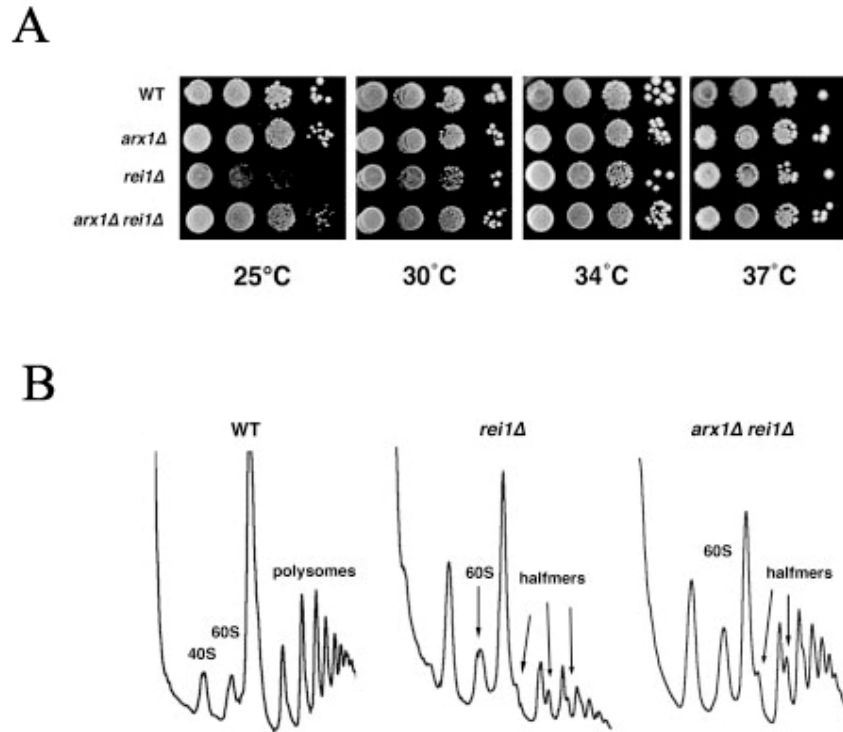
Figure 3.4 Deletion of *ARX1* suppresses the cold sensitivity of a *rei1Δ* mutant

(A) Tenfold serial dilutions of saturated cultures were spotted onto yeast extract-peptone-glucose plates and incubated for 3 days at the indicated temperatures. The strains used were the following: AJY1905 (wild-type (WT) *ARX1-HA*), AJY1901 (*arx1Δ*), AJY1907 (*rei1Δ ARX1-HA*), AJY1903 (*arx1 Δrei1Δ*) (B) Extracts were prepared from mid-log-phase cultures of strains AJY1911 (WT), AJY1907 (*rei1Δ*) and AJY1903 (*arx1Δ rei1Δ*) at room temperature (25°C) and fractionated by sucrose gradient sedimentation as described in the legend to Figure. 3.2.

Taking into consideration that *REI1* genetically interacts with *ARX1* and that Rei1p is found in the same Nmd3p-60S subunit complex, I next examined its possible involvement in 60S subunit biogenesis by monitoring its binding to 60S subunits and its impact on 60S subunit levels and export. To keep track of cellular behavior of Rei1p, I introduced 13MYC tag in frame to the C-terminus of *REI1* at its genomic locus and also made a functional plasmid carrying Rei1-GFP. Sucrose gradient sedimentation analysis using cells expressing Rei1-13myc revealed that Rei1p predominately sedimented with the 60S peak, similar to Arx1p (Figure 3.5A). As deletion of *REI1* gave a cold-sensitive phenotype, I decided to examine polysome profiles of *rei1Δ* cells at different temperature. As seen in Figure 3.5B, at low temperature, *rei1Δ* cells displayed several signs of 60S subunit biogenesis defects, including a very small free 60S peak, the appearance of large half-mers and poor polysomes. However, these defects could be corrected by raising temperature (compare 25℃ to 37℃). In addition, deletion of *REI1* impaired 60S subunit export and this effect was also temperature-dependent (Figure 3.5C). While Rpl25-eGFP is trapped in the nucleus at low temperature, the effect is rescued at higher temperatures (compare 25℃ to 30℃ and 37℃). The degree of suppression of 60S biogenesis and 60S subunit export by increasing temperature corresponded to its improved growth rate (Figure 3.4), suggesting that the primary role of Rei1p is a 60S subunit biogenesis factor.
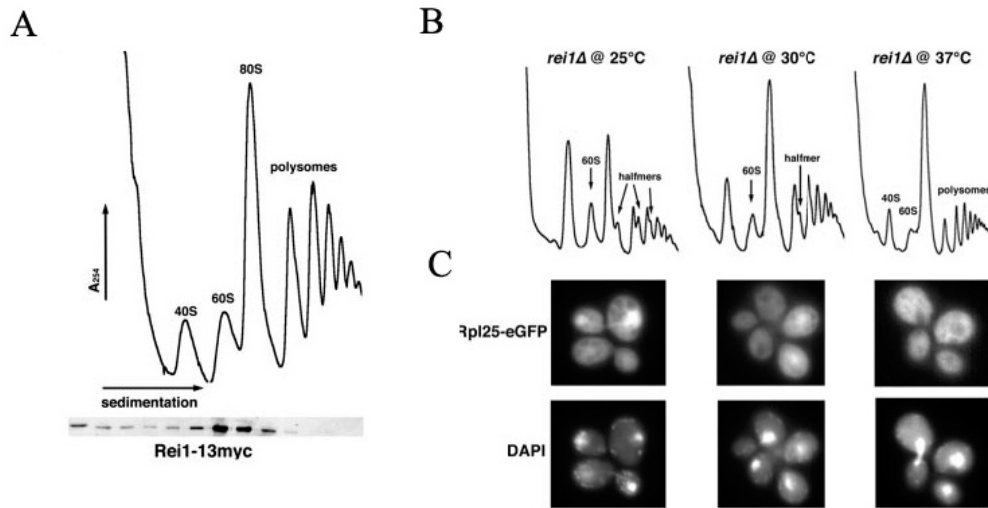
Figure 3.5 Sucrose gradient sedimentation of Rei1p and its impact on 60S subunit biogenesis

(A) Lysates were prepared from AJY1910 (*REI1-13myc*) in the presence of cycloheximide (50 µg/ml) and fractioned on 7% to 47% sucrose gradients by ultracentrifugation. Buffer conditions were as described in Chapter 2.1.2. Western blotting of Rei1p using anti-myc antibodies (Covance) was performed similarly as described in Figure 3.3. (B) Extracts from strain AJY1902 (*rei1Δ*) grown at the temperatures indicated were fractionated by sucrose gradient sedimentation as described in the legend to Figure. 3.2. (C) Strain AJY1902 (*rei1Δ*) carrying plasmid pAJ908 (*RPL25-eGFP*) was incubated at the indicated temperatures, and the *in vivo* localization of Rpl25-eGFP was monitored by fluorescence microscopy.

3.3.3 Rei1p is a cytoplasmic protein but could interact with Arx1p transiently

While Arx1p and Rei1p were both found in Nmd3p-60S subunit complexes, they may load on to 60S subunit in different cellular compartments as Nmd3p co-purified with a mixture of nuclear/cytoplasmic 60S subunits. To address whether Rei1p resides in the same or different cellular compartments as Arx1p does, I monitored Rei1p localization using Rei1p-GFP. Unlike Arx1p, Rei1p-GFP was seen throughout the cell (Figure 3.6A). However, it was not possible to judge from the steady state localization of Rei1p whether or not the protein shuttles. I tested this by treating cells with Leptomycin B (LMB). LMB is an antibiotic that inhibits Crm1p-dependent nuclear export by binding to Crm1p and interfering with Crm1p-NES interaction ((Ossareh-Nazari, 1997)(Fukuda, 1997). Nuclear export of 60S subunits requires the export adaptor Nmd3p with its nuclear export signal that can be recognized by Crm1p (Ho, 2000). If Rei1p rides out of the nucleus on the pre-60S subunit, its export should also rely on Crm1p, and thus be sensitive to LMB. Rei1p-13myc was introduced into the LMB sensitive mutant strain (*CRM1T593C*). As a positive control, Nmd3p-13myc was introduced into the same yeast strain. After LMB treatment, a substantial amount of Nmd3p was enriched in the nucleus, consistent with its previously characterized function in nuclear shuttling (Ho, 2000). Conversely, Re1ip did not relocalize to the nucleus in the presence of LMB (Figure 3.6B), suggesting that Rei1p does not shuttle in a Crm1mp-dependent manner. Moreover, Rei1p remained in the cytoplasm in the presence of a dominant-negative Nmd3p mutant lacking its functional NES (data not shown) that leads to a block of 60S subunit export. These data suggested that the cellular localization of Rei1p did not rely on Crm1p or active nuclear export of 60S subunits.

Though Arx1p and Rei1p seemed to localize to different cellular

compartments, it was still possible that they may transiently reside on the same 60S subunit complex. Arx1p has been shown to bind to relatively mature pre-60S particles in the nucleolus and may be involved in nuclear export of 60S subunits (Nissan, 2002). On the other hand, the cytoplasmic protein Rei1p may bind to 60S subunits only when they are exported into the cytoplasm. Thus loading of Arx1p and Rei1p should be sequential and the interplay of Arx1p and Rei1p may take place shortly after 60S subunits reach the cytoplasm. To investigate this, I preformed a co-immunoprecipitation experiment to ask if Arx1p and Rei1p co-exist in the same complex. For this reason, I introduced Arx1p-3HA and Rei1p-13myc into cells and affinity purified complexes with antibodies against each tag. As seen in Figure 3.6C, Rei1-13myc could be found in the Arx1-3HA co-immunoprecipitated complex and vice versa. These results support the idea that Arx1p and Re1ip interact transiently on the same 60S subunit complex.
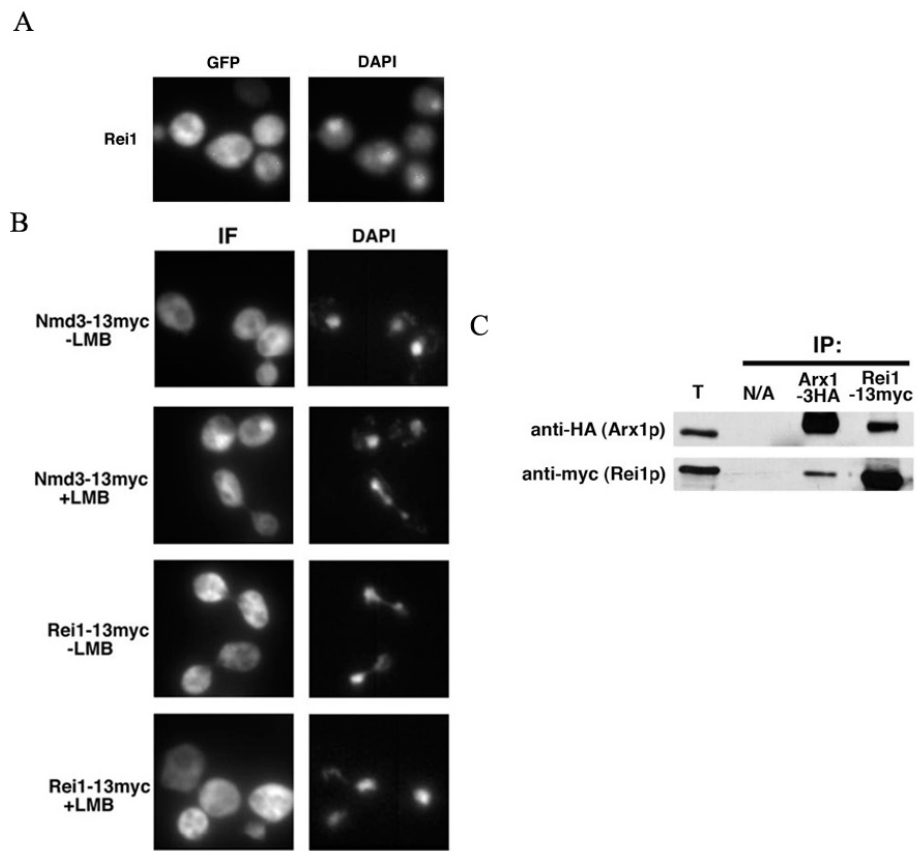
Figure 3.6 Rei1p is a cytoplasm protein but can be found in the Arx1p containing 60S particles

(A)　Strain AJY1902 (*rei1Δ*) harboring pAJ1017 (*REI1-GFP*) was grown to mid-log phase and the in vivo localizations of Rei1-GFP was monitored by fluorescence microscopy. DAPI staining was used to identify the position of nuclei. (B) To test if Rei1p shuttles in a Crm1-dependent fashion, the LMB-sensitive strain AJY1539 (*CRM1T539C*) carrying plasmid pAJ538 (*Nmd3-13myc*) or pAJ1018 (*REI1-13myc*) was cultured in selective media at room temperature. Cells were concentrated 20-fold in fresh media, LMB was added to a final concentration of 0.1 μg/ml, and cultures were incubated for 30 min. Cells were then fixed with 3.7% formaldehyde (final concentration) and subjected to indirect immunofluorescence microscopy (IF). (C) Extract from strain AJY1907 (*rei1Δ Arx1-HA*) with pAJ1018 (*REI1-13myc*) was incubated without addition of antibody (N/A) or with anti-HA or anti-myc antibody and protein A beads. Precipitated proteins were eluted from protein A beads in sample buffer and separated by SDS-polyacrylamide gel electrophoresis. Total protein extract (T) was included as a loading control for the immunoprecipitations (IP). Western blotting was performed against the HA or c-*myc* epitopes.

3.3.4 Nuclear recycling of Arx1p depends on Rei1p

The genetic interaction between *ARX1* and *REI1* suggested that Arx1p is toxic in the absence of Rei1p. Microscopy and co-immunoprecipitation work demonstrated that Arx1p binds to 60S subunits in the nucleus and accompanies them during nuclear export. Loading of Rei1p onto 60S subunits occurred shortly after Arx1p-containing 60S subunits arrive in the cytoplasm. One explanation for the interplay of Arx1p and Rei1p would be that loading of Rei1p releases Arx1p from the 60S subunits in the cytoplasm. To investigate this possibility, I examined the cellular localization of Arx1p in the *rei1Δ* strain by indirect immunofluorescence microscopy. As seen previously, Arx1p is predominately localized in the nucleus in wild type cells. However, the bulk of Arx1p relocalized to the cytoplasm in the absence of Rei1p (Figure 3.7A), suggesting that Rei1p is required for the proper cellular localization of Arx1p. Taking into account that deletion of *ARX1* rescued the growth defects of *rei1Δ* cells and that Rei1p is needed for nuclear localization of Arx1p, we speculated that the persistence of Arx1p on cytoplasmic 60S subunits is detrimental. For this reason, I decided to test if the bulk of cytoplasmic Arx1p remained bound to 60S subunits in the absence of Rei1p. Arx1p-HA was introduced into wild type and *rei1Δ* cells. Extracts were prepared and subjected to sucrose gradient sedimentation for monitoring co-sedimentation of Arx1p with 60S subunits. Indeed, Arx1p was found on the 60S peak in a *rei1Δ* strain as well as a wild type strain (Figure 3.7B). Thus nuclear recycling of Arx1p requires Rei1p and its failure of releasing from 60S subunits is problematic.
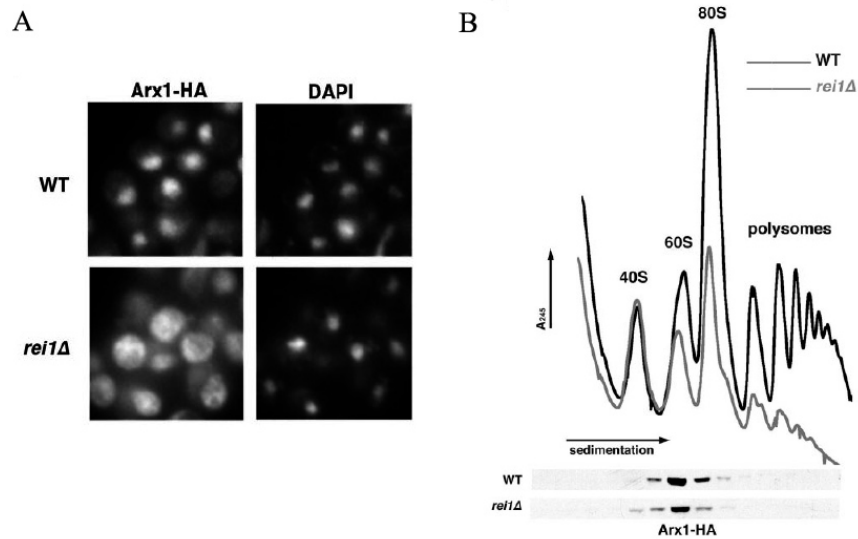
Figure 3.7 Cellular localization and sucrose gradient sedimentation of Arx1p in a
rei1Δ mutant

(A)   Cultures of strains AJY1905 (*ARX1-HA*) and AJY1907 (*rei1Δ ARX1-HA*)
were grown to mid-log phase at room temperature, and the localization of
Arx1-HA was monitored by indirect immunofluorescence microscopy as described
in Chapter 2. (B) Lysates were prepared in the presence of cycloheximide from
room-temperature cultures of strain AJY1907 (*rei1Δ ARX1-HA*) and fractioned on
sucrose gradients as described in the legend to Figure 3.2. Visualization of Arx1p
was carried out as described in Figure 3.2.

66

To test the idea that a failure to release Arx1p in a *rei1Δ* mutant is detrimental, I mutagenized Arx1p in the hope of identifying mutations that could suppress the growth defect of a *rei1Δ* mutant. PCR mutagenized plasmid borne Arx1p-GFP constructs were transformed into *arx1Δ rei1Δ* cells to identify suppressor mutants. Because deletion of *ARX1* suppresses a *rei1Δ* mutant, wild type Arx1p in the *arx1Δ rei1Δ* strain background renders a slow growth phenotype. Possible suppressor clones were identified by virtue of their better growth on plates. From the screen, one mutant, referred to as B6, in *rei1Δ* cells, was identified (Figure 3.8A). Whereas wild type Arx1p was found throughout the cytoplasm, the B6 mutant was predominately nuclear (Figure 3.8B). Thus the nuclear localization of the B6 mutant in *rei1Δ* cells resembled the normal Arx1p localization in wild type cells. This result supports the idea that the B6 mutant results from reduced Arx1p levels on cytoplasmic 60S subunits. Next, I assayed the ability of the B6 mutant to bind to 60S subunits by coimmunoprecipitation. While wild type Arx1p was able to co-purify with 60S subunits, the B6 mutant co-immunoprecipitated complex did not exhibit any detectable level for 60S subunits (Figure 3.8C). Sequence analysis of the B6 mutant revealed multiple mutations throughout the protein (refer to Chapter 2.1.8 for detailed information) and thus identification of any single residue or domain responsible for ribosome binding was not feasible. Nevertheless, these results suggested that a *rei1Δ* mutant can be suppressed by an Arx1p mutant that is defective for 60S subunits binding. Moreover, the nuclear accumulation of the B6 mutant also agreed with its potential role in bypassing the toxic effect resulting from the persistence of Arx1p on cytoplasmic 60S subunits.
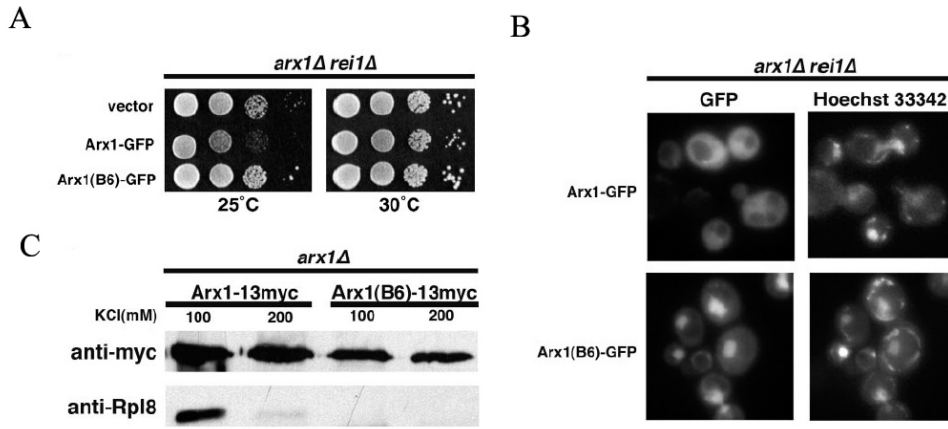
Figure 3.8 A *rei1Δ* mutant can be suppressed by an *arx1* mutant that exhibits reduced binding to 60S subunits.

(A) Tenfold serial dilution of saturated cultures were spotted onto Leu- dropout plates to select for the control or mutant *arx1* plasmid and incubated for 3 days at the indicated temperatures. The strains used were AJY1903 (*arx1Δ rei1Δ*) with empty vector (pRS416), Arx1-GFP (pAJ1015), and Arx1(B6)-GFP (pAJ1463). (B) Cultures from strain AJY1903 (*arx1Δ rei1Δ*) carrying Arx1-GFP (pAJ1015) or Arx1(B6)-GFP (pAJ1463) were grown to midlog phase. Cultures were incubated for a further 30 min in the presence of 4 μM Hoechst 33342 dye to stain nuclei before visualization by microscopy. (C) Cell extracts from strain AJY1901 (*arx1Δ*) carrying Arx1-13myc (pAJ1016) or Arx1(B6)-13myc (pAJ1464) plasmids were prepared and incubated with anti-myc antibodies and protein A beads. The immunoprecipitation was carried out as described in Figure 3.6 and Western blotting was performed against myc or Rpl8p as a marker for 60S subunits.

3.3.5 Interplay of *RPL25* with *ARX1* and *REI1*

The initial discovery of the involvement of Rpl25p in the *ARX1* and *REI1* pathway came from an unexpected genetic observation. As a means of analyzing 60S subunit export, the reporter Rpl25p-eGFP was introduced into a *rei1Δ* mutant (refer to section 3.3.2). Surprisingly, the Rpl25-eGFP plasmid could partially suppress the cold-sensitivity of a *rei1Δ* mutant (initial observation by J. Hedges, Figure 3.9A, *rei1Δ*+Rpl25-eGFP). The degree of suppression was even greater if Rpl25-eGFP was the only copy of Rpl25p in the cells (Figure3.9A, *rei1Δrpl25Δ*+Rpl25-eGFP). In agreement with the suppression of growth of a *rei1Δ* mutant, the addition of Rpl25-eGFP also rescued 60S subunits levels in *rei1Δ* cells, as monitored by polysome profile analysis (Figure 3.9B).

The cold sensitivity of a *rei1Δ* mutant was not suppressed by another 60S subunit export reporter, Rpl8-YFP, suggesting that this effect is only specific to C-terminally tagged Rpl25p. Moreover, the similar suppression effect was also observed by fusion of 13 tandem repeats of the c-myc epitope tag (~20kDa) but not a smaller 3HA epitope tag (~5kDa) to the C-terminus of Rpl25p (data not shown). Taken together, these results suggested that the suppression of the cold-sensitivity of a *rei1Δ* mutant was specific to a large fusion to the C-terminus of Rpl25. Notably, the suppression of a *rei1Δ* mutant by Rpl25-eGFP or by deletion of *ARX1* was similar (Figure 3.9A), suggesting that a large fusion to the C-terminus of Rpl25p has a common effect as that of the deletion of *ARX1* (Illustration 3.1).
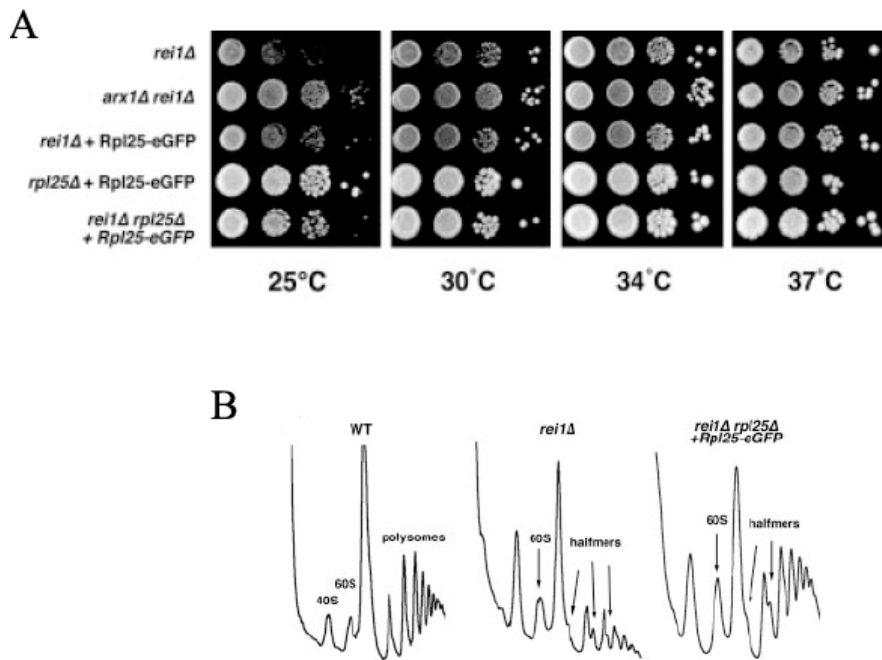
Figure 3.9   The fusion of *eGFP* to *RPL25* suppresses the cold sensitivity and 60S subunit deficiency of a *rei1Δ* mutant.

(A) Tenfold serial dilution of saturated cultures were spotted onto YPD plates and incubated for 3 days at the indicated temperatures. The strains used were the following: AJY1907 (*rei1Δ ARX1-HA*), AJY1903 (*arx1Δ rei1Δ*), AJY1907 (*rei1Δ ARX1-HA*) carrying plasmid pAJ908 (*RPL25-eGFP*), AJY1906 (*rpl25Δ ARX1-HA* pAJ908), and AJY1908 (*rei1Δ rpl25Δ ARX1-HA* pAJ908). (B) Extracts were prepared from mid-log-phase cultures of strains AJY1911 (WT), AJY1907 (*rei1Δ*) and AJY1908 (*rei1Δ rpl25Δ* Rpl25-eGFP) at room temperature (25°C) and fractionated by sucrose gradient sedimentation as described in the legend to Figure 3.2.

70
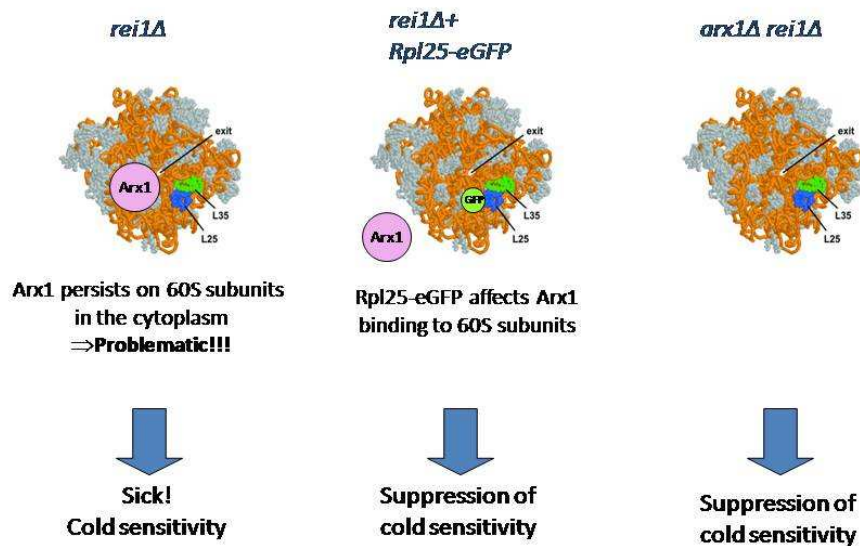
Illustration 3.1 Models for the suppression of the cold sensitivity of a *rei1Δ* mutant

The cold sensitivity of a *rei1Δ* mutant can be suppressed either by deletion of *ARX1* or the presence of Rpl25-eGFP. This common effect suggests that the persistence of Arx1p on the 60S subunit in a *rei1Δ* mutant is detrimental. The 60S subunit is shown from the view of the polypeptide exit tunnel (exit). The position of Rpl25p and its neighbor, Rpl35p, are shown in blue and green, respectively.

Because the cold sensitivity of a *rei1*Δ mutant can be suppressed by deletion of *ARX1* or an *arx1* mutant that is defective in 60S subunit binding, I suspected that large fusions to the Rpl25p interfere with Arx1p's binding to 60S subunits. To investigate this possibility, I examined Arx1p sedimentation in the presence of Rpl25-eGFP. While Arx1p co-sedimentated with free 60S subunits in wild type cells, it was largely absent from the 60S peak, and shifted to top of the gradients, in the presence of Rpl25-eGFP (Figure 3.10A), indicating a loss of 60S subunit binding. This assay was carried out under relatively high ionic conditions, in which the difference of Arx1p binding could be enhanced. At low ionic strength, Arx1p was still found to cosediment with 60S peak, suggesting that Rpl25-eGFP alters but does not completely block Arx1p's access to 60S subunits (data not shown).

For this reason, I then asked if Arx1p binding to 60S subunits could be altered by other ribosomal proteins in the close proximity of Rpl25p. According to the yeast ribosome Cryo-EM structures, six ribosomal proteins surround the polypeptide exit tunnel, including Rpl25p, Rpl35p, Rpl19p, Rpl26p, Rpl17p and Rpl31p (Beckmann, 2001). Among these, I tested if large fusions to the two closest neighbors of Rpl25p, namely Rpl35p and Rpl19p, affect Arx1p binding to 60S subunits. I first constructed Rpl19A-GFP Rpl19B-GFP and Rpl35A-GFP Rpl35-GFP expression strains as Rpl19p and Rpl35p are each encoded by two loci: A and B. The Rpl19A-GFP Rpl19B-GFP strain did not reveal any obvious slow-growth phenotype. On the other hand, GFP fusions to both Rpl35A and Rpl35 resulted in a severe growth defect and low 60S subunit levels. However, no nuclear retention of Rpl35-GFP was observed, thus the growth defects observed for the Rpl35A-GFP Rpl35-GFP strain may be a consequence of the failure in nuclear import of Rpl35p or the instability of cytoplasmic 60S subunits.

To test Arxp-60S subunit association in the presence of GFP fusions to either Rpl19p or Rpl35p, Arx1p-13myc was introduced into Rpl19A-GFP Rpl19B-GFP and Rpl35A-GFP Rpl35-GFP cells. Co-immunoprecipitated Arx1p complexes and Western blotting for Rpl8p showed that Rpl19A-GFP Rpl19B-GFP cells did not affect Arx1p association with 60S subunits (Figure 3.10C). Conversely, Arx1p-bound Rpl8p level was significantly reduced in the presence of Rpl35A-GFP Rpl35-GFP (Figure 3.10C). These findings suggested that Arx1p binds to 60S subunits in close proximity to Rpl25p and Rpl35p at the polypeptide exit tunnel.

Considering that GFP fusions to ribosomal proteins may impair their functions, as a severe growth defect was observed for Rpl35A-GFP Rpl35-GFP cells, the reduced Rpl8p level co-purified from the strain may simply reflect overall lower 60S subunit levels. To address this issue, I tested various trans-acting factors for their binding to 60S subunits in Rpl35A-GFP Rpl35-GFP cells. These factors, including Nmd3p, Lsg1p, Tif6p and Nog2p, have been shown to localize in different cellular compartments and thus participate in 60S subunit biogenesis at various steps (Basu, 2001)(Fromont-Racine, 2003)(Ho, 2000)(Kallstrom, 2003)(Milkereit, 2001). From the panel of factors tested, only Arx1p showed reduced binding to ribosomes when Rpl35Ap and Rpl35Bp carried GFP fusions (Figure 3.10D), indicating that the reduced Arx1p binding to 60S subunits was not an artifact of low 60S subunits.
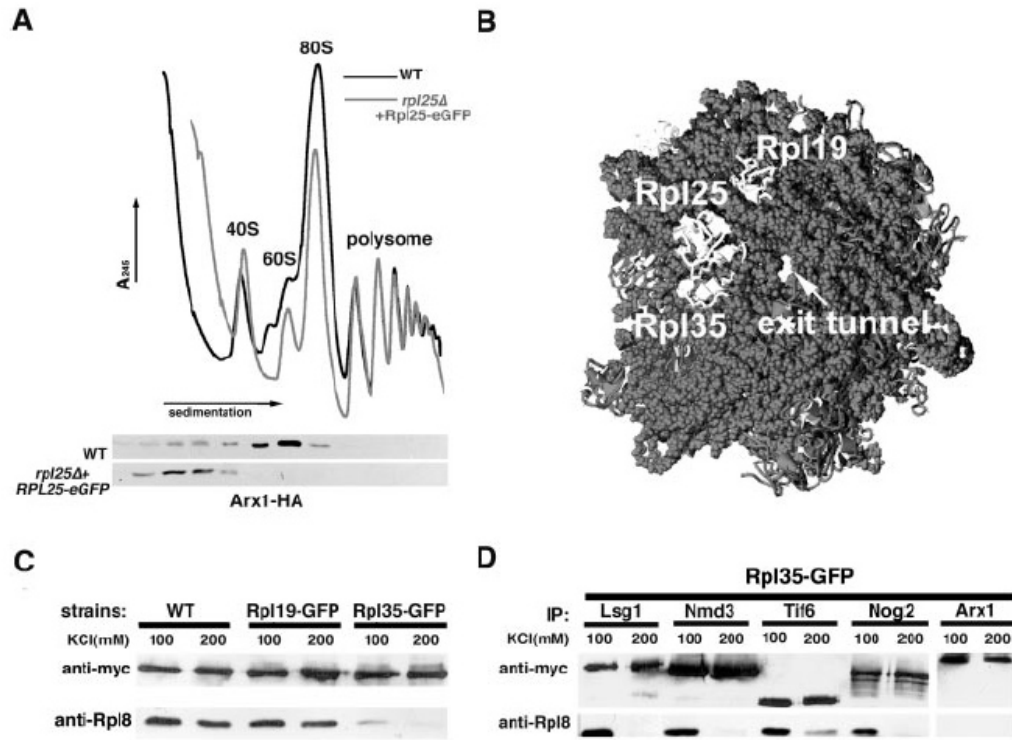
Figure 3.10 Rpl25-eGFP and Rpl35A-GFP and Rpl35B-GFP alter Arx1-60S subunit association.

(A) Lysates were prepared in the presence of cycloheximide from room-temperature cultures of strain AJY1905 (*ARX1-HA*) and AJY1906 (*rpl25Δ ARX1-HA Rpl25-eGFP*) and fractioned on sucrose gradients as described in the legend to Figure 3.2. Fractions were collected, and proteins were precipitated with trichloroacetic acid, separated on SDS-polyacrylamide gel electrophoresis gels, transferred to nitrocellulose membrane, and immunoblotted for HA. (B) Cartoon of ribosomal proteins surrounding the exit tunnel (modified from (Spahn, 2001 19)). (C) Cell extracts from strains AJY2128 (Rpl19A-GFP Rpl19B-GFP), AJY2125 (Rpl35A-GFP Rpl35B-GFP), and an isogenic wild type carrying Arx1-13myc (pAJ1016) plasmids were prepared and incubated with anti-myc antibodies and protein A beads. Precipitated proteins were eluted from protein A beads in sample buffer and separated by SDS-polyacrylamide gel electrophoresis. Western blotting was performed against myc or Rpl8. (D) Cell extracts were prepared from Rpl35A-GFP Rpl35B-GFP strain AJY2125 expressing c-*myc* tagged Lsg1 (pAJ901), Nmd3 (pAJ1001), Tif6 (pAJ1010), Nog2 (pAJ1014), and Arx1 (pAJ1026). The tagged proteins were immunoprecipitated, and their association with 60S subunits was monitored by blotting for Rpl8.

3.3.6 Functions of Arx1p at the polypeptide exit tunnel

Data presented thus far suggest that Arx1p binds to 60S subunits at the polypeptide exit tunnel. If so, what is the function of Arx1p at this specific location and how would it relate to the 60S subunit biogenesis? A number of co-translationally acting factors have been shown to bind to ribosomal proteins in the vicinity of the polypeptide exit tunnel. In particular, the signal recognition particle (SRP) has been shown both by cross-linking experiment and Cryo-EM structure to interact with Rpl25p and Rpl35p (Pool, 2002)(Halic, 2006). In addition, several sites close to the polypeptide exit tunnel have also been identified to make contacts with the translocon (Sec61 complex) during the process of peptide translocation through the ER tunnel (Beckmann, 2001). The translocon interacts with four ribosomal proteins surrounding the polypeptide exit tunnel: Rpl19p, Rpl25p, Rpl35p and Rpl26p.

Considering that Arx1p binding to the subunits also depends on Rpl25p and Rpl35p, its binding site may overlap binding sites for SRP and the translocon. One possibility for the function of Arx1p at the polypeptide exit tunnel may be to modulate binding of these factors to the nascent 60S subunits. In addition to SRP and the translocon, additional factors work on nascent chains co-translationally. These include nascent-chain associated complex (NAC), ribosome-associated complex (RAC), methionine aminopeptidases and N-acetyltransferases. These factors are now known as ribosome-associated protein biogenesis factors (RPBs) (Raue, 2007). Though most of their binding sites on 60S subunits remain to be determined, it is likely that they bind to some of the same proteins at the polypeptide exit tunnel. Temporal and spatial binding of these factors to 60S subunits could be of crucial importance as their premature occupancy on 60S subunits may be detrimental. For example, SRP is assembled in the nucleus (Grosshans, 2001)(Andrews, 1989) and NAC shuttles

through the nucleus (Franke, 2001). Taking into account that the size of 60S subunits almost reaches the upper limit of nuclear pore complexes (NPCs), association of additional factors (for example, SRP (~0.5MDa)) to exporting 60S subunits may impede their passage through the NPC. In this sense, Arx1p may act as a packaging factor that prevents premature association of these factors to the 60S subunits to facilitate its export. In addition, as ribosomes arrive in the cytoplasm; Arx1p's departure from the 60S subunit may serve as another signal to recruit these factors to the 60S subunit.

To test this idea, I examined the effect of Arx1p on the binding of a panel of RPBs to 60S subunits. For this, two trans-acting factors, Lsg1p and Tif6p, representing cytoplasmic and predominately nuclear 60S species, respectively, were used as baits to co-purify 60S subunit complexes from wild type and *arx1Δ* cells. The resulting complexes were then subjected to Western blotting using a panel of antibodies against various factors. From a selective list of RPBs tested thus far, a significantly enhanced signal was observed for Sec65 (a component of SRP) in *arx1Δ* cells (Figure 3.11, compare lane 2 to 3), consistent with the idea that Arx1p blocks access of RPBs to the polypeptide exit tunnel. Because Arx1p seems to persist on 60S subunits in an *rei1Δ* mutant, the same experiment was also carried out in *rei1Δ* cells for comparison. However, no obvious reduction of RPBs levels was found in *rei1Δ* cells, compared to wild type. This result was not a surprise due to the fact that only a very low level of RPBs on 60S subunits can be observed in wild type strain, consistent with their transient residence on emerging nascent chains.
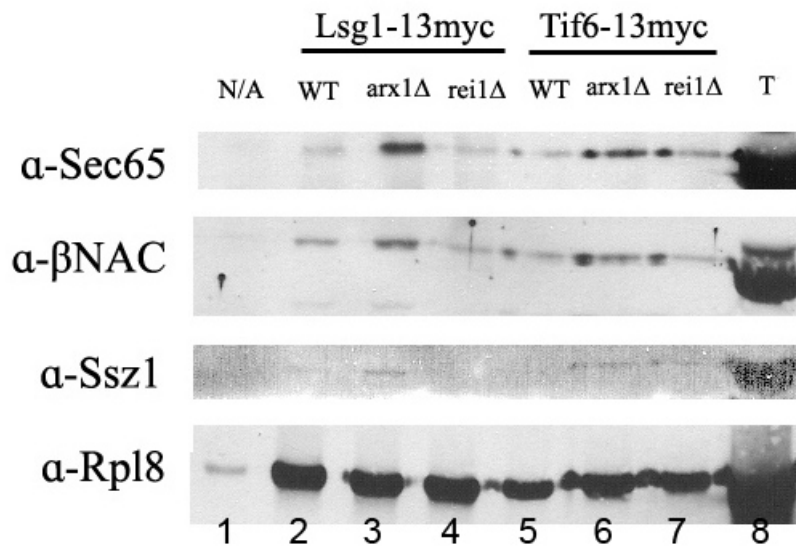
Figure 3.11 Arx1p affects RBPs binding to 60S subunits

Cell extracts of strain AJY1911 (WT), AJY1901 (*arx1Δ*) and AJY1902 (*rei1Δ*) carrying Lsg1-13myc (pAJ901) or Tif6-13myc (pAJ1010) were prepared and incubated with anti-myc antibodies and protein A beads. Precipitated proteins were eluted from protein A beads in sample buffer and separated by SDS-polyacrylamide gel electrophoresis. Western blotting was performed against Sec65, βNAC, Ssz1 and Rpl8. (N/A: negative control)

3.3.7 Association of Rei1p to the 60S subunit is altered by ES27, an rRNA expansion on the 60S subunit

The persistence of Arx1p on 60S subunits may block access of RPBs to the polypeptide exit tunnel, resulting in a severe growth defect as observed in a *rei1Δ* mutant. Alternatively, the cold sensitivity could result from mutations within RNPs (either on RNAs or RNA binding proteins) that causes unfavorable RNA structures that impede RNP function (Zavanelli, 1994). Thus the cold sensitivity of a *rei1Δ* mutant could be the consequence of a defective 60S subunit due to the failure of releasing Arx1p that alters ribosome structure and affects translation.

One candidate rRNA structure in this respect is the expansion sequence 27 (ES27). ES27 is highly variable in length in different organisms and forms a double-stranded extension (Jeeninga, 1997)(Schnare, 1996). ES27 has been shown by cryo-EM to exist in two positions: either close to the L1 arm (L1 position) or rotated past the polypeptide exit tunnel (exit position) (Illustration 3.2) (Beckmann, 2001). In the reconstituted ribosome-translocon complex, ES27 has been shown to locate exclusively at the L1 position, where interference of the contact site between translocon and ribosome exit tunnel is minimized (Beckmann, 2001). The cold sensitivity of *rei1Δ* could be due to a problem with RNA folding. Since ES27 is dynamic and in the vicinity of where we think Arx1p and Rei1p might bind, we suggested the dynamics of ES27 may be altered in the *rei1Δ* strain. Along this line, Rei1p has also been shown by gel shift assay to bind to *in vitro* synthesized ES27 with high affinity (M. Parnell, personal commncation, and unpublished data), supporting the idea that Rei1p interacts with ES27.

To investigate the impact of ES27 on Rei1p-60S subunit binding, I engineered plasmid borne ribosomal rDNA containing a partial deletion of ES27

(ES27Δ97). According to the work by Jeeninga *et al.*, partial deletion of 97 nucleotides within ES27 was viable and did not have any obvious impact on 60S subunit biogenesis (Jeeninga, 1997). The ES27Δ97 plasmid was then introduced into a yeast strain to provide the sole source of rRNA. This strain and a wild type strain were transformed with either an Arx1p-13myc or a Rei1p-13myc plasmid to immunoprecipitate 60S subunits. Under low ionic strength condition (50mM KCl), ES27Δ97 did not seem to alter the binding affinity of Arx1p to 60S subunits (Figure 3.12A). However, a slightly reduced level of Rpl8p was found in the Rei1p IP in the ES27Δ97 strain. Strikingly, this difference was more obvious under high ionic strength condition (200mM KCl) and essentially no detectable Rpl8p was found in Rei1p complexes from the ES27Δ97 strain (Figure 3.12B). The ES27Δ97 also seemed to alter Arx1p-60S subunit binding, though to a lesser extent. Together, these results pointed out a possible docking site for Rei1p on the 60S subunit that is likely to communicate with the polypeptide exit tunnel in the close proximity.
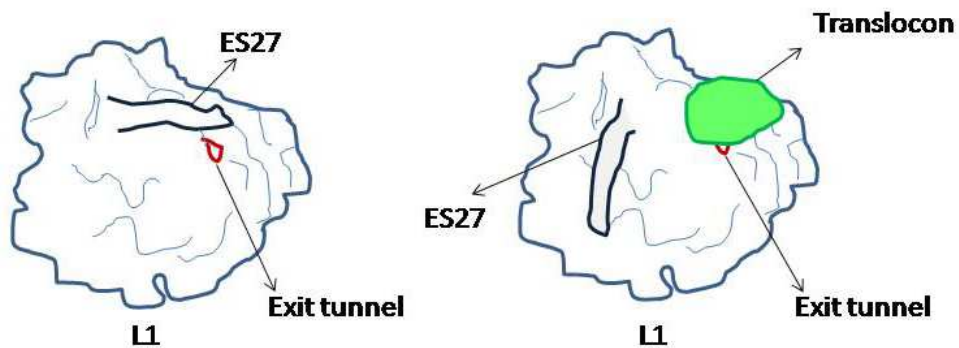
Illustration 3.2 Two modes of ES27 on the 60S subunit

Dynamic ES27 are shown above. Cartoon depicts the cryo-EM structure of ribosomes in the translocon unbound (left) or bound state (bound) and is adapted from (Beckmann, 2001 20). The ES27 locates with its end in the vicinity of the polypeptide exit tunnel in the absence of translocon (left). In the reconstruction of a ribosome-translocon (Sec61) complex, ES27 was found to adopt the L1 position exclusively (right). Two modes of ES27 location on 60S subunits indicate that it is a dynamic structure and can rotate along the surface of ribosomes. (L1: L1 protrusion).

		A				B		
IP:	N/A	Arx1 Rei1	Arx1 Rei1		N/A	Arx1 Rei1	Arx1 Rei1	
ribosome:		WT	ES27Δ97			WT	ES27Δ97	

anti-myc

anti-Rpl8

50mM KCl   200mM KCl
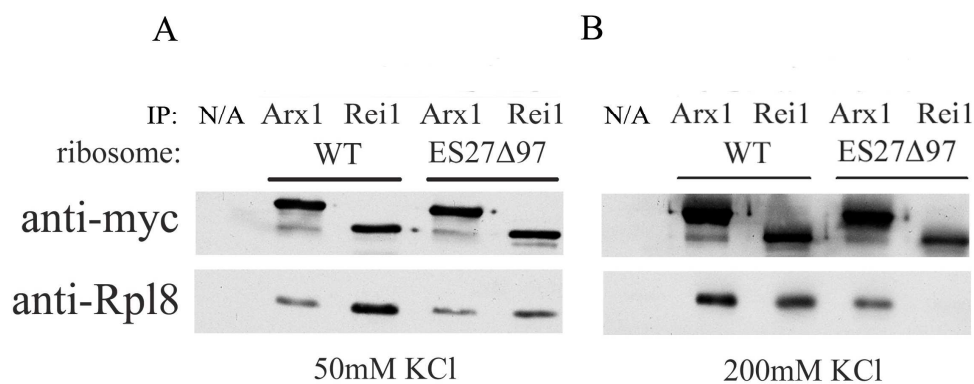
Figure 3.12 Partial deletion of ES27 affects Rei1p binding to 60S subunits

Wild type rDNA plasmid (pAJ1181) and ES27Δ97 rDNA plasmid (pAJ1489) were shuffle into AJY1185 to replace endogenous wild type plasmids. These strains were then transformed with Arx1-13myc (pAJ1016) or Rei1-13myc (pAJ1018). Cell extracts were prepared in buffer conditions: 5mM $MgCl_2$, 20mM Hepes, pH7.5 and KCl (50mM or 200mM) and incubated with anti-myc antibodies and protein A beads. Precipitated proteins were eluted from protein A beads in sample buffer and separated by SDS-polyacrylamide gel electrophoresis. Western blotting was performed against myc and Rpl8. (N/A: negative control)

3.4 Discussion

The combination of genetic, mass-spectrometric and proteomic assays has identified more than ~170 factors involved in the ribosome biogenesis in *Saccharomyces cerevisiae* (Kallstrom, 2003)(Stage-Zimmermann, 2000)(Hurt, 1999)(Gavin, 2002)(Bassler, 2001)(Fromont-Racine, 2003)(Tschochner, 2003). While most of these factors contribute to nuclear maturation of 60S subunits, few of the trans-acting factors accompany the 60S subunit during export. With respect to 60S subunit export, our lab has focused on the role of Nmd3p as the Crm1p-dependent export adaptor (Ho, 2000).

In view of understanding nuclear export of 60S subunits, my work has focused on characterizing two novel proteins that are co-purified with Nmd3p. I have shown in this study that Arx1p, a shuttling protein, first binds to the pre-60S particle in the nucleolus and accompanies it during nuclear export. On the other hand, Rei1p does not appear to shuttle and binds to the 60S subunit only when it reaches the cytoplasm. While neither Arx1p nor Rei1p is essential, deletion of *REI1* leads to severe cold sensitivity for 60S biogenesis. Interestingly, this phenotype can be suppressed by deletion of *ARX1* or by conditions that block Arx1p binding to the 60S subunits (mutations within Arx1p or large fusions to Rpl25p). These results indicated that the primary defect in *rei1Δ* cells results from a failure to release Arx1p from cytoplasmic 60S subunits. The Rpl25p-eGFP and Rpl35Ap-GFP Rpl35Bp-GFP effects on Arx1p binding to 60S subunits suggested that Arx1p binds at the polypeptide exit tunnel. However, the possibility of indirect effects mediated by long-range conformation remodeling on 60S subunits due to these fusions to Rpl25p or Rpl35p cannot be excluded. On the other hand, Arx1p is related to MetAP2, an enzyme that works co-translationally on nascent chains. Thus, if they share a common

binding site, again, it would be expected to be in the vicinity of the polypeptide exit tunnel.

Though accumulating data has identified a considerable number of factors involved in 60S subunit biogenesis, none of their binding sites on 60S subunits has been reported thus far. Several lines of evidence have strongly suggested that Arx1p binds at the exit tunnel, however, solid data to support this idea are lacking. Efforts to reconstitute Arx1p-60S subunit complexes for cross-linking studies have not been successful. The failure of obtaining such complexes may indicate that the binding of Arx1p to 60S subunits requires additional factors. Alternatively, the mature ribosomes that we used may not be in the proper conformation for Arx1p binding. The recent work by Lebreton *et al.* has identified Alb1p as an interaction partner for Arx1p (Lebreton, 2006). In this sense, Alb1p may enhance Arx1p binding to 60S subunits. However, initial attempts to express and purify Alb1p were unsuccessful.

The preliminary result that Arx1p affects SRP binding to 60S subunits is consistent with the proposed Arx1p binding site. The signal recognition particle (SRP), a large RNP with molecular weight about 0.5MD, is initially assembled in the nucleus (Andrews, 1989)(Grosshans, 2001). While nuclear export of SRP appears to be independent of the 60S subunit, SRP has been shown to associate with nontranslating ribosomes at low affinity. Because the size of 60S subunit probably reach the upper limit of the inner tunnel of the nuclear pore complex (NPC), premature association of SRP to its intrinsic substrate– the pre-60S subunit in the nucleus may sterically hinder export. Thus, Arx1p may have evolved as a packaging factor that facilitates ribosome translocation through the NPC by minimizing premature association of additional factors. Because Arx1p binding likely occludes the binding of other RBPs on the 60S

subunits, its release from cytoplasmic ribosomes may be necessary for subsequent interaction of RBPs with 60S subunits.

At the time my work on Rei1p recycling of Arx1p was published (Hung, 2006), similar work was published from another group (Lebreton, 2006). In this study, Lebreton *et al.* showed that Arx1p can form a stable complex with Alb1p, a small protein that also requires Rei1p for its nuclear shuttling. However, in their study, the Arx1p-Alb1 small complex does not bind to 60S subunits in *rei1Δ* cells, a result that is contradictory to my data. The discrepancy may due to different buffer conditions used in these sucrose gradients, as we know that high ionic strength has significant impacts on altering binding of trans-acting factors to 60S subunits. Alternatively, they carried out the experiment in a strain where Alb1p is fused with GFP. Though it has not been reported that C-terminal fusions to Alb1p affects its function, it is possible that it affects Arx1p-60S subunit association. Considering that the cold sensitivity of an *rei1Δ* can be suppressed by an Arx1p mutant that is defective in 60S subunit association, we preferred the idea that Arx1p, and perhaps the Arx1p-Alb1p complex, persisted on the 60S subunit in *rei1Δ*. Lastly, Alb1p can physically interact with Arx1p (Longtine, 1998), and thus Arx1p may work cooperatively with Alb1p respect to 60S subunit biogenesis.

In addition to its role in 60S ribosome biogenesis, Arx1p may be involved in other metabolic pathways. Arx1p has a human homolog, Ebp1, a cytoplasmic protein that is associated with the transmembrane protein ErbB-3 (a member of the epidermal growth factor receptor family (Yoo, 2000). Upon stimuli, Ebp1 translocates into the nucleus, where it is thought to act as a transcription factor (Xia, 2001)(Zhang, 2003). In this respect, Ebp1 has been shown to inhibit cell proliferation in human breast cancer (Lessor, 2000). Meanwhile, human Ebp1 has also been identified as a

nucleolar protein that is associated with pre-60S particles (Squatrito, 2006). These results raise the possibility that yeast Arx1p could act analogously to Ebp1 as its involvement in transcriptional regulation of cell proliferation. On the other hand, Rei1p has been implicated to function in the mitotic signaling network that negatively regulates Swe1 kinase, a protein kinase that regulates the G2/M transition (Iwase, 2004). In addition, Rei1p was also identified as a two-hybrid interaction partner of Nis1p (Iwase, 2001). Nis1p, another G2/M transition regulator, is a septin-binding protein that localizes to the bud neck in M phase. While Rei1p is localized in the cytoplasm throughout the cell cycle, its association with Nis1p could indicate a role in coordinating the cell cycle and ribosome biogenesis pathways. Alternatively, it could provide a mechanism for targeting nascent ribosomes to the site of active cell growth.

Chapter 4: Interplay of the Hsp40 J-protein, Jjj1p, with Arx1p and Rei1p in the 60S subunit biogenesis

4.1 Introduction

Data presented in the preceding chapter demonstrate functional interaction of the nuclear biogenesis factor Arx1p and its cytoplasmic release factor Rei1p. These results also enrich our current understanding of the late cytoplasmic maturation event. Recycling of biogenesis factors back to the nucleus is crucial for supporting 60S subunit export, and in some cases, their release could serve as a last check point before ribosomes are engaged in translation. The work in this chapter was resulted from a collaboration with the laboratory of Dr. Elizabeth Craig. Dr. Craig's group had identified the J-protein Jjj1p as an Hsp40 protein involved in 60S subunit maturation. Together, our work suggests that Jjj1p, along with the Hsp70 Ssa1p, act with Rei1p to release Arx1p in the cytoplasm. This work was published in Proc Natl Acad Sci USA vol.104 p.1558-1563 2007 (Meyer, 2007).

4.2 Background

Protein synthesis is a fundamental process that converts genetic information into polypeptides to fulfill various biological functions. Although ribosomes play the primary role of synthesizing polypeptides, a host of factors recognize the nascent polypeptide to facilitate processing, folding and targeting. Upon translation, the emerging nascent chain must avoid unfavorable folding during the course of its synthesis. For this reason, a class of specialized factors, namely chaperones, have evolved and devoted into various processes. Two classes of chaperons act on cytosolic proteins. Chaperones that bind to polypeptides post-translationally belong to the

Hsp70/40 and Hsp60/10 families (Fink, 1999)(Bukau, 1998). The other class of chaperones regulates the fate of nascent chains by binding to both the ribosome and the emerging polypeptide, thereby promoting protein folding co-translationally. Such apparatus can be found both in eukaryotes and prokaryotes. Whereas Trigger Factor (TF) has been shown to crosslink to nascent polypeptide chains in bacteria, chaperone systems such as the RAC (ribosome-associated complex) and the NAC (nascent chain-associated complex) system in eukaryotes are considered as the first contact partners of nascent chains on ribosomes (Craig, 2003)(Hartl, 2002).

In *Saccharomyces cerevisiae*, the main ribosome-associated chaperone is the Hsp70 Ssb, which has been shown to bind to ribosomes and can be cross-linked to nascent chains as short as about 50 amino acids (Pfund, 1998) (Hundley, 2002). Unlike the prokaryotic TF, which can function alone as a monomer on ribosomes, the Ssb requires an additional J-protein, Zuo, as its co-chaperone. Like all Hsp70s, Ssb interacts transiently with nascent chain substrates by its intrinsic ATPase activity that is stimulated by its J-protein Zuo, promoting polypeptide folding. In addition, Zuo has been found to associate with another Hsp70 chaperone Ssz, and together forms a stable complex, termed ribosome-associated complex (RAC) (Gautschi, 2002). It has been suggested that Ssb by itself could not be cross-linked to nascent chains on ribosomes in the absence of RAC, substantiating the dependence of RAC on recruiting Ssb to ribosomes (Gautschi, 2002)(Hundley, 2002).

The prototype of the Hsp40 J-protein is the cytosolic chaperone DnaJ from *E. Coli*. Members of the J-protein family act as co-factors of Hsp70 chaperones by stimulating their intrinsic ATPase activity when a polypeptide is bound in the substrate-bound pocket (Qiu, 2006). BLAST search against yeast genome using the J-domain of DnaJ revealed 22 J-proteins that can be further classified into three

classes (Walsh, 2004). Type I J-proteins have all three well defined domains of the DnaJ structure, including the helical J-domain, a linker glycine-rich region and a zinc-finger domain followed by a carboxyl-terminal domain. An example of a J-protein of this class is Ydj1, a co-chaperone of the cytosolic Hsp70 Ssa1/2. Type II J-proteins simply lack the zinc-finger domain, whereas Type III J-proteins lack both the zinc-finger domain and the glycine-rich region. A well characterized Type III J-protein is the ribosome-associated chaperone Zuo1. While these J-like proteins, by definition, function as Hsp40 chaperones, they participate in various processes of protein assembly, disassembly and translocation.

4.3 Results

4.3.1 Identification of a cytosolic J-protein, Jjj1p

Sequence alignment of the J-domain of the ribosome-associated J-protein Zuo1p and other J-proteins of *Saccharomyce cerevisiae* revealed a highly homologus region that is unique to a Jjj1p but not other J-proteins. Amino acids 205-287 of Zuo1p shares about 50% similarity with amino acids 179-261 of Jjj1p. While Zuo1p has an internal J-domain, the J-domains of Jjj1p and most J-proteins are located at N-termini. Adjacent to the J-domain of Zuo1p is an interdomain that links to a highly charged region (Figure 4.1A, modified from A. Meyer). It has been hypothesized that the interdomain of Zuo1p may contribute to its ribosome binding, and more interestingly, a similar region was also found in Jjj1p. In addition, Jjj1p has two C_2H_2 type zinc finger motifs flanking a highly charged region. These unique signatures shared between Zuo1p and Jjj1p inspired our collaborator Dr. Craig and her graduate student A. Meyer to investigate the possibility whether Jjj1p could function similarly

as Zuo1p in modulating chaperone activity on ribosomes.

4.3.2 Jjj1p co-sediments with 60S subunits

To determine if Jjj1p co-sedimented specifically with 60S subunits, cell extracts obtained from a wild type strain were prepared in a magnesium free condition and fractionated on sucrose gradients to separate 40S and 60S subunits. As seen in Figure 4.1B, Jjj1p co-migrates with the 60S peak, as does Zuo1p, consistent with the idea that Jjj1p binds to the 60S subunit (data taken from A. Meyer). The specific association of Jjj1p with 60S subunits was further confirmed by co-immunoprecipitation. Cell extracts from strains expressing Jjj1p-HA or Arx1-HA were prepared and incubated with anti-HA antibodies to immune-purify associated complexes. In both cases, Arx1p and Jjj1p were able to co-immunoprecipitate with 60S subunits, as monitored by Rpl8p signal (Figure 4.1C). Taken together, these results show that Jjj1p associates with 60S subunits.
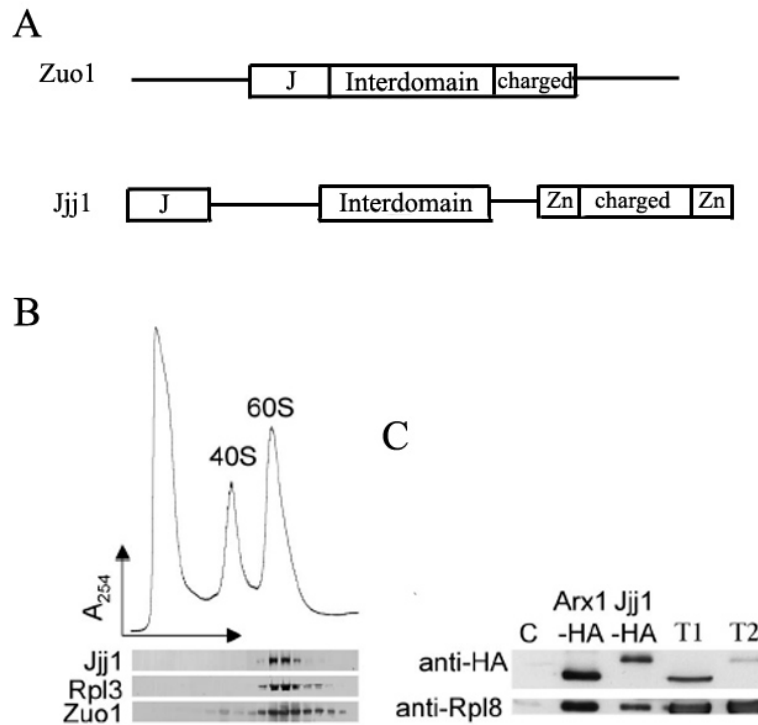
Figure 4.1 Jjj1p associates with 60S subunits

(B)   Cartoon of Zuo1p and Jjj1p domain alignment. (Modified from A. Meyer)
(B) Co-sedimentation of Jjj1p with 60S subunits. Cell lysates from wild type strain were prepared in magnesium-free buffer and separated on 15-30% sucrose gradient. Samples were monitored at OD_{254}, fractionated and collected for Western blotting to detect Jjj1p, Rpl3 and Zuo1p signal. (Taken from A. Meyer) (C) Cell extracts from strain AJY1946 (Arx1-HA) and *jjj1Δ* carrying Jjj1-3HA on plasmid were incubated without addition of antibody (N/A) or with anti-HA antibody and protein A beads. Precipitated proteins were eluted from protein A beads in sample buffer and separated by SDS-polyacrylamide gel electrophoresis. Total protein extract (T)

was included as a loading control for the immunoprecipitations (IP). Western blotting was performed against the HA epitopes and Rpl8p.

4.3.3 Jjj1p has functions distinct from Zuo1p

Because Jjj1p and Zuo1p share several similar features and both bind to 60S subunits, it is then intriguing to test if they perform overlapped functions. For this, Jjj1p was over-expressed in a *zuo1Δ* mutant to seek for potential complementation for growth. Deletion of *ZUO1* leads to a cold-sensitivity and hypersensitivities to various cations (i.e. Na+, Li+ and K+) and several translation inhibiting drugs, including hygromycin B and paromomycin (Kim, 2005). Overexpression of Jjj1p seemed to partially rescue these defects caused by deletion of *ZUO1* (data not shown, A. Meyer), suggesting that Jjj1p is able to fulfill Zuo1p function to some extent. Analogously, to ask if Zuo1p overlaps Jjj1p's function, the reverse experiment was applied to a *jjj1Δ* mutant. Deletion of *JJJ1* also causes a cold-sensitivity but not hypersensitivity to any cation or translation inhibitor (data not shown, A. Meyer). The J-domain confers Jjj1p function, as deletion of the entire J-domain or point mutations of the conserved residues histidine-proline-aspartic acid (HPD) of the J-domain render cell slow growth phenotype (data not shown, A. Meyer). The impact of overexpression of Zuo1p in a *jjj1Δ* mutant was tested, and surprisingly, no obvious improvement of growth was observed, even in the presence of Jjj1p's co-chaperone Ssz1p. These results indicated that Jjj1p possesses cellular function distinct from Zuo1p.

4.3.4 Deletion of *JJJ1* affects 60S subunit biogenesis

The finding that Jjj1p associates with 60S subunits but possesses distinct functions other than Zuo1p encouraged our collaborator Dr. Craig and A. Meyer to examine Jjj1p's functional involvement in the 60S subunit biogenesis. For this reason,

they further examined Jjj1p's co-sedimentation pattern with ribosomes in a more detailed manner, where cell extract from a wild type strain was prepared and subjected to sucrose gradient sedimentation to resolve different species of ribosomes. As a control, Zuo1p sedimentation was also monitored, and consistent with previous results, it was found to sedimentate with 60S and 80S peaks and throughout polysomes (Figure 4.2A, A. Meyer). However, Jjj1p was found predominately on the 60S peak with some trailing signal on polysome fractions. While Zuo1p was found almost in every fraction containing 60S subunits, Jjj1p seemed to co-sediment only with the free 60S peak. The difference in sedimentation pattern with ribosomes supports the idea that these two proteins fulfill different cellular functions on ribosomes.

As a step forward, our collaborator further examined the impact of deletion of *JJJ1* on 60S subunit levels analyzed by polysome profiles. While wild type as well as *zuo1Δ* cells did not reveal any obvious 60S subunit associated defects, deletion of *JJJ1* displayed several characteristics of a 60S subunit defect in the cells (Figure 4.2B, A. Meyer), including a decreased 60S peak and the appearance of half-mers. This result together with the finding that Jjj1p co-sediment primarily with the free 60S peak led our collaborators Dr. Craig and A. Meyer to suspect that Jjj1p acts as a 60S subunit biogenesis factor in addition to its chaperone function. More interestingly, the polysome profile of a *jjj1Δ* mutant is reminiscent of a *rei1Δ* mutant (Figure 4.2B, A. Meyer). Rei1p, as I discussed earlier in Chapter 3, is a non-essential cytoplasmic protein that binds to the 60S subunit presumably after 60S subunits are exported to the cytoplasm. In addition to the similar impacts on 60S subunit levels, Jjj1p resembles Rei1p in many other aspects; for example, null mutants of these two cytoplasmic proteins are both cold sensitive. The similarities in phenotype, ocalization and subunit

association suggested that Jjj1p and Rei1p may act together in 60S subunit biogenesis.
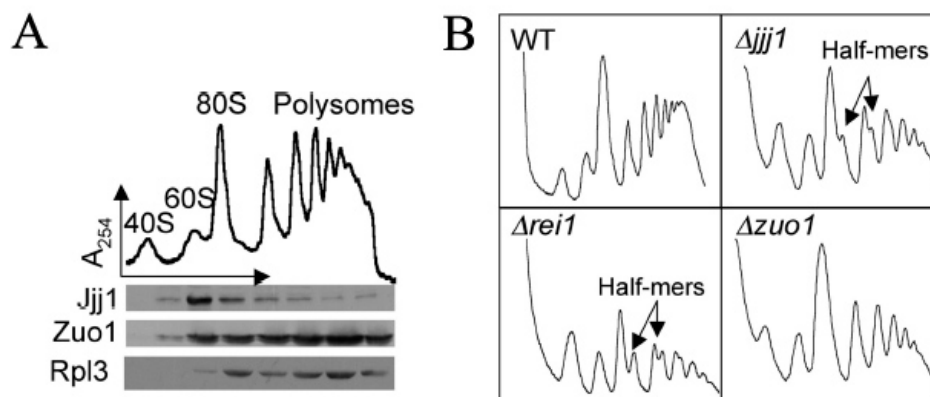
Figure 4.2 Jjj1p is a 60S subunits biogenesis factor

(A) Cell lysates prepared from a wild type strain were prepared in magnesium-free buffer and separated on 5 to 50% sucrose gradient. Samples were monitored at OD_{254}, fractionated and collected for Western blotting to detect Jjj1p, Rpl3 and Zuo1p. (B) Cell lysates prepared from wild type, *rei1Δ*, *jjj1Δ* and *zuo1Δ* were centrifuged through 7 to 47% sucrose gradients and samples were monitored at OD_{254}. (A: taken from A. Meyer)

4.3.5 Interplay between *JJJ1*, *REI1* and *ARX1*

Because Jjj1p behaves similarly to Rei1p, it is possible that Jjj1p acts cooperatively with Rei1p to promote 60S subunit biogenesis and most likely, through interactions with common factors. As Rei1p was shown in Chapter 3 to be a cytoplasmic recycling factor for Arx1p (and perhaps the Arx1p-Alb1p complex), it is possible that Jjj1p would functionally interact with Arx1p (or the Arx1p-Alb1p complex) as 60S subunits reach the cytoplasm. For this reason, a *jjj1*Δ mutant was crossed to an *arx1*Δ mutant to test for genetic interaction. As seen in Figure 4.3A (data adopted from A. Meyer), deletion of *ARX1* or its binding partner, *ALB1*, suppresses the cold-sensitivity of a *jjj1*Δ mutant. This suppression was similar to that observed when *arx1*Δ was combined with *rei1*Δ, suggesting that the persistence of Arx1p-Alb1p small complex is also detrimental in a *jjj1*Δ mutant (refer to Chapter 3). Consistently, the suppression of growth also corresponded to rescued levels of 60S subunits (Figure 4.3B, A. Meyer). However, deletion of *JJJ1* did not enhance the cold sensitivity of an *rei1*Δ mutant (Figure 4.3A, A. Meyer). This result indicates that Jjj1p may work together with Rei1p, as deletion of the second player on top of the first mutant does not cause additional effects to the cells. These genetic observations further suggested the involvement of Jjj1p in recycling the cytoplasmic Arx1p-Alb1p complex, likely coordinately with Rei1p.

The steady-state cellular localization of Jjj1p is cytoplasmic, however, this does not exclude the possibility that it transiently passes into the nucleus. To examine if Jjj1p acts similar to Rei1p, exclusively on cytoplasmic 60S subunits, I asked if Jjj1p exports as 60S ribosomes in a Crm1-dependent manner. The same strategy used to determine if Re1ip shuttles was applied to Jjj1p. A LMB-sensitive yeast strain harboring the T539C allele at *CRM1* locus was subjected to LMB treatment and

indirect immunefluorescence microscopy for detecting endogenous Jjj1p localization using antibodies specific to Jjj1p. If Jjj1p shuttles, it will be trapped in the nucleus as nuclear export of 60S subunits is blocked in the presence of LMB. As a positive control, the effect of LMB on Nmd3p was also monitored. While Nmd3p was largely enriched in the nucleus upon LMB treatment, Jjj1p remained in the cytoplasm (Figure 4.4A), similarly to Rei1p. Taken together, Jjj1p may function as Rei1p solely on cytoplasmic 60S subunits after nuclear export.
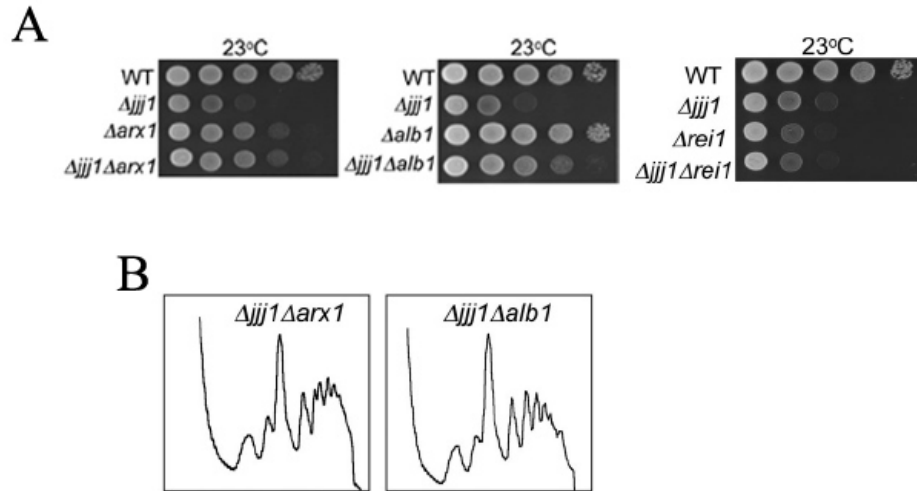
Figure 4.3 Suppression of the cold-sensitivity of a *jjj1*Δ mutant

(A) Tenfold serial dilutions of approximately equal amount of cells were spotted onto yeast extract-peptone-glucose plates and incubated at the indicated temperatures; (B) Cell lysates prepared from *jjj1*Δ*arx1*Δ and *jjj1*Δ*alb1*Δ were centrifuged through 5 to 50% sucrose gradients and samples were monitored at OD_{254}. (A and B: taken from A. Meyer)

anti-Nmd3 anti-Jjj1 anti-Nmd3 anti-Jjj1
-LMB   -LMB   +LMB   +LMB

anti-rabbit Rhod

DAPI
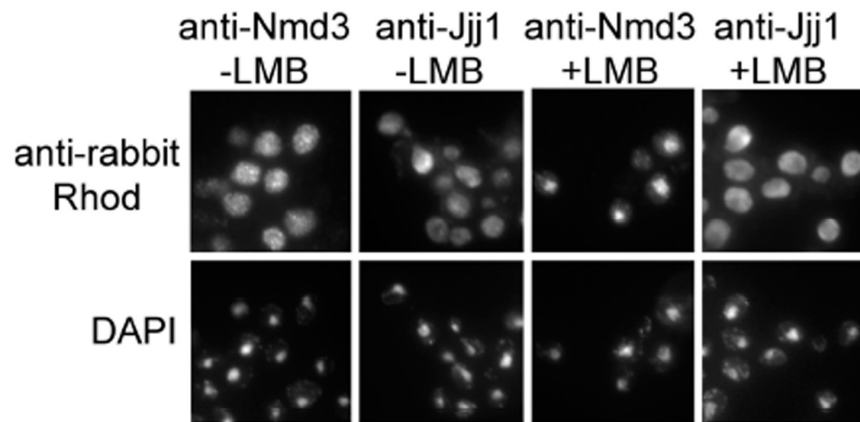
Figure 4.4 Jjj1p does not shuttle in the Crm1-dependent pathway

The LMB-sensitive strain AJY1539 (*CRM1T539C*) was cultured in rich media at room temperature to log-phase. Cells were concentrated 20-fold in fresh media, LMB was added to a final concentration of 0.1 μg/ml, and cultures were incubated for 30 min. Cells were then fixed with 3.7% formaldehyde (final concentration) and subjected to indirect immunofluorescence microscopy (IF) by using antibodies against Jjj1p or Nmd3p. Localization of these proteins was monitored by using anti-rabbit rhodamine-conjugated antibodies. DAPI was used for visualization of nuclei.

To determine if Jjj1p has similar effects similar to Rei1p on recycling Arx1p, I next investigated the cellular localization of Arx1p in a *jjj1Δ* mutant. For this, I integrated GFP fusions to the C-terminus of *ARX1* at its genomic locus in wild type and *jjj1Δ* cells. As seen previously and in Figure 4.5A, wild type Arx1p-GFP is predominately nuclear/nucleolar. However, Arx1p-GFP was found to redistribute to the cytoplasm in *jjj1Δ* cells. The re-localization of Arx1-GFP from the nucleus to the cytoplasm was seen previously in *rei1Δ* cells, suggesting that Jjj1p functions like Rei1p in recycling Arx1p back to the nucleus. Interestingly, Jjj1p function in maintaining Arx1p localization seemed to also depend on its co-chaperone activity, as Arx1p-GFP was still predominately cytoplasmic in a *jjj1$_{HPD->AAA}$* mutant (Figure 4.5A).

Failure of Arx1p recycling in a *jjj1Δ* mutant could be due to a failure to release Arx1p from the 60S subunit, or from a failure to re-import free Arx1p into the nucleus. To ask if Arx1p persists on 60S subunits in the absence of Jjj1p, cell extracts prepared from wild type or *jjj1Δ* cells harboring genomic HA tagged *ARX1* were subjected to co-immunoprecipitation. Similar levels of 60S subunits co-purified with Arx1p from *jjj1Δ* and wild type cells (Figure 4.5B). Moreover, Arx1p was also found by sucrose gradient sedimentation analysis to persist on the free 60S peak in a *jjj1Δ* mutant (Figure 4.5C). From these results, we concluded that Jjj1p has similar effects as Rei1p on recycling Arx1p and that the persistence of Arx1p on cytoplasmic 60S subunits caused a general cold-sensitivity effect.
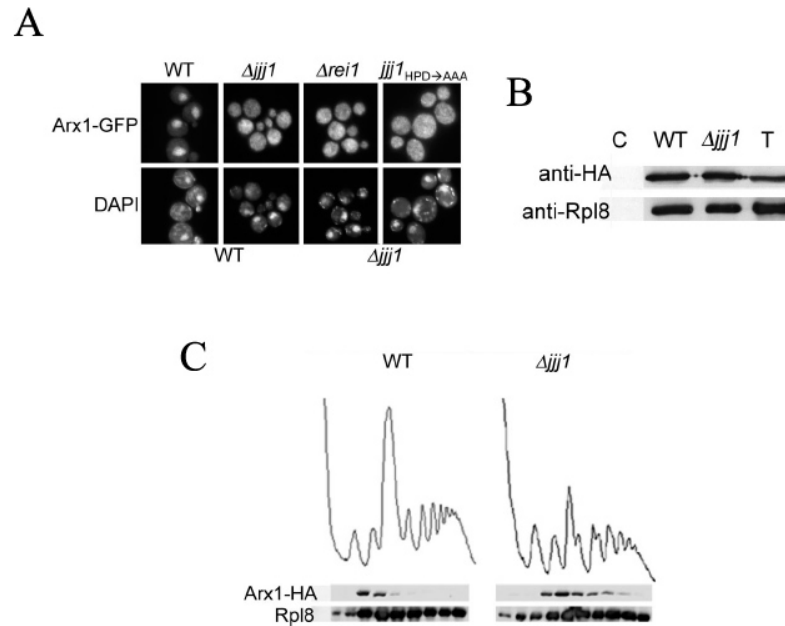
Figure 4.5 Arx1p remains bound to 60S subunits and fails to recycle in a *jjj1*Δ mutant.

(A) Cell cultures of wild type, *rei1*Δ, *jjj1*Δand *jjj1*Δ+ *jjj1*$_{HPD->AAA}$ strains carrying genomic Arx1-GFP were collected at mid-log phase. Cellular localization of Arx1-GFP was monitored by fluorescence microscopy. (B) Extracts from wild type or *jjj1*Δ cells containing genomically integrated Arx1-HA were incubated without addition of antibody (C: negative control) or with anti-HA antibody and protein A beads. Precipitated proteins were eluted from protein A beads in sample buffer and separated by SDS-polyacrylamide gel electrophoresis. Total protein extract (T) was included as a loading control for the immunoprecipitations (IP). Western blotting was performed against the HA epitopes and Rpl8p. (C) Lysates from wild type or *jjj1*Δ cells containing genomically integrated Arx1-HA were prepared and centrifuged through 7 to 47% sucrose gradients. Samples were monitored at OD$_{254}$, fractionated and collected for Western blotting using anti-bodies specific to HA epitopes and Rpl8p.

4.4 Discussion

The study of Jjj1p was initiated because of its sequence similarities with the Hsp40 chaperone member, Zuo1p. Hsp40 J-proteins are co-chaperones of Hsp70s that are involved in a variety of cellular functions, including protein folding, disassembly of protein complexes and translocation of polypeptides across organellar membrane (Craig, 2006). While some classes of chaperones are ribosome-associated as they recognize nascent polypeptides to prevent premature folding, none of them has been shown to participate in the 60S subunit biogenesis. Data presented in this chapter provide evidences that a J-protein Jjj1p acts as a 60S subunit biogenesis factor in the cytoplasm.

Several pieces of data supported the idea that Jjj1p functions similar to the previously characterized biogenesis factor, Rei1p. Rei1p was shown, both by my work and by Lebreton *et al.*, as one of the few cytoplasmic biogenesis factors that are required for proper recycling of shuttling factors. Strikingly, Jjj1p seemed to function similarly as Rei1p in recycling the Arx1p-Alb1p complex from cytoplasmic 60S subunits. Interestingly, this function also depends on the J-domain of Jjj1p, a functional domain that is essential for stimulating ATPase activity of its Hsp70 co-chaperone, Ssa1p (data not shown, A. Meyer).

Given that deletion of *JJJ1* revealed a cold-sensitivity that is reminiscent of a *rei1Δ* mutant and that both mutants can be suppressed by an additional deletion of *ARX1*, it is likely that they function together in recycling the Arx1p-Alb1p complex. If so, how would this occur? Release of factors from complexes can be driven by structural remodeling and conformational changes, which in turn, alter substrate binding affinity. Examples seen in the late cytoplasmic 60S subunit are the nuclear recycling of Nmd3p and Tif6p. Nmd3p accompanies 60S subunit to the cytoplasm

and is released by a GTPase Lsg1p. It has been suggested that the GTPase activity of Lsg1p may trigger 60S subunit remodeling that is required for correct loading of a ribosomal protein, Rpl10p. The release of Nmd3p is thought to be coupled to the loading of Rpl10p and the subsequent release of its chaperone, Sqt1p, from 60S subunits (Hedges, 2005)(West, 2005). On the other hand, release of Tif6p from 60S subunits requires another cytoplasmic GTPase, Efl1p. By analogy with the role of Lsg1p in cytoplasmic recycling, it has been suggested that the GTP hydrolysis of Efl1p triggers a conformational rearrangement that stimulates Tif6p release (Senger, 2001).

Examples of J-protein:Hsp70 complexes in modulating protein-protein interaction or RNP structure have also been observed (Walsh, 2004). For example, auxilin, a brain specific J-protein, interacts with Hsp70 chaperon to uncoat clathrin-coating vesicles (Lemmon, 2001). From this point of view, Jjj1p may work together with its Hsp70 partner, Ssa1p, in remodeling cytoplasmic 60S subunits to facilitate release of shuttling factors. Because Jjj1p binding to 60S subunits seems to be reduced in the absence of Rei1p, but not *vice versa* (data not shown), it is likely that Jjj1p binding to the 60S subunit partially depends on Rei1p. Thus, Rei1p may provide a binding platform for Jjj1p on the 60S subunit, and upon some molecular cue, the chaperone activity initiates and triggers structural rearrangement to facilitate release of the Arx1p-Alb1p complex.

Chapter 5: Arx1p interacts with 60S subunit export constituents: Nmd3p, Crm1p and nucleoporins

5.1 Introduction

The results presented in Chapter 3 and 4 describe the interplay between Arx1p, its cytoplasmic recycling factors Rei1p and Jjj1p, and the ribosomal protein Rpl25p. These data further suggested a potential role of Arx1p in mediating the association of various co-translationally acting factors with the polypeptide exit tunnel. While most of these data have contributed to an understanding of how Arx1p is recycled from the cytoplasm and the consequence of failing to release Arx1p, they have not addressed potential nuclear roles of Arx1p.

Data presented in this chapter provide evidence that Arx1p functions directly in nuclear export of 60S subunits. Specifically, Arx1p is essential if the nuclear export signal (NES) within Nmd3p is impaired. In addition, mutations within nuclear pore complex (NPC) components are synthetic sick or lethal in combination with an *arx1Δ* mutant, further suggesting a potential function of Arx1p in modulating Nmd3p-Crm1p-dependent 60S subunit export through the NPC channel. The results presented in this chapter strongly suggest that Arx1p functions in 60S subunit export, however, further experiments are needed to clarify the molecular mechanism. At the end of the chapter, I will discuss possible models of Arx1p function in facilitating the 60S subunit export.

5.2 Background

The large and small ribosomal subunits are assembled in the nucleolus/nucleus and subsequently exported into the cytoplasm independently

(Tschochner, 2003)(Takahashi, 2003)(Fromont-Racine, 2003). In *Saccharomyces cerevisiae*, the 60S subunit export pathway is well characterized and relies on the nuclear-cytoplasmic shuttling export adaptor Nmd3p, which acts in a Crm1p-dependent manner (Ho, 2000)(Trotta, 2003). Crm1p belongs to the importin-β family and exports Leucine-rich nuclear export signal-containing proteins from the nucleus into the cytoplasm. Efforts have also been made to understand export of the small subunit. While the small subunit also relies on the Crm1p pathway, no comparable 40S subunit export adaptor has yet been identified.

Nmd3p is an essential 59 kDa protein that is 519 amino acids in length. A consensus Leucin-rich NES is located within the C-terminal portion of Nmd3p. Leucine-rich NESs are typified by those of HIV-1 Rev protein and protein kinase A inhibitor (PKI) (Kutay, 2005)(Fischer, 1995)(Hauer, 1999). These Leucine-rich NESs have been well characterized as substrates for Crm1p. In the nucleus, the stable interaction of Crm1p with a NES requires the cooperative binding of RanGTP, resulting in the assembly of a stable ternary export complex that is ready for translocation through the NPC channel. After its passage through the NPC channel, the export complex is then dissociated upon GTP hydrolysis of RanGTP to RanGDP (Bischoff, 1995)(Lounsbury, 1997). In this sense, effector molecules that modulate the nucleotide binding status of Ran are positioned in different cellular compartments. In the nucleus, the chromatin-bound nucleotide exchange factor RCC1 (Prp20p) loads GTP to Ran, thus stimulating the formation of a stable export complex (Gorlich, 1996). Conversely, Ran GTPase activating protein 1 (RanGAP1) and RanGTP-binding proteins (RanBP1) are exclusively localized in the cytoplasm. Both stimulate RanGTP hydrolysis cooperatively with Ran and dissociate the export complex (Bischoff, 1994)(Bischoff, 1995)(Klebe, 1995).

As work has continued on the 60S subunit export system, it has become apparent that the mechanism is more complicated then what is described above. Loading of Nmd3p onto the 60S subunit and the subsequent binding of Crm1p and RanGTP allows the establishment of the export quaternary complex (Nmd3p/60S subunit/Crm1p/RanGTP). While Nmd3p binding to the 60S subunit (Thomas, 2003)(Ho, 1999) and the interaction between Nmd3p, Crm1p and RanGTP have been reconstituted *in vitro* ((Thomas, 2003) and Kallstrom and Johnson, unpublished), no such Nmd3p/60S subunit/Crm1p/RanGTP quaternary complex has been successfully established thus far ((Thomas, 2003)(West, 2007) and Kallstrom and Johnson, unpublished). These results suggested that additional factors exist are required to recapitulate the export machinery.

Upon formation of the export complex, Crm1p transports 60S subunits to NPCs for export. However, subsequent translocation of this huge RNP through the channel of the NPC would pose another challenge for cells. Taking into account that the size of a 60S subunit almost reaches the upper limit of the NPC channel (~30nm), its passage through the NPC may require additional export factors for efficient export (also refer to section 5.4 for detailed discussion). (For a given yeast cell growing at log phase, more than 2000 ribosomes are synthesized per minute (Warner, 2001), with a nuclear export rate of about 25 ribosomes per minute (Winey, 1997)). Recent analysis of the *Dyctiostelium* NPC by cryo-electron tomography revealed distinct structural states of the NPC (Beck, 2004). It has been suggested that such flexibility of the NPC structure represents its accommodation for translocation of large cargos. Beyond the steric problem of translocating large cargos bulk, the second challenge is the intrinsic hydrophobic nature inside the NPC channel that would impede its passage. It has been reported that particularly large cargos require multiple receptors

for efficient export (Ribbeck, 2002). In agreement with this view, it has been postulated that additional factors exist and function as "export receptors" to promote the physical translocation of the 60S subunit through the NPC channel.

Finally, the dissociation of the 60S subunit export complex at the NPC sets the stage for completing its departure from the nucleus. One nucleoporin sub-complex composed of Nup82p-Nup159p-Nsp1p has been shown previously to be required for Crm1p-mediated export (Fornerod, 1997)(Askjaer, 1999). The Nup82p sub-complex is located at the cytoplasmic face of the NPC and acts as a terminal-binding site for disassociation of Crm1p-export complexes at NPCs (Kehlenbach, 1999). Strikingly, mutations within this sub-complex caused accumulation of Nmd3p as well as pre-ribosomal particles in the nucleoplasm (Gleizes, 2001)(West, 2007). Moreover, a stable interaction between the Nup82p sub-complex, Crm1p and conditional *nmd3* NE (nuclear envelope-associated) mutants has also been observed (West, 2007). This aberrant behavior is reminiscent of that of a supraphysiological NES peptide, whose high affinity for Crm1p is independent of RanGTP and prevents it from releasing from the NPC (Engelsma, 2004). Notably, *nmd3* NE mutants are defective in 60S subunit binding. Thus, the persistence of *nmd3* NE mutants and Crm1p on the Nup82p sub-complex suggests that the ribosome itself, or other factors on it, contribute to the disassembly of the export complex from NPC (West, 2007).

5.3 Results

5.3.1 Screen for mutations that are synthetic lethal with *arx1Δ*

During characterization of the Nmd3p-60S subunit complex, several additional non-ribosomal proteins were identified (Kallstrom, 2003). Chapters 3 and 4 describe mechanisms of recycling Arx1p from the cytoplasm but not its function on

60S subunits. Here, I have investigated its role in the nucleus. I decided to begin this work by identifying other genes that functionally interact with Arx1p. Genetic interactions between genes can provide insights into the function of a gene by identifying functionally related pathways. Considering that Arx1p is not essential and that an *arx1Δ* mutant displayed only a mild growth defect, a synthetic lethality screen appeared to me as one of the most feasible means to identify functionally related genes (Kranz, 1990). This scheme has been widely applied in yeast to establish complex functional networks between proteins (Costigan, 1992)(Care, 2004). With its potential roles in the 60S subunit biogenesis, I hoped to isolate non-lethal mutations that would exacerbate the phenotype of an *arx1Δ* mutant. The identification of such *ARX1* interacting genes would hopefully suggest functions for Arx1p.

The classic synthetic lethality screen performed in yeast is monitored by colony color. Briefly, this screen is carried out in an *ade2 ade3 ura3* yeast strain with the gene of interest deleted in the genomic locus but carried by an *ADE3 URA3* based plasmid. Yeast cells with mutations in the *ADE2* gene will cause accumulation of a red pigmented intermediate 5-aminoimidazole ribonucleotide (AIR) in the adenine biosynthesis pathway. However, the red phenotype of an *ade2* mutant can be masked by mutations in the *ADE3* gene, which acts upstream of Ade2 (5-aminoimidazole ribonucleotide carboxylase). Thus the *ade2 ade3* genotype is non-pigmented (white), whereas the *ade2 ADE3* genotype will give rise to red colonies. Under no selection pressure, random loss of the wild type *ADE3 URA3* plasmid from the *ade2 ade3* strain will result in a color change from red to white, reflecting the status of plasmid maintenance in the cells.

UV mutagenesis was carried out in an *arx1Δ ade2 ade3 ura3* strain that expresses an *ARX1 ADE3 URA3* plasmid. From about 34,300 mutagenized colonies

107

that were screened, approximately 490 solid red colonies were selected for further characterization. (Refer to Methods and Materials section 2.3.2 for detailed information with respect to experimental procedures.)

5.3.2 Elimination of putative *ade3* revertants and convertants

All solid red isolates were restreaked on YPD medium to confirm their "solid" phenotype. Solid red colonies were then tested for their sensitivity to 5-fluoroorotic acid (5-FOA). *URA3* encodes orotine-5'-monophosphate decarboxylase that converts non-toxic 5-FOA into toxic 5-flurouracil. Because genomic mutations that are synthetic lethal with *arx1Δ* will be unable to lose the plasmid-borne copy of *ARX1*, these mutants will be sensitive to 5-FOA due to the *URA3* gene carried on the same plasmid. 5-FOA resistant colonies that are viable after loss of the *URA3*-containing plasmid were eliminated and considered as non-plasmid dependent mutations. These solid red, 5-FOA resistant colonies may be generated via gene conversion between the plasmid borne *ADE3* gene to the genomic *ade3* loci. 11 potential *URA3*-plasmid dependent synthetic lethal mutants were identified by their 5-FOA sensitivity and subjected to further analysis.

5.3.3 Identification of recessive *ARX1*-dependent synthetic lethal mutants

These potential mutants were then tested for their dependence on *ARX1*. An *ARX1*-containing *LEU2* plasmid was transformed into the mutants. Selection of *LEU2 ARX1* plasmid should allow loss of the *URA3 ARX1* plasmid and a red/white sectored phenotype on Leu- low Ade dropout medium. Mutants that were unable to lose the *URA3 ARX1* plasmid must rely on genetic elements of the plasmid other than *ARX1*. Up to this point, four isolated colonies, which were solid red, 5-FOA sensitive and

sectored after the *LEU2-ARX1* plasmid transformation, were identified and considered as true mutants that are synthetic lethal with an *arx1Δ* mutant.

The four synthetic lethal mutants were mated to an *ade2 ade3 arx1Δ* mutant of the opposite mating type. Diploids were then scored for color. Retention of the *URA3*-plasmid would indicate a dominant mutation. All four mutants behaved as recessive mutants and were pursued for further analysis.

5.3.4 Cloning of *arx1Δ* synthetic lethal mutants by complementation

Because the mutagenized strains likely have multiple mutations in their genomes, it is possible that the synthetic lethality with *arx1Δ* is due to mutations of more than one gene. To eliminate mutants containing multiple mutations contributing to the phenotype, the previously mated diploids that were homozygous for *arx1Δ* and heterozygous for synthetic lethality mutations (from section 5.3.3) were sporulated and dissected. Spore clones were analyzed for red/white color and on 5-FOA plates for sensitivity. Single mutations should segregate with a 2:2 ratio of white to red colonies and 2:2 ratio of 5-FOA resistance to sensitivity. All four clones displayed a 2:2 segregation pattern for color and 5-FOA sensitivity assay, indicating a single locus conferring *arx1Δ* synthetic lethality within each of mutants.

To identify specifically which gene, when mutated, was synthetic lethal with *arx1Δ*, a *LEU2* centromeric yeast genomic library was transformed into the synthetic lethal mutant strains to identify complementing clones. Transformants on Leu- low Ade dropout media were scored by sectoring and 5-FOA resistance. Complementing plasmids obtained by this means could contain the wild type allelic of the genomic locus of the synthetic lethality mutation or simply *ARX1*. Alternatively, complementation could be attributed to a dosage suppressor. Plasmids containing

ARX1 were eliminated based on restriction digest analysis and only those that displayed distinct digestion patterns were retransformed into the synthetic lethality mutant strains to confirm the red/white sector phenotype. Plasmids were then submitted for sequencing using primers specific to the plasmid vector-genomic DNA insert junction. Although I attempted to clone all four strains, I was successful with only two mutants: SYL118 and SYL348.

5.3.5 Identification of *arx1Δ* synthetic lethal clone SYL118

The SYL118 mutant was synthetic sick but not synthetic lethal with an *arx1Δ* mutant. BLAST search against GeneBank revealed that the SYL118 complementing clone contained a DNA insert spanning the *NUP120* gene. *NUP120* encodes a nucleorporin within the well-characterized Nup84p sub-complex in yeast and has been shown to be involved in the assembly of central core of NPC and the maintenance of NPC architecture (Aitchison, 1995)(Heath, 1995). Complementation of SYL118 was indeed due to *NUP120* but not other genes from the same genomic DNA insertion since the SYL118 strain could also be complemented by *NUP120* alone on a plasmid. In addition, SYL118 also exhibited similar growth defects as the null *nup120* strain. Both showed slow growth at 25 ℃ or 30 ℃ and were dead at 37 ℃ (Figure 5.1A). The SYL118 mutant allele was sequenced and found to contain a one nucleotide deletion at G3065 in the *NUP120* open reading frame which is 3113bp. This mutation causes a premature stop codon at A3082, resulting in a truncated protein lacking the C-terminal 16 amino acids. The C-terminal portion of Nup120p is predicted to be α-helical and is thought to be responsible for its NPC anchoring (Devos, 2006). Thus, defects in this portion of the protein may impair its proper

assembly into the NPC and affect NPC architecture in general, resembling that of a *nup120* null mutant. Lastly, the genetic interaction between *ARX1* and *NUP120* was confirmed by a cross of an *arx1Δ* strain to a *nup120Δ* strain. The double deletion strains displayed a severe growth defect (Figure 5.1B).

A.
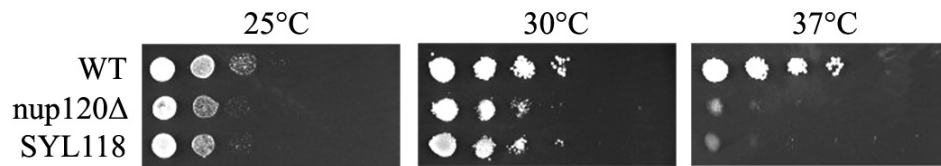
B.
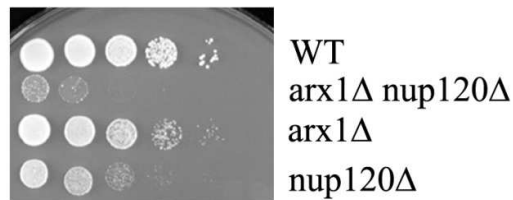
Figure 5.1 Identification of *NUP120* as an *arx1*Δ synthetic lethality player

(A)   Strain SYL118 phenocopies a *nup120* null mutant. Wild type strain, *nup120*Δ strain and strain SYl118 were grown on YPD plate at various temperatures. Growth defects were observed for both *nup120*Δ strain and strain SYl118 at semi-permissive (25℃) and non-permissive (37℃) temperature. (B) *arx1*Δ is synthetic sick with *nup120* mutant. Tetrads derived from a cross of *arx1*Δ *nup120*Δ were grown on YPD plates and the severe growth defect of a double mutant of *arx1*Δ *nup120*Δ can be visualized.

5.3.6 Synergistic effects of *arx1Δ* and nucleoporin mutants

Nup120p belongs to the Nup84p sub-complex, comprising the central core of the NPC, a spoke complex perforating the nuclear envelope. Unlike the FG-repeat Nups, which function directly in cargo transport through the NPC channel, the Nup84p-subcomplex lacks karyopherin binding motifs and is thought to act as structural constituent of the NPC architecture (Suntharalingam, 2003)(Wente, 2000). Deletion of this type of nucleoporin not only causes clustering of NPCs but also affects nuclear pore assembly (Heath, 1995)(Siniossoglou, 2000).

Identification of a genetic interaction between *NUP120* and *ARX1* was not a surprise. Despite the fact that the initial characterization of *NUP120* revealed a role in mRNA export (Aitchison, 1995)(Heath, 1995), subsequent analysis has also implicated its involvement in 60S subunit export (Stage-Zimmermann, 2000). *NUP120*, however, is dispensable for cell viability under normal growth conditions, but is essential at elevated temperatures.

Since both *arx1Δ* and *nup120Δ* have defects in 60S subunit export, it is likely that the double mutant is lethal because of an enhanced defect in export. To examine export in the double mutant requires conditional expression of one of the genes. For this reason, I engineered a rapidly degradable Arx1p construct by fusing it to a ubiquitin moiety under the inducible galactose promoter (Dong, 2004) (P_{GAL}-UBI-R-ARX1) (Figure 5.2). The ubiquitin moiety can be co-translationally cleaved, resulting in rapid degradation of the remaining Arx1p protein through the N-end rule pathway (Park, 1992). Expression of this rapidly degradable Arx1p construct can be induced by culturing cells in galactose containing medium and, conversely, can be repressed in the presence of glucose. As a control, another stable Arx1p construct, designated as P_{GAL}-UBI-M-ARX1, was engineered by replacing the

destabilizing Arginine with a stabilizing Methionine. To monitor expression of these Arx1p expression constructs, a fusion of either GFP or 13MYC was introduced in frame to the C-terminus of Arx1p. Using this strategy, I hoped to analyze the synergistic effect of *arx1Δ nup120Δ* on 60S subunit export.
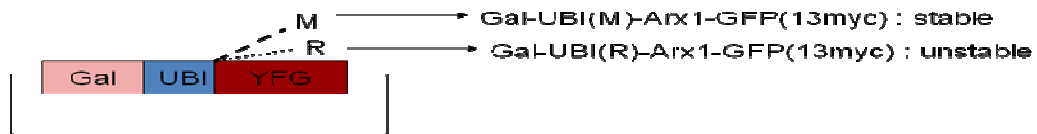
Figure 5.2 Cartoon depicting UBI-Arx1p constructs

Degradable Arx1p constructs were designed as above according to Dong *et al.* 2004. Two unstable Arx1p constructs were made: (Gal-UBI(R)-Arx1-GFP and Gal-UBI(R)-Arx1-13MYC). As controls, two other unstable Arx1p constructs were made as follows: Gal-UBI(M)-Arx1-GFP and Gal-UBI(R)-Arx1-13MYC.

To verify the rapid degradation effect of these Arx1p constructs, I first monitored the Arx1p-GFP signal by microscopy upon shifting cells from media containing galactose (induced) to glucose (repressed). The expression level of the P_{GAL}-UBI-R-ARX1-GFP construct was barely detectable even when it was driven by the galactose promoter (Figure 5.3), indicating a very low level of protein. Side by side comparison revealed that the stable P_{GAL}-UBI-M-ARX1-GFP construct was expressed at a relatively high level in galactose media and the signal diminished after cultures were switched to glucose media for two hours (Figure 5.3A). The effect of ubiquitin-mediated reduction of Arx1p expression levels was also monitored by Western blotting using the myc-tagged constructs (Figure 5.3B). Consistent with what was observed from the GFP versions, the P_{GAL}-UBI-M-ARX1-13MYC construct revealed a sustained protein level whereas the P_{GAL}-UBI-R-ARX1-13MYC construct produced an almost undetectable protein signal after repression for less than an hour.

These two degradable Arx1-GFP constructs with varied protein expression levels *in vivo* also yielded different levels of complementation of strain SYL118 (data not shown). The stable P_{GAL}-UBI-M-ARX1-13MYC construct supported cell viability better than the unstable P_{GAL}-UBI-M-ARX1-13MYC construct on galactose plates, indicating that a substantiated Arx1p protein level is required in the context of a *nup120* mutant.
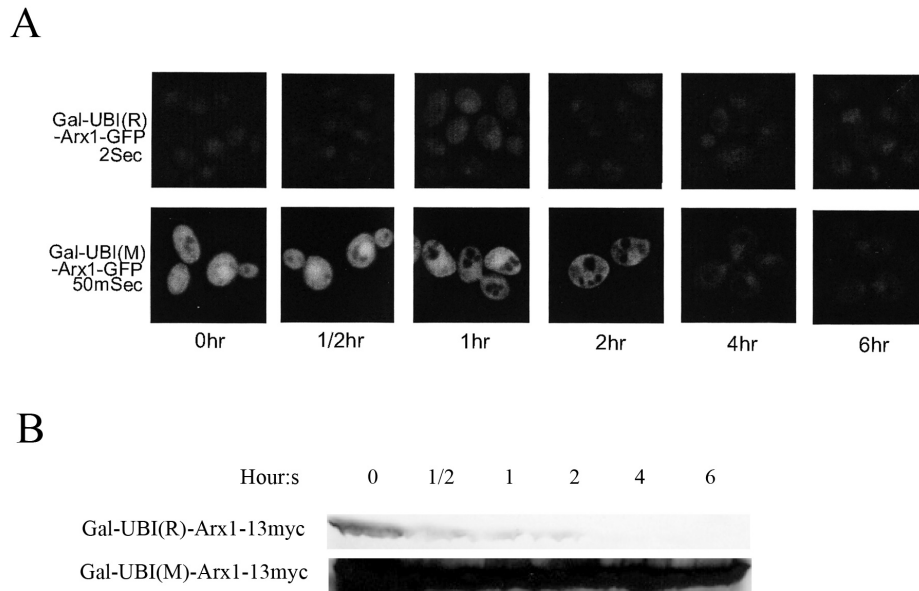
Figure 5.3 Expression of degradable Arx1p constructs

(A)   Time course for Gal-UBI-Arx1-GFP expression in glucose containing media. Wild type strain (AJY1911) carrying either Gal-UBI(M)-Arx1-GFP (pAJ1480) or Gal-UBI(R)-Arx1-GFP (pAJ1483) plasmid were cultured in galactose containing media to mid-log phase and transfer to glucose containing media for various time before they were subjected to microscopy. Note that different exposure times were applied to samples harboring different constructs. (B) Expression of regulatable Arx1-13MYC expression constructs. Wild type cells (AJY1911) harboring either Gal-UBI(M)-Arx1-13MYC (pAJ1481) or Gal-UBI(R)-Arx1-13MYC (pAJ1484) plasmid were cultured in galactose containing media to mid-log phase and transfered to glucose containing media for various times before they were collected and subjected to Western blotting using an anti-myc antibody.

In order to investigate the effect of the *arx1Δ nup120Δ* double mutant on 60S subunit export, I monitored the localization of Rpl25p and Nmd3p. Strain SYL118 harboring the degradable Arx1p construct: P_{GAL}-UBI-R-ARX1-13MYC or P_{GAL}-UBI-M-ARX1-13MYC was co-transformed with either an Nmd3p-GFP or a Rpl25p-eGFP plasmid. Cells were shifted from galactose media to maintain Arx1p expression to glucose media and aliquots were taken at different time points for microscopy. As shown in Figure 5.4A, cells bearing the unstable P_{GAL}-UBI-R-ARX1-13MYC construct revealed a strong nuclear enrichment for Nmd3p even in galactose (very low level of Arx1p expression); however, the nuclear retention of Rpl25p-eGFP was only observed when cultures were shifted to glucose media (repression of Arx1p expression). This result is inconsistent with previous finding presented by Stage-Zimmermann *et al,* in which case *nup120Δ* alone is sufficient to block 60S subunit export (Stage-Zimmermann, 2000). Though strain SYL118 displayed a similar growth defect as that of a *nup120Δ* mutant, it is possible that these two mutants have slightly different effects on 60S subunit export. Alternatively, the discrepancy of these results could derive from using different 60S subunit ribosomal proteins as export reporters, as these authors also claimed that a more sensitive readout can be obtained using Rpl11p rather than Rpl25p. In contrast, repression of the stable P_{GAL}-UBI-M-ARX1-13MYC construct did not reveal any severe 60S subunit export defect (Figure 5.4B), although Nmd3p accumulated in the nucleus after shifting cultures to glucose containing medium for two hours. Taken together, these results suggested that deletion of *NUP120* exacerbates *arx1Δ* phenotype, resulting in a block of the Nmd3p-mediated 60 subunit export.

117

A.
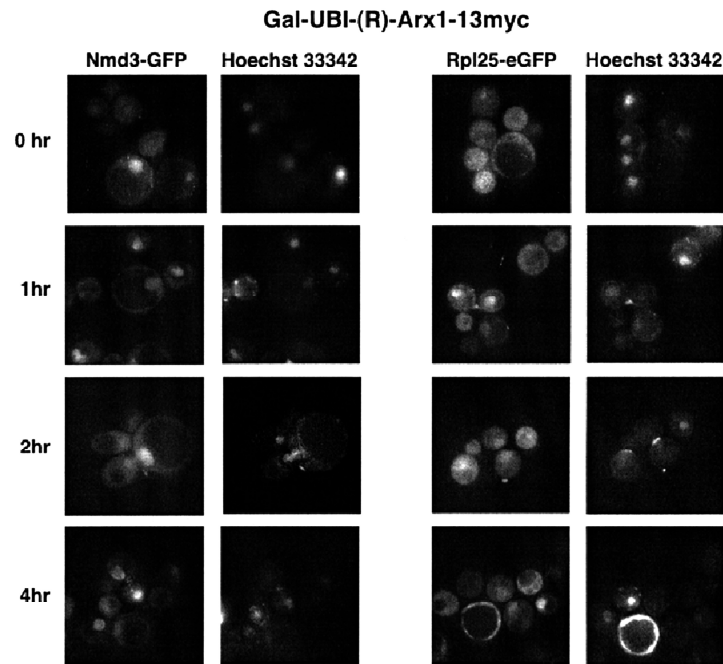
Figure 5.4 Localization of Nmd3p and Rpl25-eGFP in SYL118 after repression of Arx1p expression

(A) Stain SYL118 transformed with the unstable Gal-UBI(R)-Arx1-13MYC (pAJ1484) and Rpl25-eGFP (pAJ908) or Nmd3p-GFP (pAJ755), was cultured in galactose containing media to mid-log phase and transfered to glucose containing media for various time before they were subjected to microscopy. Nuclear DNA was stained with Hoechst 33342.

B.
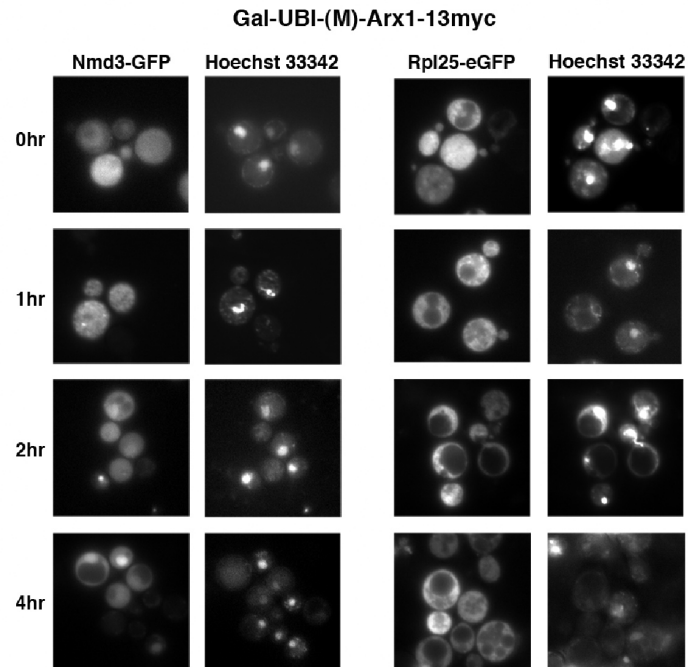
Gal-UBI-(M)-Arx1-13myc

(B)   Stain   SYL118   transformed,   with   stable   Gal-UBI(M)-Arx1-13MYC
(pAJ1481) and Rpl25-eGFP (pAJ908) or Nmd3p-GFP (pAJ755), was cultured in
galactose containing media to mid-log phase and transfered to glucose containing
media for various times before they were subjected to microscopy. Nuclear DNA
was stained with Hoechst 33342.

Nucleocytoplasmic transport of macromolecules across nuclear pore complexes is largely dependent on karyopherin-mediated processes, and many nucleoporins have been identified physical docking surfaces for transport receptors. For example, Nup159p and Nup1p have been shown to interact with Crm1p and Kap95, respectively (Allen, 2001)(Allen, 2002). In addition, Nup159p and Nup116p have both been shown to interact with the NXF family of mRNA export transporters, designated as Mex67/TAP. And more recently, the yeast Nup159-Nup82-Nsp1 subcomplex homolog of the vertebrate Nup214-Nup88-Nup62 subcomplex has also been implicated in mediating ribosome export (Bernad, 2006).

Unlike the nucleoporins described above, *NUP120* has not been identified as a docking site for transport cargos; however, it is known to play an important function in the maintenance of NPC architecture (Aitchison, 1995) and the RanGTP gradient across the nuclear envelope (Gao, 2003). Thus disruption of Nup120p at NPCs may simply produce global effects disturbing nucleocytplasmic transport in general, and subsequently affect ribosome export. To distinguish between specific and indirect effects on 60S subunit export generated by deletion of *NUP120*, I decided to look for possible synergistic effects between other nucleoporin mutants and an *arx1Δ* mutant.

The yeast NPC can be grouped into several nucleoporin sub-complexes based on proteomic and biochemical analyses (Suntharalingam, 2003). The best characterized sub-complexes among these are the Nup84p sub-complex (Nup84p, Nup85p, Nup120p, Nup145p, Seh1p, and Sec13p), the Nup82p sub-complex (Nup82p, Nup159p, and Nsp1p), the Nup53p sub-complex (Nup53p, Nup59p, and Nup170p) and finally the Nic96p sub-complex (Nic96p, Nup49p, Nup57p, and Nsp1p) (Illustration 5.1). I crossed an *arx1Δ* mutant to a panel of ten different nucleoporin mutants that belong to different sub-complexes. Among the ten mutants tested, *ARX1*

interacted strongly with *NUP82*, *NUP84, NUP120*, *GLE2* and *NUP133*, moderately with *NIC96* and *NUP42*, but not with *NSP1*, *NUP100* and *NUP116* (Table 5.1)(also refer to Chapter 2.3.3 for detailed information with respect to methods and materials). Taken together, these results revealed that *ARX1* could genetically interact with a broad range of nucleoporins that are involved in 60S subunit export, suggesting that Arx1p is directly involved in the NPC-mediated 60S subunit export.

Table 5.1 Nucleoporin mutants that were tested for genetic interactions with *arx1Δ*

NPC component	Localizatoin	Genetic interaction with *arx1Δ*	Roles in ribosome export
Nup82	Cytoplasmic	Strong	Yes
Nup84	Symmertic	Strong	No
Nup133	Symmertic	Strong	Yes
Nup42	Cytoplasmic	Weak	No
Nsp1	Symmertic	No	Yes
Nic96	Symmertic	Weak	Yes
Nup100	Cytoplasmic -biased	No	No
Nup116	Cytoplasmic -biased	No	Yes
Nup120	Symmertic	Strong	Yes
Gle2	Cytoplasmic	Strong	?
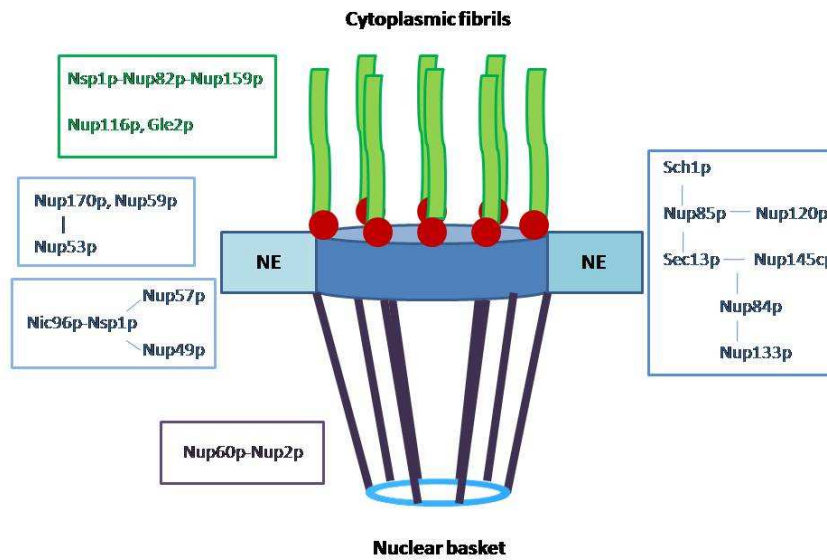
Illustration 5.1 Architecture of the yeast NPC

A typical yeast NPC is shown above and comprises three major sub-structures: cytoplasmic fibrils, a central disc and a nuclear basket. Interactions between different nucleoporins within a sub-complex are indicated by dashes. Different nucleoporin sub-complexes are grouped and indicated by different colors. Green: cytpoplasmic bias Nup sub-complexes; Blue: symmetric distributed Nup sub-complexes; Purple: Nuclear bias Nup sub-complexes. (Adopted from Suntharalingam and Wente 2003)

5.3.7 Identification of *arx1Δ* synthetic lethality clone SYL348

Isolate SYL348 was complemented by a genomic clone containing a fragment of chromosome VIII. This plasmid DNA covered several genes; including *THP2*, *MTG2*, *DBP8*, *NMD3* and *ATG7*. Among these, *NMD3* was the likely candidate. Indeed, strain SYL348 could be complemented by a functional NMD3 plasmid (data not shown). To determine the mutation in *NMD3* that causes synthetic lethality, the genomic locus of *NMD3* from strain SYL348 was amplified by PCR and subjected to DNA sequencing. Sequencing results revealed that SYL348 contained a mutation in *NMD3* converting T1514 to A. This mutation introduces a stop codon, eliminating the last 14 amino acids of the protein, and produces a truncated Nmd3 protein: *Nmd3Δ14* (Figure 5.5).

A

Nmd3p

399 419   496   505

cc cc cc   cc   NLS   coil   NES

1   518

NMD3   D E D E D E D A P Q I N I D E L L D E L D E M T L E D G V E N T P V E S Q Q   518
nmd3#348   D E D E D E D A P Q I N I D E L L D E L D E M T - - - - - - - - - - - - - -   504
           *

B

Protein	NES sequence ΦX$_{2-3}$ΦX$_{2-3}$ΦXΦ
PKI	LAL KLAGLDI
Sc Nmd3 (1)	I N I DEL LDEL
Sc Nmd3 (2)	LLD ELDEMTL
Hs Nmd3	LAEMLED LHI

C

nmd3-AA: A A
                             ↑ ↑
aa: 491   500
            I N I DEL LDEL
             ↓   ↓   ↓
nmd3-AAA :   A   A   A
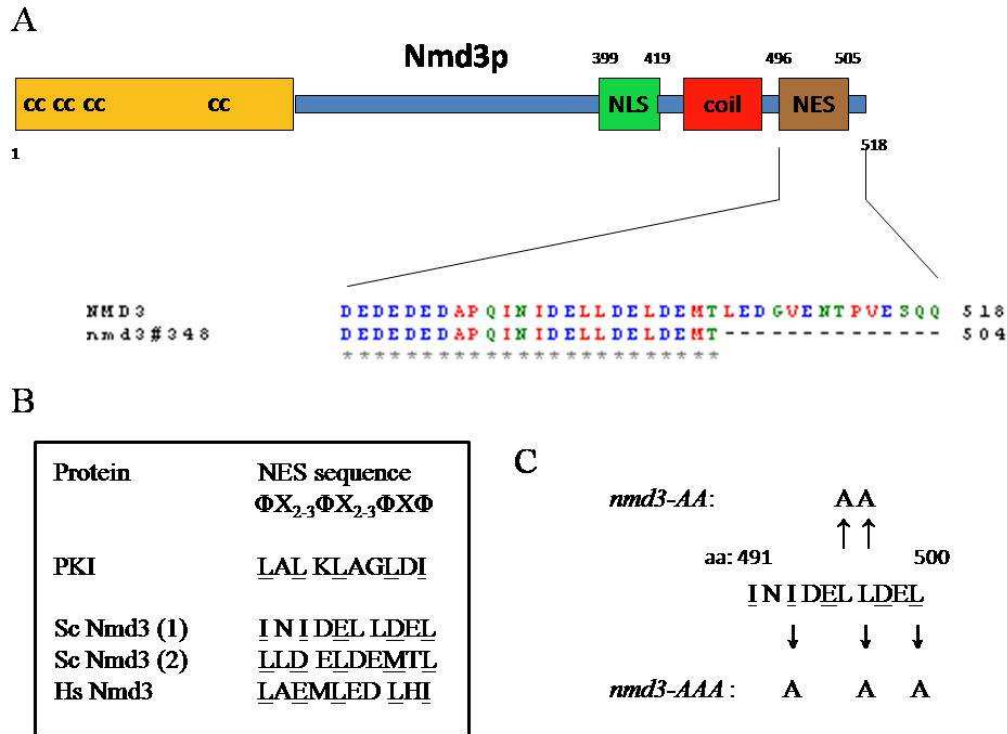
Figure 5.5 Cartoon of Nmd3ps' NES

(A) The **C**-terminal portions of Nmd3p sequence encoded by wild type strain or strain SYL348 were aligned. A premature stop codon eliminates the last 14 amino acids of Nmd3p from strain SYL348, resulting in a truncated protein. (B) An alignment of the NESs of yeast Nmd3p (sc) and human Nmd3p (Hs). (1) The previously suggested NES from aa 491 to 500. (2) The revised Nmd3p's NES from aa 496 to 505. (C) The *nmd3-AA* and *nmd3-AAA* mutant. Arrows indicate corresponding mutated residues.

5.3.8 *arx1Δ* is synthetic lethal with *nmd3* mutants

Isolate SYL348 encodes a truncated Nmd3p. A nonsense mutation could result in a truncated protein. Alternatively, nonsense codons can also target mRNAs for rapid degradation (NMD, nonsense-mediated decay) (Lykke-Andersen, 2001)(Gonzalez, 2001). Thus a trivial explanation for the synthetic lethal phenotype was reduced protein expression. However, Western blotting for Nmd3p from extract prepared from wild type and SYL348 cells indicated no significant change in protein levels (data not shown), suggesting that the truncated *Nmd3Δ14* protein is not unstable and the synthetic lethal effect is not due to insufficient Nmd3p expression in the cells.

Previously, our lab had suggested a nuclear export signal in Nmd3p from amino acids 491 to 500 (INIDELLDEL) (Figure 5.5B). This region has been shown to play an important role in Nmd3p localization and function and is mediated by the Crm1p export pathway (Ho, 2000). Furthermore, mutations of hydrophobic residues in this region (I493A, L497A and L500A) (Figure 5.5C) have also been shown to impair the 60S subunit export (Hedges, 2005). However, *Nmd3Δ14* deletes a Leucine outside the initially proposed NES. Reexamination of the sequence of Nmd3p showed that it was possible to shift the putative NES of Nmd3p further downstream, from amino acids 496 to 505 (LLDELDEMTL) (Figure 5.5A and B), which conforms well to a consensus Leucine rich NES ($\Phi X_{2-3}\Phi X_{2-3}\Phi X\Phi$). Indeed, this speculation was supported by several observations. First, the *Nmd3Δ14* mutant showed a severe growth defect, suggesting a vital function provided by the last few residues of the protein. Furthermore, microscopy revealed that the truncated *Nmd3Δ14* protein is trapped in the nucleus, and consequently caused a block of 60S subunit export (Figure

5.6A). To ask if loss of L505 was the important defect, an *nmd3* mutant was made in which L505 was changed to A in the context of the full length protein. Strikingly, the *Nmd3L505A* mutant was barely viable (Hedges, 2006). Moreover, the *Nmd3L505A* mutant protein was trapped in the nucleus, similar to the *Nmd3Δ14* mutant (Hedges, 2006). Furthermore, both *Nmd3L505A* and *Nmd3Δ14* mutants caused a defect in the 60S subunit export, as monitored by Rpl25-eGFP (Figure 5.6B). Taken together, these results demonstrated an important function of L505 in supporting nuclear export of 60S subunits.

The synthetic lethal effect of *arx1Δ Nmd3Δ14* suggested that Arx1p's function is related to 60S subunit export. In this view, I also asked if *arx1Δ* would display specific genetic interactions with previously identified *nmd3* mutants (*nmd3AA nmd3AAAA*, Figure 5.5C) that are defective for nuclear export. Not surprisingly, these *nmd3* NES mutants displayed strong synthetic effects with an *arx1Δ* mutant, supporting the idea that Arx1p functions coordinately with Nmd3p-NES in 60S subunit export (data not shown).

A.

WT   SYL348

anti-Nmd3

B.

WT   Nmd3Δ14a.a.   Nmd3L505A

Rpl25-eGFP
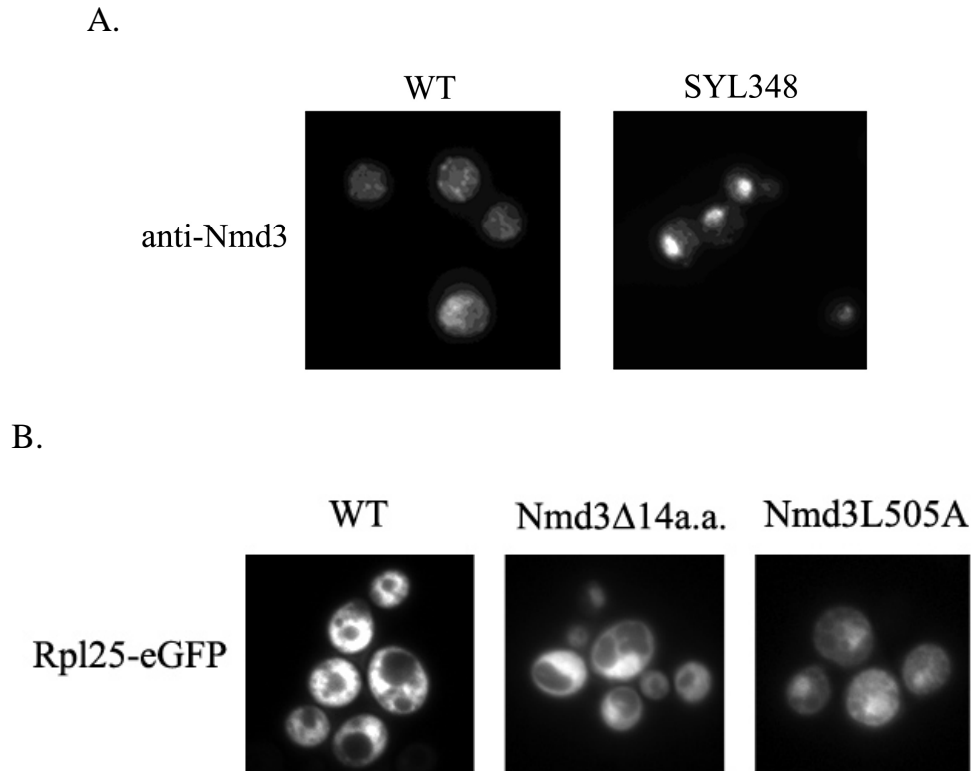
Figure 5.6 Cellular localization of *Nmd3Δ14* and its effect on 60S subunit export

(A)   Wild type (AJY1911) and strain SYL348 cells were cultured in YPD to mid-log phase and subjected to indirect immunofluoroscence for visualizing endogenous Nmd3p localization. (B) Wild type (AJY1911), srain SYL348 and strain AJY2110 carrying pAJ1593 (Nmd3L505A-13myc) as the only copy of Nmd3p were co-transformed with pAJ908 (Rpl25-eGFP). Cells were then cultured in selective media to mid-log phase and subjected to direct microscopy for visualization of GFP signal.

5.3.9 *arx1Δ* accumulates Nmd3p-Crm1p-60S subunit intermediates in the nucleus

Genetic interactions between Arx1p and various *nmd3* NES mutants suggested that Arx1p plays a role in the context of Nmd3p-mediated 60S subunit export. Nmd3p, as the Crm1-dependent 60S subunit export adaptor, binds to the 60S subunit in the nucleus to recruit Crm1p via its classic Leucine-rich NES. Whereas association of Nmd3p to either the 60S subunit or Crm1p has been documented, the assembly of Nmd3p-Crm1p-60S subunit ternary complexes has not been successful *in vitro.* These results implied that additional factors may be required for the assembly of the 60S subunit export complex.

Data above have suggested a role for Arx1p in 60S subunit export. My previous data showed that deletion of *ARX1* modestly trapped 60S subunits in the nucleus and also caused a mild growth defect (refer to Chapter 3). Furthermore, the situation can be worsened in conjunction with *nmd3* NES mutants. A likely possibility for Arx1p's function in this respect would be to assist Nmd3p-60S subunit export complex formation. In view of understanding the impact of Arx1p on Nmd3p-60S subunit export complex assembly, I first asked if Arx1p is involved in regulating Nmd3p-60S subunit association. Sucrose gradient sedimentation followed by Western blotting analysis revealed that Nmd3p remained associated with 60S subunits in an *arx1Δ* strain and the binding was virtually indistinguishable from that of a wild type strain (Figure 5.7A). These results indicated that Arx1p is not required for efficient recruitment of Nmd3p to the 60S subunit. In addition, an enriched nuclear signal of Nmd3p-GFP was observed in an *arx1Δ* strain (Figure 5.7B). Thus Nmd3p bound to 60S subunits accumulates in the nucleus in *arx1Δ* cells, suggesting that Arx1p acts after loading Nmd3p onto the 60S subunits.

A

WT   *arx1Δ*

Nmd3-GFP

B

WT   *arx1Δ*

A_{254}

sedimentation

anti-Nmd3p
anti-Rpl8p
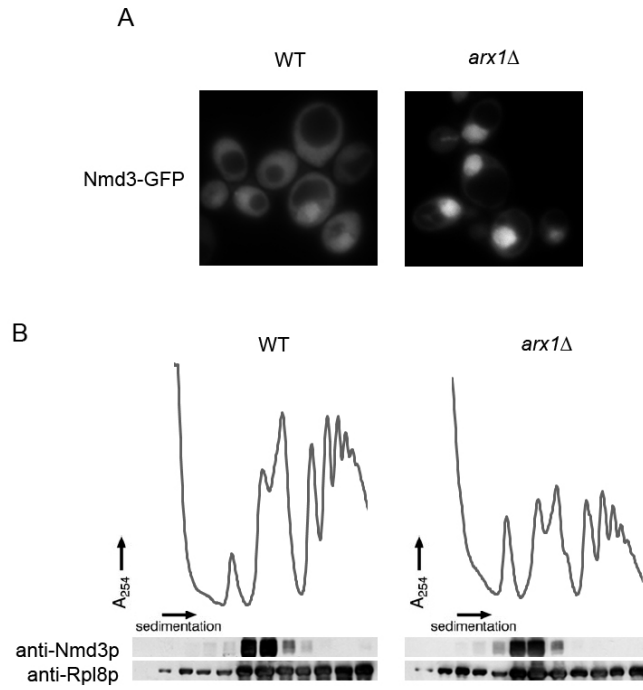
Figure 5.7 Nmd3p is enriched in the nucleus in *arx1Δ* mutant and remains bound to 60S subunits

(A) Cultures of AJY1911 (WT) and AJY1901 (*arx1Δ*) carrying pAJ582 (Nmd3-GFP) was grown to mid-log phase in selective media and the *in vivo* localizations of Nmd3 were monitored by fluorescence microscopy. (B) Lysates were prepared from AJY1911 (WT) and AJY1901 (*arx1Δ*) in the presence of cycloheximide (50 μg/ml) and fractioned on 7% to 47% sucrose gradients by ultracentrifugation. (refer to Chapter 2.1.2 for buffer conditions) Fractions were collected, and the absorbance at 254 nm was monitored continuously. Proteins were precipitated with trichloroacetic acid, separated by SDS-polyacrylamide gel electrophoresis, transferred to nitrocellulose membrane, and immunoblotted for Nmd3p or Rpl8p using specific antibodies.

Data presented so far suggested that cells lacking *ARX1* were impaired in 60S subunit export with 60S subunits trapped in the nucleus in an Nmd3p bound state. Considering that Arx1p genetically interacts with specific *nmd3* NES mutants, I speculated that Arx1p may be involved in modulating the accessibility of the NES of Nmd3p to Crm1p after loading onto the 60S subunit prior to export. The idea of a "regulated NES" was not unprecedented (Wesierska-Gadek, 2003)(Craig, 2002), and remodeling of Nmd3p's NES may regulate 60S subunit export complex formation.

Crm1p-cargo interactions are often very transient and cannot be easily observed *in vitro*. To address the prospect of Arx1p's involvement in modulating Nmd3p-Crm1p interaction, I took the advantage of utilizing a mutant *nmd3* containing a supraphysiological NES, Nmd3p-supraNES (West, 2007). Supraphysiological NESs were first identified from a screen carried out by Engelsma *et al* (Engelsma, 2004) in a screen for *in vitro* synthetic sequences that are capable of binding to Crm1p with high affinity in a RanGTP-independent manner. Replacement of Nmd3p's NES with a strong supraphysiological NES enhances the interaction between Nmd3p and Crm1p *in vitro* (West, 2007).

Cell extracts obtained from the wild type or *arx1Δ* strain carrying either Nmd3p-13myc or Nmd3p-supraNES-13myc and Crm1p-HA plasmids were subjected to affinity purification using anti-myc antibodies. The Nmd3p-specific co-immunoprecipitated complexes were then analyzed by SDS-PAGE followed by Western blotting to monitor Crm1p levels. As shown in Figure 5.8A, an enhanced Crm1p signal was observed in the Nmd3p-supraNES co-immunoprecipitated complex from the wild type strain (compare lane 1 to 3), consistent with the theory of a higher binding affinity for the supraphysiological NES. Interestingly, Crm1p signal from the Nmd3p co-purified complex is enriched in a strain lacking Arx1p (compare lane 1 to

2), and is even pronounced in Nmd3-supraNES-13myc's IP (compare lane 3 to 4). To further address if the Nmd3p co-purified Crm1p correlates with a 60S subunit-bound state, I carried out sucrose gradient sedimentation to identify possible co-sedimentation of Crm1p with 60S subunits. As seen in Figure 5.8B, an increased level of Crm1p was found to co-migrate with 60S subunits in an *arx1Δ* mutant. In combination with the microscopy work, these results suggest that a 60S subunit export intermediate containing Nmd3p and Crm1p accumulates in the nucleus in an *arx1Δ* mutant.

A
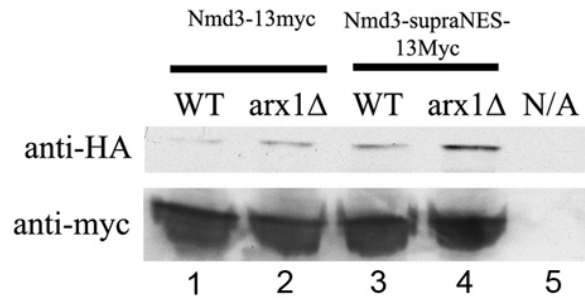
B
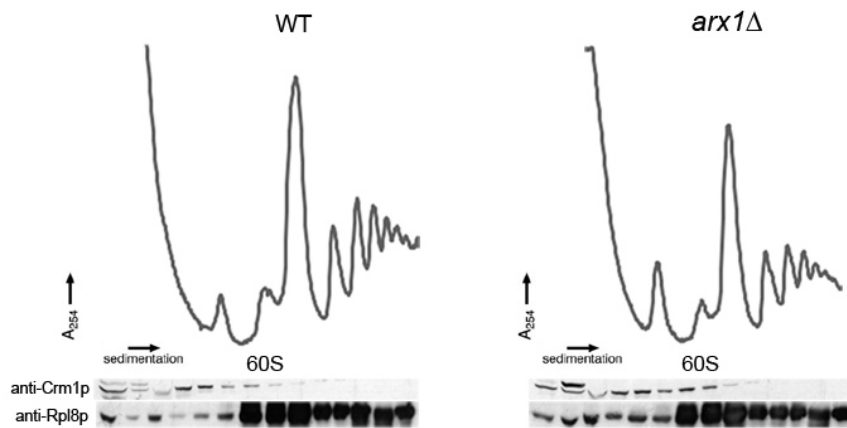
Figure 5.8 Arx1p affects Crm1p interaction with Nmd3p and 60S subunits

(A) Strains AJY1911 (wild type) and AJY1901 (*arx1Δ*) transformed with pAJ538 (Nmd3-13myc) or pAJ1594 (Nmd3-supraNES-13myc) and pAJ739 (Crm1T539C-HA) were cultured in selective media and collected at mid-log phase. Immunoprecipitations were carried out using anti-myc antibodies and subjected to Western blotting using anti-myc and anti-HA antibodies to monitor Nmd3p and Crm1p levels. (N/A: negative control) (B) Lysates from AJY1911 (WT) and AJY1901 (*arx1Δ*) carrying pAJ856 (Crm1-3HA) were prepared in the presence of cycloheximide (50 μg/ml) and fractioned on 7% to 47% sucrose gradients by ultracentrifugation. Fractions were collected, and the absorbance at 254 nm was monitored continuously. Proteins were precipitated with trichloroacetic acid, separated by SDS-polyacrylamide gel electrophoresis, transferred to nitrocellulose membrane, and immunoblotted for HA or Rpl8p using specific antibodies.

5.3.10 Arx1p interacts with nucleoporins

The data presented thus far suggested that Arx1p is needed for promoting the nuclear export of the Nmd3p-Crm1p-60S subunit intermediate. If so, how does Arx1p function? Because *arx1Δ* displayed synergistic effects with various nucleoporin mutants that are defective in 60S subunit export, one possibility is that Arx1p participates in the NPC passage of the 60S subunit export complex. In this sense, Arx1p can be involved in facilitating the recruitment of the 60S subunit export complex to the NPC or the subsequent translocation through the NPC channel.

The speculation of Arx1p's function at NPC was also inspired by a previous finding of Arx1p's interaction with two nucleoporins: Nup42p (a component of the cytoplasmic fibrils) and Nup100p (a component of the central transporter region) (Allen, 2001). In this assay, Allen and co-workers immobilized purified GST-fusion of various nucleoporins onto beads as bait to capture interacting proteins from yeast extracts. However, these results did not address if Arx1p interacts with nucleoporins directly or indirectly. Accordingly, I decided to test these interactions by the yeast two-hybrid system. For this reason, Arx1p fused to the GAL4 DNA binding domain (BD) and several nucleoporins fused to the GAL4 activating domain (AD) were transformed as pairs into a yeast two-hybrid reporter strain. Transformants were spotted onto selective media to identify possible interactions and scored for cell growth (refer to Chapter 2.3.4 for detailed information with respect to methods and materials). As seen in Figure 5.9, Arx1p showed specific interactions with Nup100p, Nup116p and week interaction with Nup57p. A panel of previously characterized nucleoporin-nucleoporin interactions was also included for comparison (Patel, 2007). Taken together, these results indicated that Arx1p is a true nucleoporin interacting partner.

136
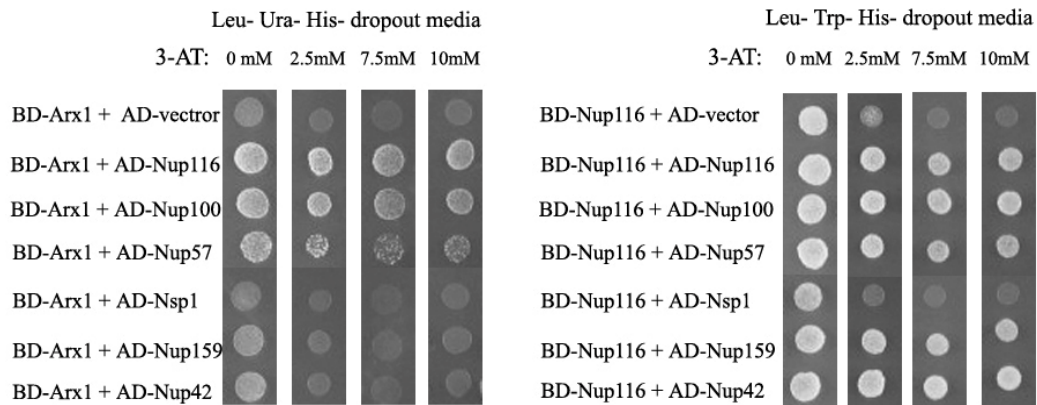
Figure 5.9 Arx1p interacts with nucleoporins

Yeast strain AJY951 containing plasmids that express Arx1 or Nup116 fusion to the Gal4-binding domain (BD) and various Nup protein fusions to the Gal4 activation domain (AD) were spotted onto selective media (Leu- Ura- His- dropout or Ura- Trp-His- dropout). Plates were incubated at 30 ℃ for 4 days. Positive interactions should drive expression of the *HIS3* reporter. Various concentrations of 3-AT were added to eliminate false-positives.

.

5.4 Discussion

In this chapter, I used a synthetic lethal screen to identify genes that functionally interact with *ARX1*. From this screen, two mutations were identified in two genes involved in 60S subunit export. Specifically, *arx1Δ* displayed synthetic lethality with an *nmd3* allele that is impaired for nuclear export. Moreover, deletion of *ARX1* exacerbated phenotypes of several Nmd3p-NES mutants, suggesting that Arx1p functions in the Nmd3p-NES mediated 60S subunit export pathway. In addition, synergistic effects were identified with several nucleoporin mutants that are implicated in 60S subunit export. Taken together, the results that deletion of *ARX1* led to nuclear accumulation of the Nmd3p-Crm1p-60S subunit intermediate and the interaction of Arx1p with nucleoporins suggest that Arx1p acts as an export receptor.

Why do pre-60S particles require multiple receptors? To answer this question, one should consider the nature of the karyopherin-mediated nuclear transport. Unlike passive transport that allows relatively free diffusion of small molecules (up to 20~40kDa) through NPCs, bi-directional transport of macromolecules between the nucleus and the cytoplasm requires transport receptors. These karyopherins interact with FG-repeats of the nucleoporins. These FG-repeats, present as: FG, GLFG and FXFG that are usually separated by spacers of different length. In addition to their hydrophobic nature, these FG-repeats are mostly natively unfolded and flexible, creating a hydrophobic meshwork that poses a selective mechanism for translocations through NPCs.

In view of karyopherin-mediated nuclear transport through NPCs, several models have been proposed. Among them, the "selective phase model" is now generally favored (Ribbeck, 2001). This model assumes that the nuclear envelope conduits filled with FG-repeats would provide a permeability barrier, which limits the

138

flux of macromolecules but can be compromised by receptors that can diffuse into the hydrophobic mesh. Transport receptors interact with FG-Nups with low-binding affinity; transiently dissolving the meshwork to allow passage of cargo through the NPC channel. In agreement with this, FG-repeats containing nucleoporins interact with karyopherins *in vitro* (Paschal, 1995)(Radu, 1995)(Clarkson, 1996)(Bachi, 2000). Furthermore, structural analysis by X-ray crystallography has explained the interactions between FG-repeats and transport factors at the molecular level. Particularly, the FG-repeats have been solved in complex with importin-β (Bayliss, 2002) and the mRNA export mediator TAP-NXT1 heterodminer (Grant, 2002). In both cases, the interactions between transport factors and NPCs seem to be hydrophobic, primarily mediated by the phenylalanine of FG-repeats and hydrophobic pockets within transport factors. Karyopherins are also notable for their large surface hydrophobicity (Ribbeck, 2002) that facilitates their movement through the hydrophobic channel of the NPC.

The same model for translocation can be applied to cases for large RNPs, such as the 60S subunit. Large molecules have been shown to be considerably delayed in their translocation through NPCs. However, such hindrance can be removed by increasing the receptor-to-cargo ratio (Ribbeck, 2002). Considering the complexity of 60S subunit and its large molecular size, approaching to the upper limit of the inner NPC tunnel, export of such large RNPs may also be enhanced by having multiple receptors.

Consistent with this speculation; the recent discovery by Yao et al. has illustrated a functional involvement of general mRNA export receptors, Mtr2p/Mex67p heterodimers, in the 60S subunit export (Yao, 2007). In this study, they suggested that a loop-confined heterodimeric surface on Mtr2-Mex67 binds to 5S

rRNA on the 60S subunit. This loop was also suggested to be on the opposite face of the predicted FG-repeat Nup binding sites on Mtr2-Mex67. In this sense, the Mtr2-Mex67 heterodimer acts as a "transport receptor", binding to the 60S subunit and interacting with nucleoporins simultaneously to shield unfavorable surfaces on the 60S subunit and promote translocation through the NPC. From this point of view, Arx1p's contribution in the passage of the 60S subunit export complex through the NPC channel may be analogous. It will be intriguing to determine binding sites of these factors on the 60S subunit surface, perhaps translocation-unfavorable exposed domains, to relate their possible function as translocation-prompting factors. Considering that Arx1p binding to pre-60S subunit particles is required at a step after recruitment of Crm1p to the Nmd3p-60S subunit complex and interacts with nucleoporins, I suggest that Arx1p acts as a third export adaptor for the 60S subunit.

References

Aitchison, J.D., Blobel, G. and Rout, M.P. (1995) Nup120p: a yeast nucleoporin required for NPC distribution and mRNA transport. *J Cell Biol*, **131**, 1659-1675.

Alcazar-Roman, A.R., Tran, E.J., Guo, S. and Wente, S.R. (2006) Inositol hexakisphosphate and Gle1 activate the DEAD-box protein Dbp5 for nuclear mRNA export. *Nat Cell Biol*, **8**, 711-716.

Allen, N.P., Huang, L., Burlingame, A. and Rexach, M. (2001) Proteomic analysis of nucleoporin interacting proteins. *J Biol Chem*, **276**, 29268-29274.

Allen, N.P., Patel, S.S., Huang, L., Chalkley, R.J., Burlingame, A., Lutzmann, M., Hurt, E.C. and Rexach, M. (2002) Deciphering networks of protein interactions at the nuclear pore complex. *Mol Cell Proteomics*, **1**, 930-946.

Amrani, N., Dong, S., He, F., Ganesan, R., Ghosh, S., Kervestin, S., Li, C., Mangus, D.A., Spatrick, P. and Jacobson, A. (2006) Aberrant termination triggers nonsense-mediated mRNA decay. *Biochem Soc Trans*, **34**, 39-42.

Andrews, D.W., Lauffer, L., Walter, P. and Lingappa, V.R. (1989) Evidence for a two-step mechanism involved in assembly of functional signal recognition particle receptor. *J Cell Biol*, **108**, 797-810.

Askjaer, P., Bachi, A., Wilm, M., Bischoff, F.R., Weeks, D.L., Ogniewski, V., Ohno, M., Niehrs, C., Kjems, J., Mattaj, I.W. and Fornerod, M. (1999) RanGTP-regulated interactions of CRM1 with nucleoporins and a shuttling DEAD-box helicase. *Mol Cell Biol*, **19**, 6276-6285.

Bachi, A., Braun, I.C., Rodrigues, J.P., Pante, N., Ribbeck, K., von Kobbe, C., Kutay, U., Wilm, M., Gorlich, D., Carmo-Fonseca, M. and Izaurralde, E. (2000) The C-terminal domain of TAP interacts with the nuclear pore complex and promotes export of specific CTE-bearing RNA substrates. *Rna*, **6**, 136-158.

Bai, S.W., Rouquette, J., Umeda, M., Faigle, W., Loew, D., Sazer, S. and Doye, V. (2004) The fission yeast Nup107-120 complex functionally interacts with the small GTPase Ran/Spi1 and is required for mRNA export, nuclear pore distribution, and proper cell division. *Mol Cell Biol*, **24**, 6379-6392.

Ban, N., Nissen, P., Hansen, J., Moore, P.B. and Steitz, T.A. (2000) The complete atomic structure of the large ribosomal subunit at 2.4 A resolution. *Science*, **289**, 905-920.

Bassler, J., Grandi, P., Gadal, O., Lessmann, T., Petfalski, E., Tollervey, D., Lechner, J. and Hurt, E. (2001) Identification of a 60S preribosomal particle that is closely linked to nuclear export. *Mol Cell*, **8**, 517-529.

Basu, U., Si, K., Deng, H. and Maitra, U. (2003) Phosphorylation of mammalian eukaryotic translation initiation factor 6 and its Saccharomyces cerevisiae homologue Tif6p: evidence that phosphorylation of Tif6p regulates its nucleocytoplasmic distribution and is required for yeast cell growth. *Mol Cell Biol*, **23**, 6187-6199.

Basu, U., Si, K., Warner, J.R. and Maitra, U. (2001) The Saccharomyces cerevisiae TIF6 gene encoding translation initiation factor 6 is required for 60S ribosomal subunit biogenesis. *Mol Cell Biol*, **21**, 1453-1462.

Bataille, N., Helser, T. and Fried, H.M. (1990) Cytoplasmic transport of ribosomal subunits microinjected into the Xenopus laevis oocyte nucleus: a generalized, facilitated process. *J Cell Biol*, **111**, 1571-1582.

Bayliss, R., Littlewood, T., Strawn, L.A., Wente, S.R. and Stewart, M. (2002) GLFG and FxFG nucleoporins bind to overlapping sites on importin-beta. *J Biol Chem*, **277**, 50597-50606.

Beck, M., Forster, F., Ecke, M., Plitzko, J.M., Melchior, F., Gerisch, G., Baumeister, W. and Medalia, O. (2004) Nuclear pore complex structure and dynamics revealed by cryoelectron tomography. *Science*, **306**, 1387-1390.

Becker, J., Melchior, F., Gerke, V., Bischoff, F.R., Ponstingl, H. and Wittinghofer, A. (1995) RNA1 encodes a GTPase-activating protein specific for Gsp1p, the Ran/TC4 homologue of Saccharomyces cerevisiae. *J Biol Chem*, **270**, 11860-11865.

Beckmann, R., Spahn, C.M., Eswar, N., Helmers, J., Penczek, P.A., Sali, A., Frank, J. and Blobel, G. (2001) Architecture of the protein-conducting channel associated with the translating 80S ribosome. *Cell*, **107**, 361-372.

142

Beckmann, R., Spahn, C.M., Frank, J. and Blobel, G. (2001) The active 80S ribosome-Sec61 complex. *Cold Spring Harb Symp Quant Biol*, **66**, 543-554.

Benard, L., Carroll, K., Valle, R.C. and Wickner, R.B. (1998) Ski6p is a homolog of RNA-processing enzymes that affects translation of non-poly(A) mRNAs and 60S ribosomal subunit biogenesis. *Mol Cell Biol*, **18**, 2688-2696.

Bernabeu, C. and Lake, J.A. (1982) Nascent polypeptide chains emerge from the exit domain of the large ribosomal subunit: immune mapping of the nascent chain. *Proc Natl Acad Sci U S A*, **79**, 3111-3115.

Bernad, R., Engelsma, D., Sanderson, H., Pickersgill, H. and Fornerod, M. (2006) Nup214-Nup88 nucleoporin subcomplex is required for CRM1-mediated 60 S preribosomal nuclear export. *J Biol Chem*, **281**, 19378-19386.

Bischoff, F.R., Klebe, C., Kretschmer, J., Wittinghofer, A. and Ponstingl, H. (1994) RanGAP1 induces GTPase activity of nuclear Ras-related Ran. *Proc Natl Acad Sci U S A*, **91**, 2587-2591.

Bischoff, F.R., Krebber, H., Smirnova, E., Dong, W. and Ponstingl, H. (1995) Co-activation of RanGTPase and inhibition of GTP dissociation by Ran-GTP binding protein RanBP1. *Embo J*, **14**, 705-715.

Bischoff, F.R., Scheffzek, K. and Ponstingl, H. (2002) How Ran is regulated. *Results Probl Cell Differ*, **35**, 49-66.

Bradshaw, R.A., Brickey, W.W. and Walker, K.W. (1998) N-terminal processing: the methionine aminopeptidase and N alpha-acetyl transferase families. *Trends Biochem Sci*, **23**, 263-267.

Braun, I.C., Herold, A., Rode, M. and Izaurralde, E. (2002) Nuclear export of mRNA by TAP/NXF1 requires two nucleoporin-binding sites but not p15. *Mol Cell Biol*, **22**, 5405-5418.

Bukau, B. and Horwich, A.L. (1998) The Hsp70 and Hsp60 chaperone machines. *Cell*, **92**, 351-366.

Care, A., Vousden, K.A., Binley, K.M., Radcliffe, P., Trevethick, J., Mannazzu, I. and Sudbery, P.E. (2004) A synthetic lethal screen identifies a role for the cortical actin patch/endocytosis complex in the response to nutrient deprivation in Saccharomyces cerevisiae. *Genetics*, **166**, 707-719.

143

Chook, Y.M., Jung, A., Rosen, M.K. and Blobel, G. (2002) Uncoupling Kapbeta2 substrate dissociation and ran binding. *Biochemistry*, **41**, 6955-6966.

Clarkson, W.D., Kent, H.M. and Stewart, M. (1996) Separate binding sites on nuclear transport factor 2 (NTF2) for GDP-Ran and the phenylalanine-rich repeat regions of nucleoporins p62 and Nsp1p. *J Mol Biol*, **263**, 517-524.

Costigan, C., Gehrung, S. and Snyder, M. (1992) A synthetic lethal screen identifies SLK1, a novel protein kinase homolog implicated in yeast cell morphogenesis and cell growth. *Mol Cell Biol*, **12**, 1162-1178.

Craig, E., Zhang, Z.K., Davies, K.P. and Kalpana, G.V. (2002) A masked NES in INI1/hSNF5 mediates hCRM1-dependent nuclear export: implications for tumorigenesis. *Embo J*, **21**, 31-42.

Craig, E.A., Eisenman, H.C. and Hundley, H.A. (2003) Ribosome-tethered molecular chaperones: the first line of defense against protein misfolding? *Curr Opin Microbiol*, **6**, 157-162.

Craig, E.A., Huang, P., Aron, R. and Andrew, A. (2006) The diverse roles of J-proteins, the obligate Hsp70 co-chaperone. *Rev Physiol Biochem Pharmacol*, **156**, 1-21.

Dahlberg, J.E., Lund, E. and Goodwin, E.B. (2003) Nuclear translation: what is the evidence? *Rna*, **9**, 1-8.

Devos, D., Dokudovskaya, S., Williams, R., Alber, F., Eswar, N., Chait, B.T., Rout, M.P. and Sali, A. (2006) Simple fold composition and modular architecture of the nuclear pore complex. *Proc Natl Acad Sci U S A*, **103**, 2172-2177.

Dong, J., Lai, R., Nielsen, K., Fekete, C.A., Qiu, H. and Hinnebusch, A.G. (2004) The essential ATP-binding cassette protein RLI1 functions in translation by promoting preinitiation complex assembly. *J Biol Chem*, **279**, 42157-42168.

Driessen, H.P., de Jong, W.W., Tesser, G.I. and Bloemendal, H. (1985) The mechanism of N-terminal acetylation of proteins. *CRC Crit Rev Biochem*, **18**, 281-325.

Egea, P.F., Stroud, R.M. and Walter, P. (2005) Targeting proteins to membranes: structure of the signal recognition particle. *Curr Opin Struct Biol*, **15**, 213-220.

Engelsma, D., Bernad, R., Calafat, J. and Fornerod, M. (2004) Supraphysiological nuclear export signals bind CRM1 independently of RanGTP and arrest at Nup358. *Embo J*, **23**, 3643-3652.

Ferbitz, L., Maier, T., Patzelt, H., Bukau, B., Deuerling, E. and Ban, N. (2004) Trigger factor in complex with the ribosome forms a molecular cradle for nascent proteins. *Nature*, **431**, 590-596.

Fink, A.L. (1999) Chaperone-mediated protein folding. *Physiol Rev*, **79**, 425-449.

Fischer, U., Huber, J., Boelens, W.C., Mattaj, I.W. and Luhrmann, R. (1995) The HIV-1 Rev activation domain is a nuclear export signal that accesses an export pathway used by specific cellular RNAs. *Cell*, **82**, 475-483.

Fornerod, M. and Ohno, M. (2002) Exportin-mediated nuclear export of proteins and ribonucleoproteins. *Results Probl Cell Differ*, **35**, 67-91.

Fornerod, M., Ohno, M., Yoshida, M. and Mattaj, I.W. (1997) CRM1 is an export receptor for leucine-rich nuclear export signals. *Cell*, **90**, 1051-1060.

Frank, J., Zhu, J., Penczek, P., Li, Y., Srivastava, S., Verschoor, A., Radermacher, M., Grassucci, R., Lata, R.K. and Agrawal, R.K. (1995) A model of protein synthesis based on cryo-electron microscopy of the E. coli ribosome. *Nature*, **376**, 441-444.

Franke, J., Reimann, B., Hartmann, E., Kohlerl, M. and Wiedmann, B. (2001) Evidence for a nuclear passage of nascent polypeptide-associated complex subunits in yeast. *J Cell Sci*, **114**, 2641-2648.

Fromont-Racine, M., Senger, B., Saveanu, C. and Fasiolo, F. (2003) Ribosome assembly in eukaryotes. *Gene*, **313**, 17-42.

Fukuda, M., Asano, S., Nakamura, T., Adachi, M., Yoshida, M., Yanagida, M. and Nishida, E. (1997) CRM1 is responsible for intracellular transport mediated by the nuclear export signal. *Nature*, **390**, 308-311.

Gadal, O., Strauss, D., Braspenning, J., Hoepfner, D., Petfalski, E., Philippsen, P., Tollervey, D. and Hurt, E. (2001) A nuclear AAA-type ATPase (Rix7p) is required for biogenesis and nuclear export of 60S ribosomal subunits. *Embo J*, **20**, 3695-3704.

Gadal, O., Strauss, D., Kessl, J., Trumpower, B., Tollervey, D. and Hurt, E. (2001) Nuclear export of 60s ribosomal subunits depends on Xpo1p and requires a nuclear export sequence-containing factor, Nmd3p, that associates with the large subunit protein Rpl10p. *Mol Cell Biol*, **21**, 3405-3415.

Gao, H., Sumanaweera, N., Bailer, S.M. and Stochaj, U. (2003) Nuclear accumulation of the small GTPase Gsp1p depends on nucleoporins Nup133p, Rat2p/Nup120p, Nup85p, Nic96p, and the acetyl-CoA carboxylase Acc1p. *J Biol Chem*, **278**, 25331-25340.

Gautschi, M., Mun, A., Ross, S. and Rospert, S. (2002) A functional chaperone triad on the yeast ribosome. *Proc Natl Acad Sci U S A*, **99**, 4209-4214.

Gavin, A.C., Bosche, M., Krause, R., Grandi, P., Marzioch, M., Bauer, A., Schultz, J., Rick, J.M., Michon, A.M., Cruciat, C.M., Remor, M., Hofert, C., Schelder, M., Brajenovic, M., Ruffner, H., Merino, A., Klein, K., Hudak, M., Dickson, D., Rudi, T., Gnau, V., Bauch, A., Bastuck, S., Huhse, B., Leutwein, C., Heurtier, M.A., Copley, R.R., Edelmann, A., Querfurth, E., Rybin, V., Drewes, G., Raida, M., Bouwmeester, T., Bork, P., Seraphin, B., Kuster, B., Neubauer, G. and Superti-Furga, G. (2002) Functional organization of the yeast proteome by systematic analysis of protein complexes. *Nature*, **415**, 141-147.

Gerace, L. (1995) Nuclear export signals and the fast track to the cytoplasm. *Cell*, **82**, 341-344.

Gietz, D., St Jean, A., Woods, R.A. and Schiestl, R.H. (1992) Improved method for high efficiency transformation of intact yeast cells. *Nucleic Acids Res*, **20**, 1425.

Giglione, C., Boularot, A. and Meinnel, T. (2004) Protein N-terminal methionine excision. *Cell Mol Life Sci*, **61**, 1455-1474.

Gleizes, P.E., Noaillac-Depeyre, J., Leger-Silvestre, I., Teulieres, F., Dauxois, J.Y., Pommet, D., Azum-Gelade, M.C. and Gas, N. (2001) Ultrastructural localization of rRNA shows defective nuclear export of preribosomes in mutants of the Nup82p complex. *J Cell Biol*, **155**, 923-936.

Gonzalez, C.I., Bhattacharya, A., Wang, W. and Peltz, S.W. (2001) Nonsense-mediated mRNA decay in Saccharomyces cerevisiae. *Gene*, **274**, 15-25.

Gorlich, D. and Mattaj, I.W. (1996) Nucleocytoplasmic transport. *Science*, **271**, 1513-1518.

Grallath, S., Schwarz, J.P., Bottcher, U.M., Bracher, A., Hartl, F.U. and Siegers, K. (2006) L25 functions as a conserved ribosomal docking site shared by nascent chain-associated complex and signal-recognition particle. *EMBO Rep*, **7**, 78-84.

Grandi, P., Rybin, V., Bassler, J., Petfalski, E., Strauss, D., Marzioch, M., Schafer, T., Kuster, B., Tschochner, H., Tollervey, D., Gavin, A.C. and Hurt, E. (2002) 90S pre-ribosomes include the 35S pre-rRNA, the U3 snoRNP, and 40S subunit processing factors but predominantly lack 60S synthesis factors. *Mol Cell*, **10**, 105-115.

Granneman, S. and Baserga, S.J. (2004) Ribosome biogenesis: of knobs and RNA processing. *Exp Cell Res*, **296**, 43-50.

Grant, R.P., Hurt, E., Neuhaus, D. and Stewart, M. (2002) Structure of the C-terminal FG-nucleoporin binding domain of Tap/NXF1. *Nat Struct Biol*, **9**, 247-251.

Grosshans, H., Deinert, K., Hurt, E. and Simos, G. (2001) Biogenesis of the signal recognition particle (SRP) involves import of SRP proteins into the nucleolus, assembly with the SRP-RNA, and Xpo1p-mediated export. *J Cell Biol*, **153**, 745-762.

Halic, M., Gartmann, M., Schlenker, O., Mielke, T., Pool, M.R., Sinning, I. and Beckmann, R. (2006) Signal recognition particle receptor exposes the ribosomal translocon binding site. *Science*, **312**, 745-747.

Harms, J., Schluenzen, F., Zarivach, R., Bashan, A., Gat, S., Agmon, I., Bartels, H., Franceschi, F. and Yonath, A. (2001) High resolution structure of the large ribosomal subunit from a mesophilic eubacterium. *Cell*, **107**, 679-688.

Hartl, F.U. and Hayer-Hartl, M. (2002) Molecular chaperones in the cytosol: from nascent chain to folded protein. *Science*, **295**, 1852-1858.

Hauer, J.A., Barthe, P., Taylor, S.S., Parello, J. and Padilla, A. (1999) Two well-defined motifs in the cAMP-dependent protein kinase inhibitor (PKIalpha) correlate with inhibitory and nuclear export function. *Protein Sci*, **8**, 545-553.

He, F. and Jacobson, A. (1995) Identification of a novel component of the nonsense-mediated mRNA decay pathway by use of an interacting protein screen. *Genes Dev*, **9**, 437-454.

Heath, C.V., Copeland, C.S., Amberg, D.C., Del Priore, V., Snyder, M. and Cole, C.N. (1995) Nuclear pore complex clustering and nuclear accumulation of poly(A)+ RNA associated with mutation of the Saccharomyces cerevisiae RAT2/NUP120 gene. *J Cell Biol*, **131**, 1677-1697.

Hedges, J., Chen, Y.I., West, M., Bussiere, C. and Johnson, A.W. (2006) Mapping the functional domains of yeast NMD3, the nuclear export adapter for the 60 S ribosomal subunit. *J Biol Chem*, **281**, 36579-36587.

Hedges, J., West, M. and Johnson, A.W. (2005) Release of the export adapter, Nmd3p, from the 60S ribosomal subunit requires Rpl10p and the cytoplasmic GTPase Lsg1p. *Embo J*, **24**, 567-579.

Hesterkamp, T., Hauser, S., Lutcke, H. and Bukau, B. (1996) Escherichia coli trigger factor is a prolyl isomerase that associates with nascent polypeptide chains. *Proc Natl Acad Sci U S A*, **93**, 4437-4441.

Ho, J.H. and Johnson, A.W. (1999) NMD3 encodes an essential cytoplasmic protein required for stable 60S ribosomal subunits in Saccharomyces cerevisiae. *Mol Cell Biol*, **19**, 2389-2399.

Ho, J.H., Kallstrom, G. and Johnson, A.W. (2000) Nmd3p is a Crm1p-dependent adapter protein for nuclear export of the large ribosomal subunit. *J Cell Biol*, **151**, 1057-1066.

Huh, W.K., Falvo, J.V., Gerke, L.C., Carroll, A.S., Howson, R.W., Weissman, J.S. and O'Shea, E.K. (2003) Global analysis of protein localization in budding yeast. *Nature*, **425**, 686-691.

Hundley, H., Eisenman, H., Walter, W., Evans, T., Hotokezaka, Y., Wiedmann, M. and Craig, E. (2002) The in vivo function of the ribosome-associated Hsp70,

Ssz1, does not require its putative peptide-binding domain. *Proc Natl Acad Sci U S A*, **99**, 4203-4208.

Hung, N.J. and Johnson, A.W. (2006) Nuclear recycling of the pre-60S ribosomal subunit-associated factor Arx1 depends on Rei1 in Saccharomyces cerevisiae. *Mol Cell Biol*, **26**, 3718-3727.

Hurt, E., Hannus, S., Schmelzl, B., Lau, D., Tollervey, D. and Simos, G. (1999) A novel in vivo assay reveals inhibition of ribosomal nuclear export in ran-cycle and nucleoporin mutants. *J Cell Biol*, **144**, 389-401.

Ito, K. (2005) Ribosome-based protein folding systems are structurally divergent but functionally universal across biological kingdoms. *Mol Microbiol*, **57**, 313-317.

Iwase, M. and Toh-e, A. (2001) Nis1 encoded by YNL078W: a new neck protein of Saccharomyces cerevisiae. *Genes Genet Syst*, **76**, 335-343.

Iwase, M. and Toh-e, A. (2004) Ybr267w is a new cytoplasmic protein belonging to the mitotic signaling network of Saccharomyces cerevisiae. *Cell Struct Funct*, **29**, 1-15.

Jacobson, A. and Peltz, S.W. (1996) Interrelationships of the pathways of mRNA decay and translation in eukaryotic cells. *Annu Rev Biochem*, **65**, 693-739.

James, P., Halladay, J. and Craig, E.A. (1996) Genomic libraries and a host strain designed for highly efficient two-hybrid selection in yeast. *Genetics*, **144**, 1425-1436.

Jeeninga, R.E., Van Delft, Y., de Graaff-Vincent, M., Dirks-Mulder, A., Venema, J. and Raue, H.A. (1997) Variable regions V13 and V3 of Saccharomyces cerevisiae contain structural features essential for normal biogenesis and stability of 5.8S and 25S rRNA. *Rna*, **3**, 476-488.

Johnson, A.W. and Kolodner, R.D. (1995) Synthetic lethality of sep1 (xrn1) ski2 and sep1 (xrn1) ski3 mutants of Saccharomyces cerevisiae is independent of killer virus and suggests a general role for these genes in translation control. *Mol Cell Biol*, **15**, 2719-2727.

Johnson, A.W., Lund, E. and Dahlberg, J. (2002) Nuclear export of ribosomal subunits. *Trends Biochem Sci*, **27**, 580-585.

Kaiser, C., S. Michaelis, et al. (1994) *Methods in yeast genetics*.

Kallstrom, G., Hedges, J. and Johnson, A. (2003) The putative GTPases Nog1p and Lsg1p are required for 60S ribosomal subunit biogenesis and are localized to the nucleus and cytoplasm, respectively. *Mol Cell Biol*, **23**, 4344-4355.

Kass, S., Tyc, K., Steitz, J.A. and Sollner-Webb, B. (1990) The U3 small nucleolar ribonucleoprotein functions in the first step of preribosomal RNA processing. *Cell*, **60**, 897-908.

Katahira, J., Strasser, K., Podtelejnikov, A., Mann, M., Jung, J.U. and Hurt, E. (1999) The Mex67p-mediated nuclear mRNA export pathway is conserved from yeast to human. *Embo J*, **18**, 2593-2609.

Kehlenbach, R.H., Dickmanns, A., Kehlenbach, A., Guan, T. and Gerace, L. (1999) A role for RanBP1 in the release of CRM1 from the nuclear pore complex in a terminal step of nuclear export. *J Cell Biol*, **145**, 645-657.

Kempers-Veenstra, A.E., Oliemans, J., Offenberg, H., Dekker, A.F., Piper, P.W., Planta, R.J. and Klootwijk, J. (1986) 3'-End formation of transcripts from the yeast rRNA operon. *Embo J*, **5**, 2703-2710.

Kim, S.Y. and Craig, E.A. (2005) Broad sensitivity of Saccharomyces cerevisiae lacking ribosome-associated chaperone ssb or zuo1 to cations, including aminoglycosides. *Eukaryot Cell*, **4**, 82-89.

Klebe, C., Bischoff, F.R., Ponstingl, H. and Wittinghofer, A. (1995) Interaction of the nuclear GTP-binding protein Ran with its regulatory proteins RCC1 and RanGAP1. *Biochemistry*, **34**, 639-647.

Kranz, J.E. and Holm, C. (1990) Cloning by function: an alternative approach for identifying yeast homologs of genes from other organisms. *Proc Natl Acad Sci U S A*, **87**, 6629-6633.

Kressler, D., Linder, P. and de La Cruz, J. (1999) Protein trans-acting factors involved in ribosome biogenesis in Saccharomyces cerevisiae. *Mol Cell Biol*, **19**, 7897-7912.

Kruiswijk, T., Planta, R.J. and Krop, J.M. (1978) The course of the assembly of ribosomal subunits in yeast. *Biochim Biophys Acta*, **517**, 378-389.

Kumar, A. and Warner, J.R. (1972) Characterization of ribosomal precursor particles from HeLa cell nucleoli. *J Mol Biol*, **63**, 233-246.

Kutay, U. and Guttinger, S. (2005) Leucine-rich nuclear-export signals: born to be weak. *Trends Cell Biol*, **15**, 121-124.

Lebreton, A., Saveanu, C., Decourty, L., Rain, J.C., Jacquier, A. and Fromont-Racine, M. (2006) A functional network involved in the recycling of nucleocytoplasmic pre-60S factors. *J Cell Biol*, **173**, 349-360.

Lei, E.P. and Silver, P.A. (2002) Protein and RNA export from the nucleus. *Dev Cell*, **2**, 261-272.

Lemmon, S.K. (2001) Clathrin uncoating: Auxilin comes to life. *Curr Biol*, **11**, R49-52.

Lessor, T.J., Yoo, J.Y., Xia, X., Woodford, N. and Hamburger, A.W. (2000) Ectopic expression of the ErbB-3 binding protein ebp1 inhibits growth and induces differentiation of human breast cancer cell lines. *J Cell Physiol*, **183**, 321-329.

Longtine, M.S., McKenzie, A., 3rd, Demarini, D.J., Shah, N.G., Wach, A., Brachat, A., Philippsen, P. and Pringle, J.R. (1998) Additional modules for versatile and economical PCR-based gene deletion and modification in Saccharomyces cerevisiae. *Yeast*, **14**, 953-961.

Lounsbury, K.M. and Macara, I.G. (1997) Ran-binding protein 1 (RanBP1) forms a ternary complex with Ran and karyopherin beta and reduces Ran GTPase-activating protein (RanGAP) inhibition by karyopherin beta. *J Biol Chem*, **272**, 551-555.

Lowther, W.T. and Matthews, B.W. (2000) Structure and function of the methionine aminopeptidases. *Biochim Biophys Acta*, **1477**, 157-167.

Luirink, J. and Sinning, I. (2004) SRP-mediated protein targeting: structure and function revisited. *Biochim Biophys Acta*, **1694**, 17-35.

Lund, M.K. and Guthrie, C. (2005) The DEAD-box protein Dbp5p is required to dissociate Mex67p from exported mRNPs at the nuclear rim. *Mol Cell*, **20**, 645-651.

Lykke-Andersen, J. (2001) mRNA quality control: Marking the message for life or death. *Curr Biol*, **11**, R88-91.

Macara, I.G. (2001) Transport into and out of the nucleus. *Microbiol Mol Biol Rev*, **65**, 570-594, table of contents.

Maier, T., Ferbitz, L., Deuerling, E. and Ban, N. (2005) A cradle for new proteins: trigger factor at the ribosome. *Curr Opin Struct Biol*, **15**, 204-212.

Meyer, A.E., Hung, N.J., Yang, P., Johnson, A.W. and Craig, E.A. (2007) The specialized cytosolic J-protein, Jjj1, functions in 60S ribosomal subunit biogenesis. *Proc Natl Acad Sci U S A*, **104**, 1558-1563.

Milkereit, P., Gadal, O., Podtelejnikov, A., Trumtel, S., Gas, N., Petfalski, E., Tollervey, D., Mann, M., Hurt, E. and Tschochner, H. (2001) Maturation and intranuclear transport of pre-ribosomes requires Noc proteins. *Cell*, **105**, 499-509.

Miller, O.L., Jr. and Beatty, B.R. (1969) Visualization of nucleolar genes. *Science*, **164**, 955-957.

Milligan, R.A. and Unwin, P.N. (1986) Location of exit channel for nascent protein in 80S ribosome. *Nature*, **319**, 693-695.

Moroianu, J. (1998) Distinct nuclear import and export pathways mediated by members of the karyopherin beta family. *J Cell Biochem*, **70**, 231-239.

Moy, T.I. and Silver, P.A. (2002) Requirements for the nuclear export of the small ribosomal subunit. *J Cell Sci*, **115**, 2985-2995.

Neumann, S., Petfalski, E., Brugger, B., Grosshans, H., Wieland, F., Tollervey, D. and Hurt, E. (2003) Formation and nuclear export of tRNA, rRNA and mRNA is regulated by the ubiquitin ligase Rsp5p. *EMBO Rep*, **4**, 1156-1162.

Nissan, T.A., Bassler, J., Petfalski, E., Tollervey, D. and Hurt, E. (2002) 60S pre-ribosome formation viewed from assembly in the nucleolus until export to the cytoplasm. *Embo J*, **21**, 5539-5547.

Nissen, P., Hansen, J., Ban, N., Moore, P.B. and Steitz, T.A. (2000) The structural basis of ribosome activity in peptide bond synthesis. *Science*, **289**, 920-930.

Ohno, M. (1998) [Importins and exportins: receptors involved in nucleocytoplasmic transport of proteins and RNAs]. *Tanpakushitsu Kakusan Koso*, **43**, 1255-1264.

Ossareh-Nazari, B., Bachelerie, F. and Dargemont, C. (1997) Evidence for a role of CRM1 in signal-mediated nuclear protein export. *Science*, **278**, 141-144.

Panse, V.G., Kressler, D., Pauli, A., Petfalski, E., Gnadig, M., Tollervey, D. and Hurt, E. (2006) Formation and nuclear export of preribosomes are functionally linked to the small-ubiquitin-related modifier pathway. *Traffic*, **7**, 1311-1321.

Park, E.C., Finley, D. and Szostak, J.W. (1992) A strategy for the generation of conditional mutations by protein destabilization. *Proc Natl Acad Sci U S A*, **89**, 1249-1252.

Paschal, B.M. and Gerace, L. (1995) Identification of NTF2, a cytosolic factor for nuclear import that interacts with nuclear pore complex protein p62. *J Cell Biol*, **129**, 925-937.

Patel, S.S., Belmont, B.J., Sante, J.M. and Rexach, M.F. (2007) Natively unfolded nucleoporins gate protein diffusion across the nuclear pore complex. *Cell*, **129**, 83-96.

Patel, S.S., Belmont, B.J., Sante, J.M. and Rexach, M.F. (2007) Natively unfolded nucleoporins gate protein diffusion across the nuclear pore complex. *Cell*, **129**, 83-96.

Petosa, C., Schoehn, G., Askjaer, P., Bauer, U., Moulin, M., Steuerwald, U., Soler-Lopez, M., Baudin, F., Mattaj, I.W. and Muller, C.W. (2004) Architecture of CRM1/Exportin1 suggests how cooperativity is achieved during formation of a nuclear export complex. *Mol Cell*, **16**, 761-775.

Pfund, C., Lopez-Hoyo, N., Ziegelhoffer, T., Schilke, B.A., Lopez-Buesa, P., Walter, W.A., Wiedmann, M. and Craig, E.A. (1998) The molecular chaperone Ssb from Saccharomyces cerevisiae is a component of the ribosome-nascent chain complex. *Embo J*, **17**, 3981-3989.

Picking, W.D., Picking, W.L., Odom, O.W. and Hardesty, B. (1992) Fluorescence characterization of the environment encountered by nascent polyalanine and polyserine as they exit Escherichia coli ribosomes during translation. *Biochemistry*, **31**, 2368-2375.

Polevoda, B. and Sherman, F. (2003) Composition and function of the eukaryotic N-terminal acetyltransferase subunits. *Biochem Biophys Res Commun*, **308**, 1-11.

Pool, M.R., Stumm, J., Fulga, T.A., Sinning, I. and Dobberstein, B. (2002) Distinct modes of signal recognition particle interaction with the ribosome. *Science*, **297**, 1345-1348.

Qiu, X.B., Shao, Y.M., Miao, S. and Wang, L. (2006) The diversity of the DnaJ/Hsp40 family, the crucial partners for Hsp70 chaperones. *Cell Mol Life Sci*, **63**, 2560-2570.

Radu, A., Moore, M.S. and Blobel, G. (1995) The peptide repeat domain of nucleoporin Nup98 functions as a docking site in transport across the nuclear pore complex. *Cell*, **81**, 215-222.

Raska, I., Shaw, P.J. and Cmarko, D. (2006) Structure and function of the nucleolus in the spotlight. *Curr Opin Cell Biol*, **18**, 325-334.

Rassow, J. and Pfanner, N. (1996) Protein biogenesis: chaperones for nascent polypeptides. *Curr Biol*, **6**, 115-118.

Raue, U., Oellerer, S. and Rospert, S. (2007) Association of protein biogenesis factors at the yeast ribosomal tunnel exit is affected by the translational status and nascent polypeptide sequence. *J Biol Chem*, **282**, 7809-7816.

Raychaudhuri, P., Stringer, E.A., Valenzuela, D.M. and Maitra, U. (1984) Ribosomal subunit antiassociation activity in rabbit reticulocyte lysates. Evidence for a low molecular weight ribosomal subunit antiassociation protein factor (Mr = 25,000). *J Biol Chem*, **259**, 11930-11935.

Ribbeck, K. and Gorlich, D. (2001) Kinetic analysis of translocation through nuclear pore complexes. *Embo J*, **20**, 1320-1330.

Ribbeck, K. and Gorlich, D. (2002) The permeability barrier of nuclear pore complexes appears to operate via hydrophobic exclusion. *Embo J*, **21**, 2664-2671.

Rospert, S., Dubaquie, Y. and Gautschi, M. (2002) Nascent-polypeptide-associated complex. *Cell Mol Life Sci*, **59**, 1632-1639.

Russell, D.W. and Spremulli, L.L. (1979) Purification and characterization of a ribosome dissociation factor (eukaryotic initiation factor 6) from wheat germ. *J Biol Chem*, **254**, 8796-8800.

Saveanu, C., Namane, A., Gleizes, P.E., Lebreton, A., Rousselle, J.C., Noaillac-Depeyre, J., Gas, N., Jacquier, A. and Fromont-Racine, M. (2003) Sequential protein association with nascent 60S ribosomal particles. *Mol Cell Biol*, **23**, 4449-4460.

Schafer, T., Maco, B., Petfalski, E., Tollervey, D., Bottcher, B., Aebi, U. and Hurt, E. (2006) Hrr25-dependent phosphorylation state regulates organization of the pre-40S subunit. *Nature*, **441**, 651-655.

Schnare, M.N., Damberger, S.H., Gray, M.W. and Gutell, R.R. (1996) Comprehensive comparison of structural characteristics in eukaryotic cytoplasmic large subunit (23 S-like) ribosomal RNA. *J Mol Biol*, **256**, 701-719.

Segref, A., Sharma, K., Doye, V., Hellwig, A., Huber, J., Luhrmann, R. and Hurt, E. (1997) Mex67p, a novel factor for nuclear mRNA export, binds to both poly(A)+ RNA and nuclear pores. *Embo J*, **16**, 3256-3271.

Senger, B., Lafontaine, D.L., Graindorge, J.S., Gadal, O., Camasses, A., Sanni, A., Garnier, J.M., Breitenbach, M., Hurt, E. and Fasiolo, F. (2001) The nucle(ol)ar Tif6p and Efl1p are required for a late cytoplasmic step of ribosome synthesis. *Mol Cell*, **8**, 1363-1373.

Shaw, P. and Doonan, J. (2005) The nucleolus. Playing by different rules? *Cell Cycle*, **4**, 102-105.

Sherman, F., Stewart, J.W. and Tsunasawa, S. (1985) Methionine or not methionine at the beginning of a protein. *Bioessays*, **3**, 27-31.

Siniossoglou, S., Lutzmann, M., Santos-Rosa, H., Leonard, K., Mueller, S., Aebi, U. and Hurt, E. (2000) Structure and assembly of the Nup84p complex. *J Cell Biol*, **149**, 41-54.

Spahn, C.M., Beckmann, R., Eswar, N., Penczek, P.A., Sali, A., Blobel, G. and Frank, J. (2001) Structure of the 80S ribosome from Saccharomyces

cerevisiae--tRNA-ribosome and subunit-subunit interactions. *Cell*, **107**, 373-386.

Squatrito, M., Mancino, M., Sala, L. and Draetta, G.F. (2006) Ebp1 is a dsRNA-binding protein associated with ribosomes that modulates eIF2alpha phosphorylation. *Biochem Biophys Res Commun*, **344**, 859-868.

Stage-Zimmermann, T., Schmidt, U. and Silver, P.A. (2000) Factors affecting nuclear export of the 60S ribosomal subunit in vivo. *Mol Biol Cell*, **11**, 3777-3789.

Stewart, M. (2007) Ratcheting mRNA out of the nucleus. *Mol Cell*, **25**, 327-330.

Strom, A.C. and Weis, K. (2001) Importin-beta-like nuclear transport receptors. *Genome Biol*, **2**, REVIEWS3008.

Suntharalingam, M. and Wente, S.R. (2003) Peering through the pore: nuclear pore complex structure, assembly, and function. *Dev Cell*, **4**, 775-789.

Takahashi, N., Yanagida, M., Fujiyama, S., Hayano, T. and Isobe, T. (2003) Proteomic snapshot analyses of preribosomal ribonucleoprotein complexes formed at various stages of ribosome biogenesis in yeast and mammalian cells. *Mass Spectrom Rev*, **22**, 287-317.

Thiry, M. and Lafontaine, D.L. (2005) Birth of a nucleolus: the evolution of nucleolar compartments. *Trends Cell Biol*, **15**, 194-199.

Thomas, F. and Kutay, U. (2003) Biogenesis and nuclear export of ribosomal subunits in higher eukaryotes depend on the CRM1 export pathway. *J Cell Sci*, **116**, 2409-2419.

Trotta, C.R., Lund, E., Kahan, L., Johnson, A.W. and Dahlberg, J.E. (2003) Coordinated nuclear export of 60S ribosomal subunits and NMD3 in vertebrates. *Embo J*, **22**, 2841-2851.

Tschochner, H. and Hurt, E. (2003) Pre-ribosomes on the road from the nucleolus to the cytoplasm. *Trends Cell Biol*, **13**, 255-263.

Ullman, K.S., Powers, M.A. and Forbes, D.J. (1997) Nuclear export receptors: from importin to exportin. *Cell*, **90**, 967-970.

Venema, J., Dirks-Mulder, A., Faber, A.W. and Raue, H.A. (1995) Development and application of an in vivo system to study yeast ribosomal RNA biogenesis and function. *Yeast*, **11**, 145-156.

Verschoor, A., Warner, J.R., Srivastava, S., Grassucci, R.A. and Frank, J. (1998) Three-dimensional structure of the yeast ribosome. *Nucleic Acids Res*, **26**, 655-661.

Walsh, P., Bursac, D., Law, Y.C., Cyr, D. and Lithgow, T. (2004) The J-protein family: modulating protein assembly, disassembly and translocation. *EMBO Rep*, **5**, 567-571.

Warner, J.R. (2001) Nascent ribosomes. *Cell*, **107**, 133-136.

Warner, J.R. and Soeiro, R. (1967) Nascent ribosomes from HeLa cells. *Proc Natl Acad Sci U S A*, **58**, 1984-1990.

Weirich, C.S., Erzberger, J.P., Flick, J.S., Berger, J.M., Thorner, J. and Weis, K. (2006) Activation of the DExD/H-box protein Dbp5 by the nuclear-pore protein Gle1 and its coactivator InsP6 is required for mRNA export. *Nat Cell Biol*, **8**, 668-676.

Weis, K. (2002) Nucleocytoplasmic transport: cargo trafficking across the border. *Curr Opin Cell Biol*, **14**, 328-335.

Wen, W., Meinkoth, J.L., Tsien, R.Y. and Taylor, S.S. (1995) Identification of a signal for rapid export of proteins from the nucleus. *Cell*, **82**, 463-473.

Wente, S.R. (2000) Gatekeepers of the nucleus. *Science*, **288**, 1374-1377.

Wesierska-Gadek, J., Wojciechowski, J. and Schmid, G. (2003) Central and carboxy-terminal regions of human p53 protein are essential for interaction and complex formation with PARP-1. *J Cell Biochem*, **89**, 220-232.

West, M., Hedges, J.B., Chen, A. and Johnson, A.W. (2005) Defining the order in which Nmd3p and Rpl10p load onto nascent 60S ribosomal subunits. *Mol Cell Biol*, **25**, 3802-3813.

West, M., Hedges, J.B., Lo, K.Y. and Johnson, A.W. (2007) Novel interaction of the 60S ribosomal subunit export adapter Nmd3 at the nuclear pore complex. *J Biol Chem*.

Wild, K., Halic, M., Sinning, I. and Beckmann, R. (2004) SRP meets the ribosome. *Nat Struct Mol Biol*, **11**, 1049-1053.

Winey, M., Yarar, D., Giddings, T.H., Jr. and Mastronarde, D.N. (1997) Nuclear pore complex number and distribution throughout the Saccharomyces cerevisiae

cell cycle by three-dimensional reconstruction from electron micrographs of nuclear envelopes. *Mol Biol Cell*, **8**, 2119-2132.

Xia, X., Cheng, A., Lessor, T., Zhang, Y. and Hamburger, A.W. (2001) Ebp1, an ErbB-3 binding protein, interacts with Rb and affects Rb transcriptional regulation. *J Cell Physiol*, **187**, 209-217.

Yao, W., Roser, D., Kohler, A., Bradatsch, B., Bassler, J. and Hurt, E. (2007) Nuclear export of ribosomal 60S subunits by the general mRNA export receptor Mex67-Mtr2. *Mol Cell*, **26**, 51-62.

Yonath, A., Leonard, K.R. and Wittmann, H.G. (1987) A tunnel in the large ribosomal subunit revealed by three-dimensional image reconstruction. *Science*, **236**, 813-816.

Yoneda, Y., Hieda, M., Nagoshi, E. and Miyamoto, Y. (1999) Nucleocytoplasmic protein transport and recycling of Ran. *Cell Struct Funct*, **24**, 425-433.

Yoo, J.Y., Wang, X.W., Rishi, A.K., Lessor, T., Xia, X.M., Gustafson, T.A. and Hamburger, A.W. (2000) Interaction of the PA2G4 (EBP1) protein with ErbB-3 and regulation of this binding by heregulin. *Br J Cancer*, **82**, 683-690.

Zavanelli, M.I., Britton, J.S., Igel, A.H. and Ares, M., Jr. (1994) Mutations in an essential U2 small nuclear RNA structure cause cold-sensitive U2 small nuclear ribonucleoprotein function by favoring competing alternative U2 RNA structures. *Mol Cell Biol*, **14**, 1689-1697.

Zhang, Y., Woodford, N., Xia, X. and Hamburger, A.W. (2003) Repression of E2F1-mediated transcription by the ErbB3 binding protein Ebp1 involves histone deacetylases. *Nucleic Acids Res*, **31**, 2168-2177.

Vita

Nai-Jung Hung was born 27 March 1976 in Tainan, Taiwan to Jung-Chou Hung and Shu-Jen Wu. She earned a Bachelor of Science degree in Zoology from the National Taiwan University in 1998. She then joined Dr. Robert Costa's lab in University of Illinois at Chicago as a graduate student in 1999. Later, she entered the Ph.D. program in Cellular and Molecular Biology at the University of Texas at Austin at 2001 and joined the lab of Arlen Johnson.

Permanent address: 4F 6-1 LN38 Tian-Yuh St, Shih-Lin, Taipei, Taiwan, ROC

This dissertation was typed by the author